THE GEOLOGY AND GENESIS OF THE CHLORITE-CARBONATE ALTERATION IN THE FOOTWALL OF THE HELLYER VOLCANIC-HOSTED MASSIVE SULPHIDE (VHMS) DEPOSIT

Alison Bradley, B.Sc.

A research thesis submitted in partial fulfilment of the requirements of the degree of Bachelor of Science with Honours

Centre for Ore Deposit Research,
Geology Department, University of Tasmania.

November, 1997.

ABSTRACT

The chlorite-carbonate alteration assemblage is an unusual feature in the footwall of the Hellyer volcanic-hosted massive sulphide deposit, Tasmania. Carbonate alteration is common to many VHMS deposits however its origin and characteristics has been rarely studied in detail.

Chlorite-carbonate alteration is defined as texturally diverse dolomite in a matrix of fine-grained chlorite. This distinctive alteration is found at the top of the chlorite-alteration zone around the central and northern hydrothermal discharge sites beneath the deposit. On the ore contact ('contact zone'), the chlorite-carbonate assemblage occurs as thin discontinuous lenses. A lower stratiform chlorite-carbonate alteration zone ('lower zone') occurs approximately 40 metres below the contact zone, is more laterally continuous and only occurs on the west side of the east flank of the ore deposit. Carbonate alteration is associated with sericite, chlorite and quartz in the contact zone but is primarily associated with chlorite in the lower zone. Carbonate-chlorite assemblages have not been observed at greater depths in the footwall alteration pipe, or distal to the deposit.

The carbonate mineralogy is Fe-dolomite or dolomite. Carbonate textures consist of large and small spheroids, rhombs, massive carbonate and veinlets. These textures appear to be associated with the initial porosity and permeability of the host rock. The various carbonate textures formed synchronously and have no textural zonation within the contact and lower alteration zones.

Whole-rock geochemical studies indicate major gains in Ca, Mg, and Fe and losses in Si and Na in the chlorite-carbonate alteration compared to the unaltered footwall andesite. An absolute mass-gain of 18g/100g is achieved when converting an andesite to a chorite-carbonate altered rock.

Carbon isotopes ($\delta^{13}C$) range between +0.31 and +2.8‰ and oxygen isotopes ($\delta^{18}O$) range from +10.29 to +18.29‰. Isotope studies indicate that the dolomites formed from upwelling hydrothermal fluid (modified seawater with a minor magmatic input) in the lower zone or from the mixing of the hydrothermal fluid with infiltrating seawater in the contact zone. Carbon isotopic values are uncharacteristically high at Hellyer compared with other VHMS deposits and could indicate deep-seated contributions of $\delta^{13}C$.

From distribution and textural evidence, it is proposed that the dolomite alteration formed by direct precipitation within chloritised volcaniclastic units near the seafloor or in shallow sub-seafloor units in the mixing zone between upwelling hydrothermal fluids and infiltrating seawater. As the hydrothermal fluid mixed with infiltrating seawater a pH increase counteracted the affects of cooling and caused dolomite to precipitate.

Acknowledgments

I would like to thank Aberfoyle Resources Limited for their logistical support for this project. In particular, I would like to thank Dr. Gary McArthur who was helpful and supportive during the year; Chris Davies for producing some of my plans and Steve Richardson. I would also like to thank the Tasmanian Government for providing me with a scholarship which helped me complete this year.

I would also like to thank my supervisors Dr. Bruce Gemmell and Prof. Ross Large. Bruce has been of great support and offered endless advice and encouragement during the year.

I would like to extend my thanks to Karin Orth, Walter Herrman, Paul Kitto, Dr. Khin Zaw, Dr. David Cooke and Dr. Garry Davidson for their help during the year.

Thanks to fellow honours students for their friendship and memorable entertainment over the year (it has definitely been an interesting one!).

Finally, huge thanks go to my parents Tony and Carol and great friends Karin and Julianne who have heard out my many stressed phone-calls and have never ceased to provide enormous encouragement and support.

Table of Contents

Appendices

1.1 Example of a logging sheet
1.2 Drill holes logged and intervals

2.1Thin section sample locations and descriptions
2.2 Example of a petrological interpretation sheet

3.1 Whole-rock XRF results
3.2 Unaltered andesite XRF analyses
3.3 Chlorite-carbonate XRF analyses (Gemmell, 1989)
3.4 Location, TiO_2 and Zr data for the mixed dacitic sequence and Hellyer Basalt

4.1 $\delta^{13}C$ and $\delta^{18}O$ stable isotope sample locations for the stage 2A, 2B and 2C syn-mineralisation veins
4.2 $\delta^{13}C$ and $\delta^{18}O$ stable isotope sample locations and descriptions
5 Rock Catalogue

List of Figures

Chapter 6

Chapter 7

Chapter 8

List of Plates

List of Tables

CHAPTER 1

INTRODUCTION

1.1 Research Aims

Chlorite-carbonate alteration is an integral part of the footwall alteration zone associated with the Hellyer volcanic-hosted massive sulphide (VHMS) deposit and occurs near the top of the massive chlorite alteration zone (Gemmell and Large, 1992; McArthur, 1989). It is closely associated to the massive sulphide deposit as it lies in a zone on the footwall-ore contact, in the chlorite zone (McArthur, 1989) and also as a stratiform zone approximately 30-50 metres below the deposit. Footwall alteration pipes in VHMS deposits can be used as an exploration tool as they are generally mineralogically zoned and act as vectors to ore. The alteration geochemistry and textural evolution surrounding a VHMS ore deposit gives an insight into the types of hydrothermal fluids that precipitated the mineralisation and the physico-chemical conditions at that time (Gemmell, 1996).

The main aims of this research project are to:

1) Outline the spatial distribution both vertically and laterally of the chlorite-carbonate alteration zone in the footwall of the Hellyer ore deposit.

2) Characterise the mineralogical and textural variations of the chlorite-carbonate alteration on both small and large scales.

3) Investigate the whole-rock characteristics of the chlorite-carbonate alteration, including mass balance calculations

4) Use carbon and oxygen isotope data to determine the nature of the hydrothermal fluids precipitating the alteration minerals.

5) Propose a genetic model for the formation of this alteration zone.

1.2 Outline of the Research Project

Chapter Two covers the regional and local geology to give an overview of the proximal and distal geologic environments surrounding the Hellyer ore deposit.

To investigate the spatial distribution of the alteration zone (Chapter Three) select portions from diamond drill holes were logged, based on information obtained from cross-sections 10260N-10520N and 10910N-11090N.
In the logging process, variations in carbonate textures were noted as well as other alteration types associated with the chlorite-carbonate alteration.

To characterise the textural variations and evolution of the alteration zone (Chapter Four) thirty polished thin sections were examined. The carbonates were examined using cathodoluminecence (CL) techniques to determine their composition and paragenesis. Whole-rock geochemistry was determined using X-Ray Fluorescence techniques and is discussed in Chapter Five

Carbon and oxygen isotope analyses were obtained from forty samples collected from a broad area around the ore deposit. These results were used, in part, to determine a model for the genesis of the alteration zone (Chapter Six) by giving an insight as to what type of fluids the minerals precipitated from.

Chapter seven outlines a genetic model for the formation of the chlorite-carbonate alteration zone. Chapter Eight compares this study to other similar ones completed on local deposits such as Que-River (CSIRO-Division of Mineralogy, 1983) and Rosebery (Orth and Hill, 1995). Comparisons are also made with carbonate alteration associated with Mattabi-type deposits in Canada.

1.3 Previous Research

Carbonates existing in volcanic hosted massive sulphide ore deposits have been relatively over-looked and therefore a minimal amount of research on hydrothermal carbonates associated with massive sulphide deposits has been undertaken. Aberfoyle Resources Ltd. (McArthur, 1989) and Gemmell and Large (1992) have acknowledged that the chlorite-carbonate alteration at Hellyer exists mainly on the footwall-ore contact and is more prominent in the northern end of the deposit, on the east flank. They also concluded that the carbonate existed as predominantly dolomitic spheroids only associated with chlorite and overprinted by a network of massive Devonian calcite veins. A study of the host-rock alteration at Hellyer was also carried out by Jack (1989) and detailed studies into the stringer system and footwall alteration has also been documented by (Gemmell, 1988;1989; Gemmell and Large, 1992).
Alteration pipe mineralogy and chemical studies underlying a number of other volcanic-hosted sulphide deposits have been conducted. Comparisons between some Kuroko-style deposits have also been carried out (Urabe et al., 1983).

Studies carried out at Que-River deposit (Offler and Whitford, 1992), 3km south of Hellyer, indicate the presence of chlorite-carbonate alteration zones in lens-like structures associated with massive chlorite zones.

From these previous studies it is apparent that many VHMS deposits have carbonate as an important component of their hydrothermal alteration. This investigation of carbonate alteration is significant for a better understanding of the systematics of alteration associated with VHMS deposits and may yield important information to aid exploration.

CHAPTER 2

REGIONAL AND LOCAL GEOLOGY

2.1 The Regional Geological Setting

Hellyer is a high-grade, volcanic-hosted, Pb-Zn-Cu-Ag-Au ore deposit located within the middle to late Cambrian Mt. Read Volcanic Belt in the north-west of Tasmania (Fig. 2.1). This belt extends for 200km and is 10 to 15km wide and comprises rhyolites, dacites, andesites, rare basalts and volcaniclastics which fill the Dundas Trough. This is an elongate basin bound by blocks of Precambrian metasediments (Eastoe et al., 1987). At the base of the Mount Read Volcanics is the Central Volcanic Complex containing predominantly dacitic and rhyolitic lavas, mafics, tuffs and breccias. This sequence is overlain unconformably by the Dundas Group to the South west of the belt and the Mt. Charter Group to the North east (Fig. 2.2). The Hellyer massive sulphide ore deposit is located in the Que-Hellyer volcanics located towards the base of the Mt. Charter Group. This group is comprised of volcaniclastics, graywackes siltstones and shales. The Que-Hellyer volcanics are overlain by the Que River Shale and occur above the Animal Creek Greywacke (Fig. 2.3).

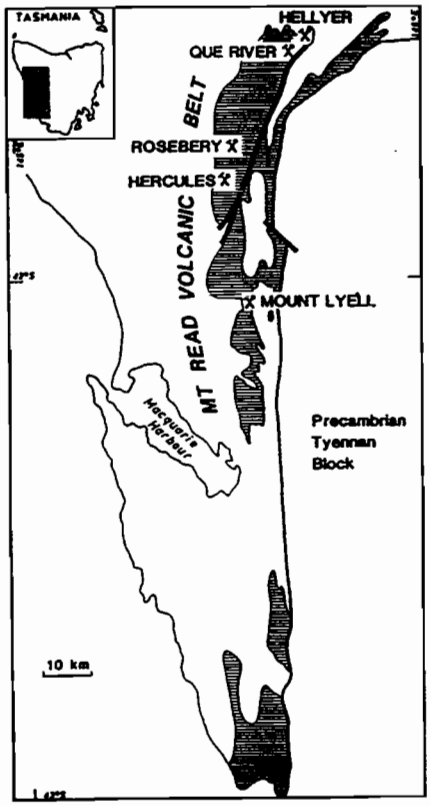

Figure 2.1: Location of the Hellyer deposit (after Gemmell and Large, 1992)

2.1.1 The Que-Hellyer volcanics

The Que-Hellyer volcanics are 18-20 km long belt of andesitic and basaltic lavas, volcaniclastics, minor intercalated sediments and debris-flow deposits up to 5km wide and 1km thick. According to Waters and Wallace (1992) and Corbett and Komyshan (1989) the Que-Hellyer Volcanics can be sub-divided into four units. At the base there is the lower tuff and lava sequence containing intercalated basaltic, andesitic and felsic lava, tuffaceous sandstones and interbedded tuff, conformably overlain by lower andesites and basalts. The mineralised horizon occurs in a conformable unit above the lower andesites and basalts called the mixed sequence and comprises volcaniclastic breccias, dacitic volcanics and polymict mass-flow units reaching up to 20m thick (Fig. 2.3). Above this sequence is the Hellyer basalt comprising pillowed to massive basalitic lavas, peperites, hyaloclastites and interbedded fine-grained sediments. The area was deformed during the Devonian Tabberabberan Orogeny producing mainly N-NW trending fold axes. This deformation event subsequently metamorphosed the rocks to prenhite-pumpellyite facies. (Mc Arthur and Dronseika, 1990; Waters and Wallace, 1992; Drown, 1990).

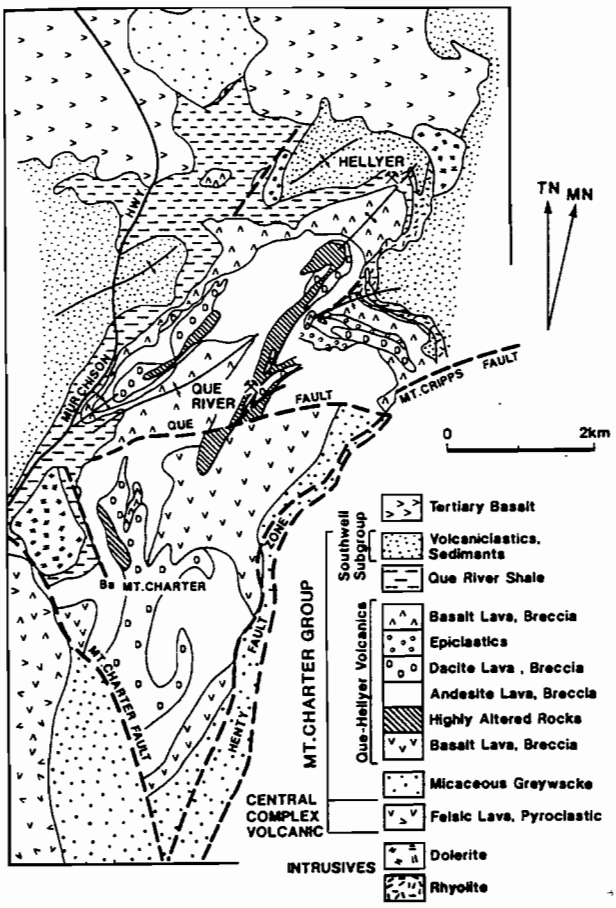

Figure 2.2: General geology around the Hellyer deposit, north-west Tasmania (after Drown, 1990)

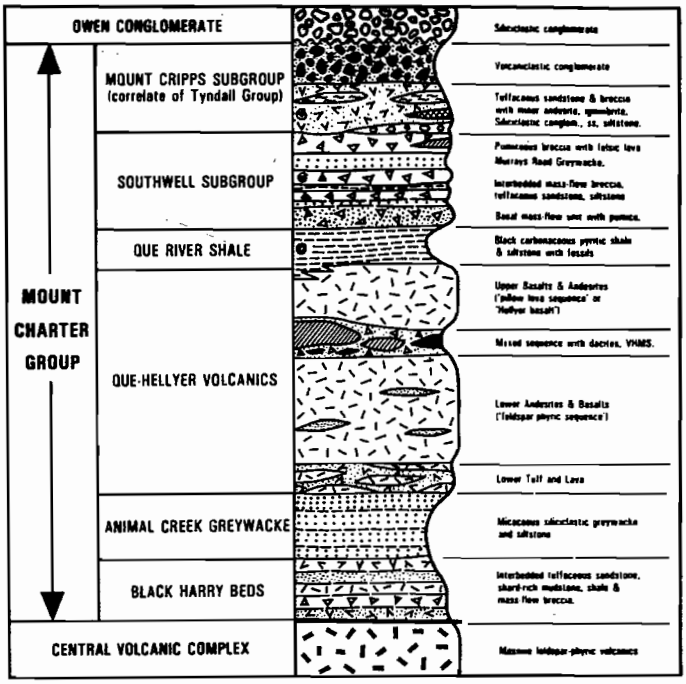

Figure 2.3: Stratigraphic column and terminology for the Mount Charter Group in the Hellyer-Que River area (after Corbett, 1992).

2.2 The Local Geological Setting

2.2.1 Stratigraphy

The footwall rocks beneath the deposit are approximately 500 metres thick and are comprise coherent fragmental mafic and felsic volcanics. These are mainly andesites, basalts, to a lesser extent dacites, volcaniclastics, auto breccias and epiclastic mass flow sediments labelled the Feldspar-Phyric Sequence (FPS). Thick epiclastic units can be found directly below the ore horizon suggesting that there was a basinal structure present before ore deposition (Drown, 1990). Directly beneath the ore horizon, these rock have been extensively altered so that none of the original volcanic textures remain (Gemmell and Large, 1992).

The ore deposit is semi-conformably overlain the Hangingwall Volcaniclastic Sequence (HVS) with varying thickness from 0 metres to up to 40 metres (McArthur and Dronseika, 1990). Over the central part of the ore deposit the basalts can be in direct contact and extensively are fractured (Waters and Wallace, 1992). Two main rock types are present, coarse-grained volcanic breccia containing polymict fragments and a finer grained, well laminated ash containing basaltic shards. The hangingwall units also have been altered by

fuchsite, carbonate and barite directly above the ore deposit. These units are covered by an 80-250 metre thick massive Pillow Lava Sequence (PLS). Above the PLS is a 100 metre thick Que River Shale. (Fig. 2.3) This is overlain by 500 metres of interbedded quartz-feldspar phyric pumiceous mass-flow breccias, massive shale and sill-like rhyolitic lava bodies that can reach up to 1km thick called the upper rhyolitic sequence (Gemmell and Large, 1992; Mc Arthur, 1996).

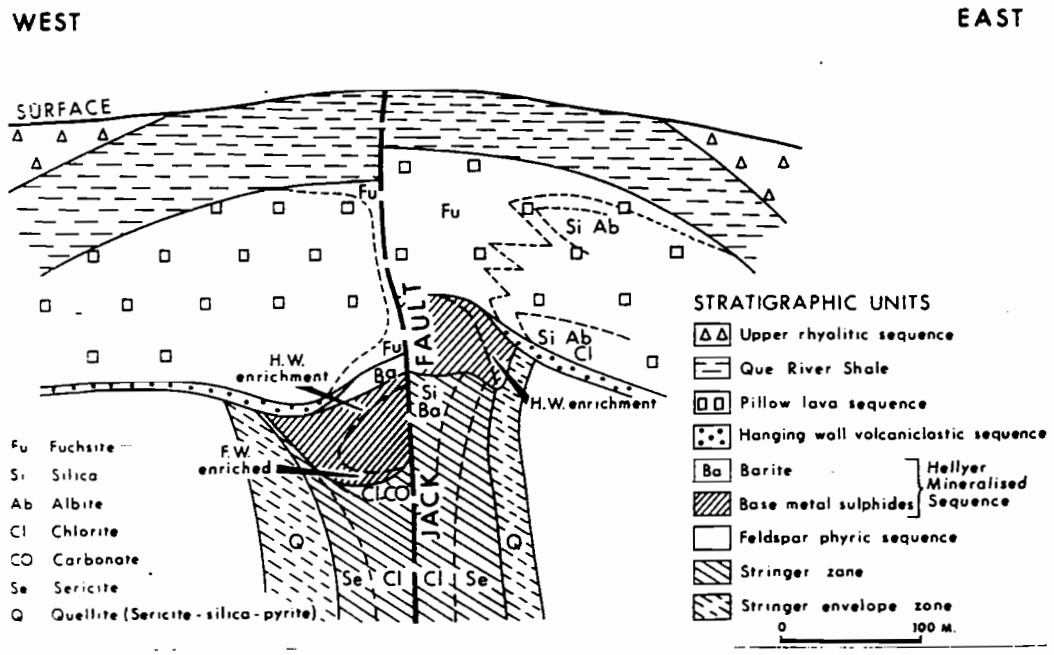

Figure 2.4: Local geology of the Hellyer ore deposit (after McArthur, 1989)

2.2.2 Structure

The middle Devonian Tabberabberan Orogeny involved compression in the east-west direction and produced predominantly N-S trending fold axes in the Mt. Read Volcanics (Fig. 2.4). The Hellyer ore-deposit is situated in the crest of an open, upright anticline plunging at 20-25°NNE. On microscopic scale there is a well developed cleavage in the alteration pipe and in the peripheral sulphides as the phyllosilicates behaved in a ductile manner under deformation (Drown, 1990). There is also a later Mesozoic sub-vertical wrench fault structure, the Jack

Fault, that truncated the ore-deposit in half and displaced the eastern half of the ore deposit 130 metres to the north and 30 metres up.

2.2.3 The Footwall Alteration Zone

Beneath the Hellyer ore deposit the footwall rocks have been extensively altered. The alteration zone is well preserved, extends in some areas up to 550m below the ore deposit and is spatially and mineralogically zoned (Fig. 2.5 a,b) (Gemmell and Large, 1992). Directly below the ore deposit there are no primary volcanic textures in the host rocks as they have been obliterated (McArthur, 1996).

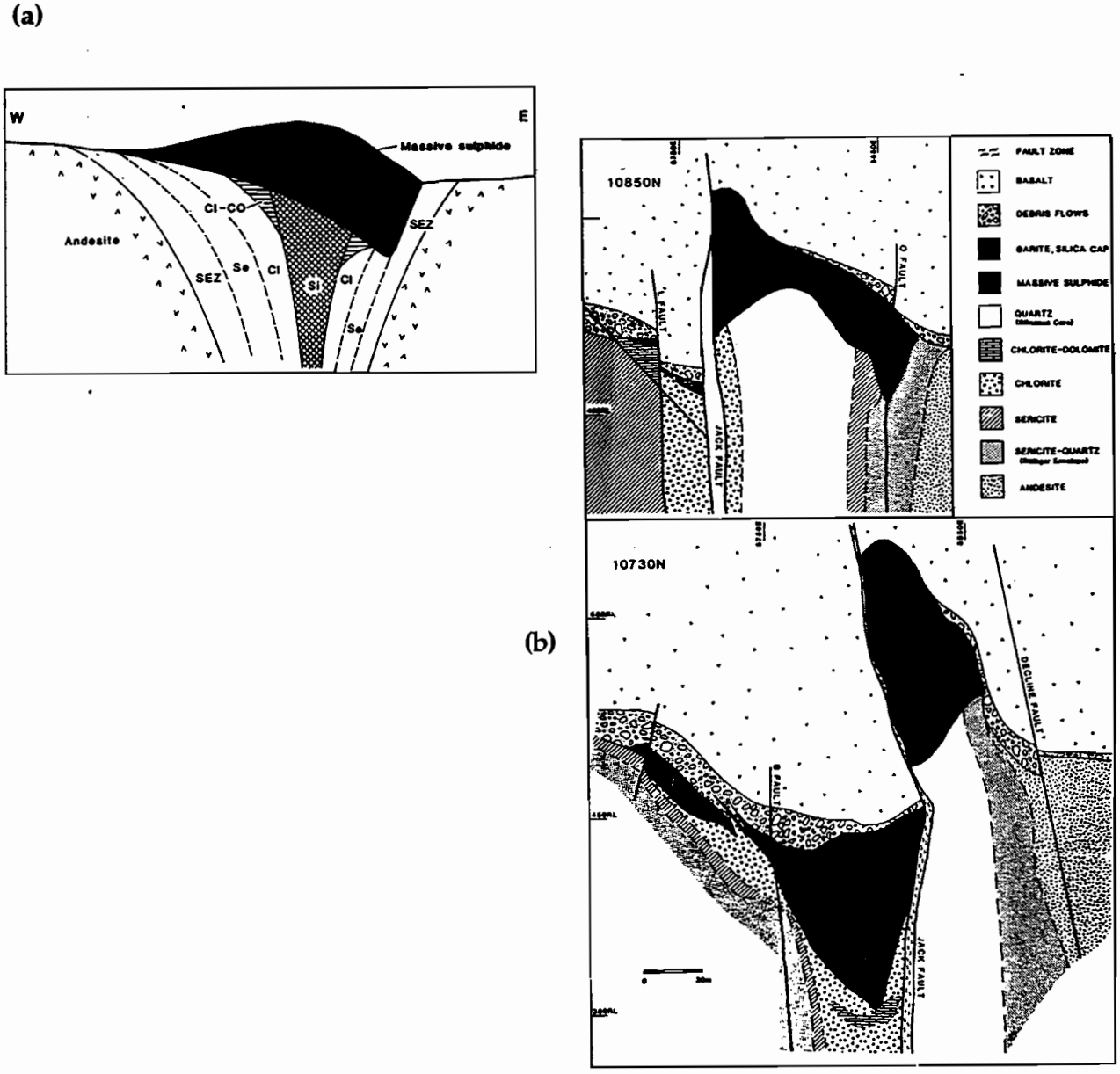

Figure 2.5: Pre-Jack Fault alteration zones (a) and two cross-sections showing alteration zones, mineralisation and geological setting of the Hellyer ore deposit, post-Jack Fault (b) (after Gemmell and large, 1992)

The central part of the alteration pipe consists of a siliceous core and represents the most intense hydrothermal alteration. This pipe has an approximate diameter of 140 metres and contains the syn-mineralisation veins responsible for carrying the economic sulphides. Moving laterally away from this core there is the chlorite zone which comprises massive, fine-grained chlorite and disseminated pyrite. McArthur (1989) noted that on the footwall-ore contact there is a chlorite carbonate zone containing spheroids, veins and veinlets of

dolomite and disseminated pyrite. They found that most of this type of alteration is concentrated in the northern end of the ore deposit, with only a minor amount in the southern end. The chlorite zone grades into the sericite zone that contains massive sericite, chlorite, disseminated pyrite and minor carbonate. On the edges of the alteration pipe is the sericite-quartz zone which is less intense than the inner core. Some of the original host rock textures still remain (Gemmell and Large, 1992).

2.2.4 Mineralisation and Dimensions

Hellyer ore-deposit is an irregular, elongate lozenge-shaped well preserved ore deposit that is 830 metres long, has a maximum east-west width of 200 metres and is 43 metres thick (McArthur, 1996). It had a pre-mining resource of 16.2 million tonnes at 0.38% Cu, 7.1% Pb, 13.9% Zn, 168ppm Ag, 2.5ppm Au, 2.2%Ba, 1.2%As and 24.8%Fe (McArthur, 1996). Mineralisation consists of 54% pyrite, 20% sphalerite, 8% galena, 2% arsenopyrite, 1% chalcopyrite, minor tetrahedrite and 15% chlorite, sericite and quartz gangue. Above the mineralisation is a barite cap which is overlain by a metal-rich siliceous layer (Gemmell and Large, 1992).

2.3 Genesis of the Ore Deposit

McArthur and Dronseika (1990) agree that the Hellyer ore deposit is a well preserved volcanogenic sea-floor vent deposit. McArthur (1996) suggests that during the Late Cambrian there were a group of volcanic rocks that lay below 3km of seawater. At this time there was a relatively tectonically active environment producing '...a series of north-south grabens and half-grabens'. These acted as a conduit for hydrothermal fluids to convect. Faults created from the initial east-west extension were then later reactivated and expanded seawater circulation. Waters and Wallace (1992) and McArthur (1996) argue that mineralisation accumulated within a depression on the Cambrian sea-floor

The intense north-south sub-vertical chlorite-sericite alteration zone was produced from waves of hot hydrothermal fluids passing upwards through the fractured rocks with an initially high water/ratio and high sea-water sulphate content. The convection cells progressively penetrated deeper in to the fracture system and sulphur from the basement rocks mixed with the fluids which had a low water/rock ratio. Siliceous alteration then overprinted the earlier pervasive chlorite-sericite alteration. These highly reduced fluids then precipitated metals from the host rocks and deposited them as a mound on the sea-floor. Barite then precipitated and capped the deposit then a later volcanic event erupted basalts onto the sea-floor covering the deposit (McArthur and Dronseika, 1990). These sulphides were precipitated from syn-mineralisation feeder veins that convected beneath the sea-floor and can be found mainly in the central siliceous alteration zone directly underlying the ore deposit (Gemmell and Large, 1992).

CHAPTER 3

SPATIAL DISTRIBUTION OF THE CHLORITE-CARBONATE ALTERATION ZONE

3.1 Introduction

McArthur (1989) initially determined that the chlorite-carbonate alteration zone was located on the footwall-ore contact and occurred as a lense-like planar feature associated with the upper part of the chlorite alteration zone. In this study, select portions from sixty diamond drill holes intersecting the chlorite-carbonate alteration were logged on cross-sections in the southern end of the ore-deposit 10260N, 10340N, 10430N, 10510N, 10520N and in the northern end of the ore-deposit 10910N, 10947.5N, 11010N, 11047.5N and 11090N (Figures 3.4 a, b, c, d and e). More detail was given to the alteration zone in the northern part of the ore deposit as the chlorite-carbonate alteration is more prevalent in this area. Compilation of drill-hole data from the north (east block) collected by previous Aberfoyle geologists indicates that the chlorite-carbonate alteration zone occurs as two horizons, one on the footwall-ore contact (contact zone) as patchy zones and another, along strike, approximately 35-45m below the ore horizon (lower zone). At the southern end of the ore deposit, the chlorite carbonate alteration is patchy and only occurs on the ore-footwall contact. Variations in alteration assemblages and carbonate textures down hole were logged, an example of a logging sheet as completed for this study can be found in Appendix 1.1. All holes and intervals logged are in Appendix 1.2.

3.2 Lateral Distribution

Most of the information concerning the lateral distribution of the chlorite-carbonate alteration zone has been previously collected by Aberfoyle geologists in the last 10 years and a distribution of all alteration zones is given by Gemmell and Large (1992). Figure 3.1(a) shows the distribution of the chlorite-carbonate alteration on a plan view as of 1990. Figure 3.2 shows the distribution of the chlorite-carbonate alteration in plan view which documents all occurrences from drill logs. In this study, cross-sections 10910N, 10947.5N, 11010N, 11047.5N and 11090N were examined to document the characteristics of the chlorite-carbonate alteration zone.

The chlorite-carbonate alteration zone is the most prominent between 10910N and 11090N on the eastern flank of the Hellyer deposit. It is located in the upper parts of the massive chlorite zone which is in the stringer zone of the footwall of the Hellyer deposit.

The chlorite-carbonate-alteration assemblages generally form around the northern and central (correlating to the siliceous core) feeder zones, outlined by Gemmell and Large (1992). This distribution is clearly displayed in Figure 3.1 (b).

Chlorite-carbonate alteration assemblages have also been documented on the western flank of the ore deposit contact at 10910N. The alteration is patchy along the ore-footwall contact and does not form well defined zones. In a north-south direction the chlorite-carbonate alteration zone occurs as discontinuous patches on the ore contact but becomes more continuous along the strike between 10947.5N and 11047.5N. The lower zone is a continuous lens from 10950N to 11050N.

(a)

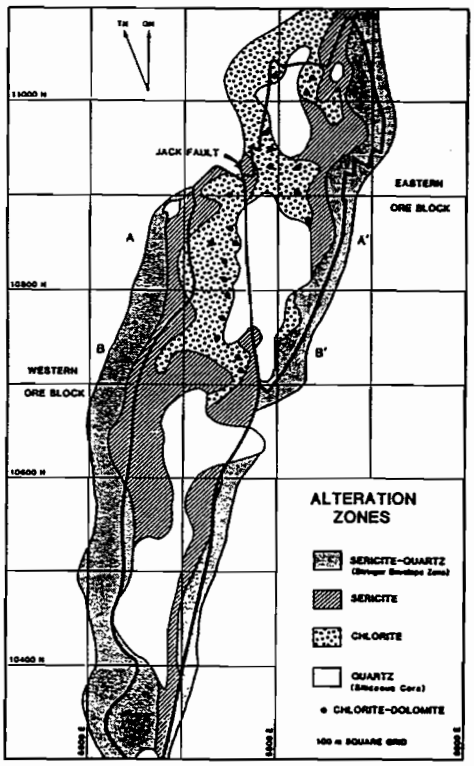

(b)

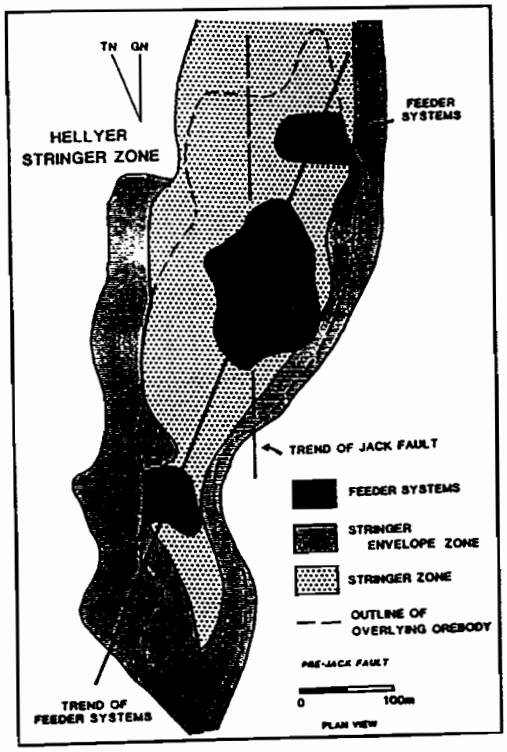

Figure 3.1 (a) Distribution (as known in 1990) of chlorite-carbonate alteration in the northern part of the ore deposit and (b) the southern, central and northern feeder zones (from Gemmell and Large, 1992)

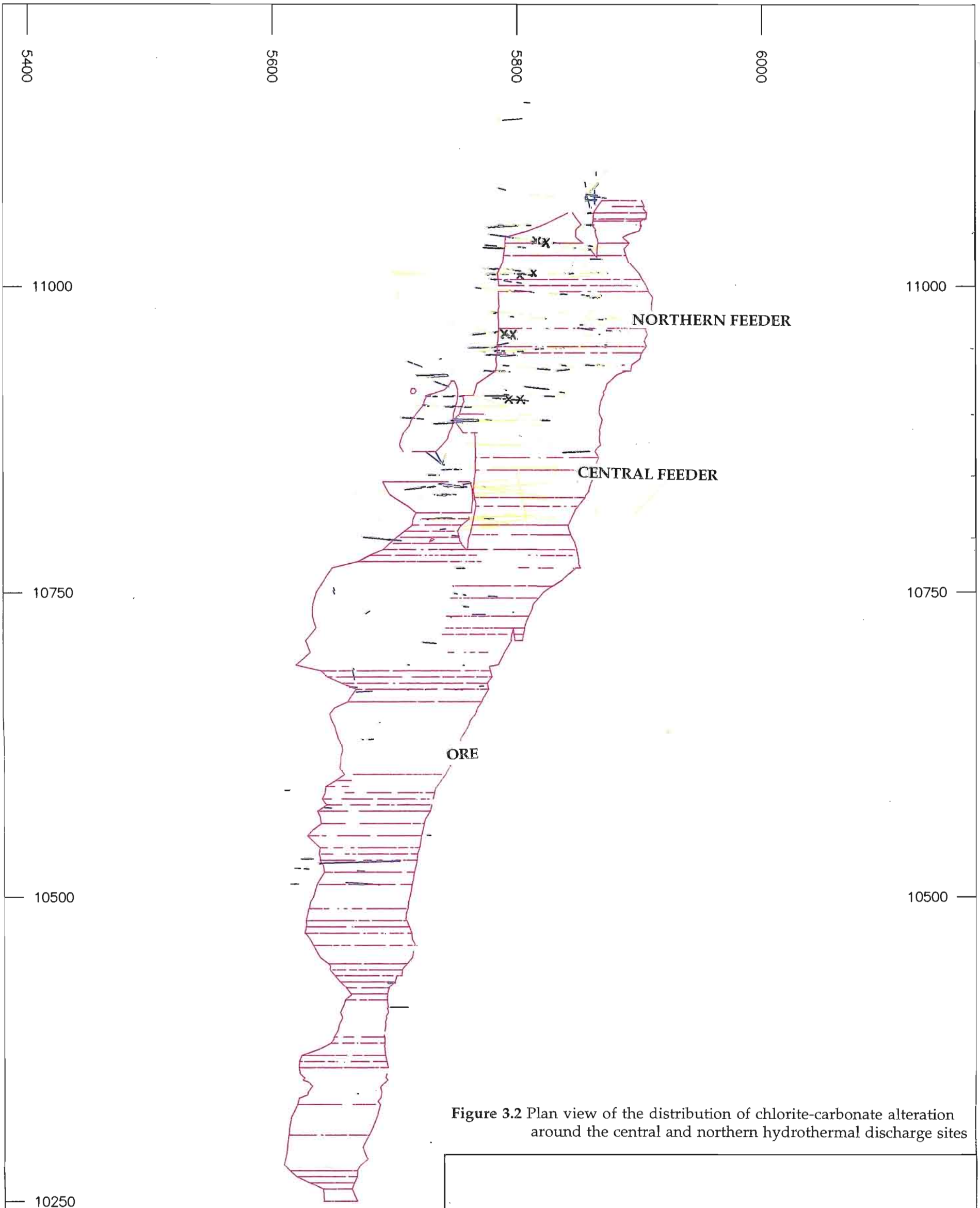

Figure 3.2 Plan view of the distribution of chlorite-carbonate alteration around the central and northern hydrothermal discharge sites

Figure 3.2

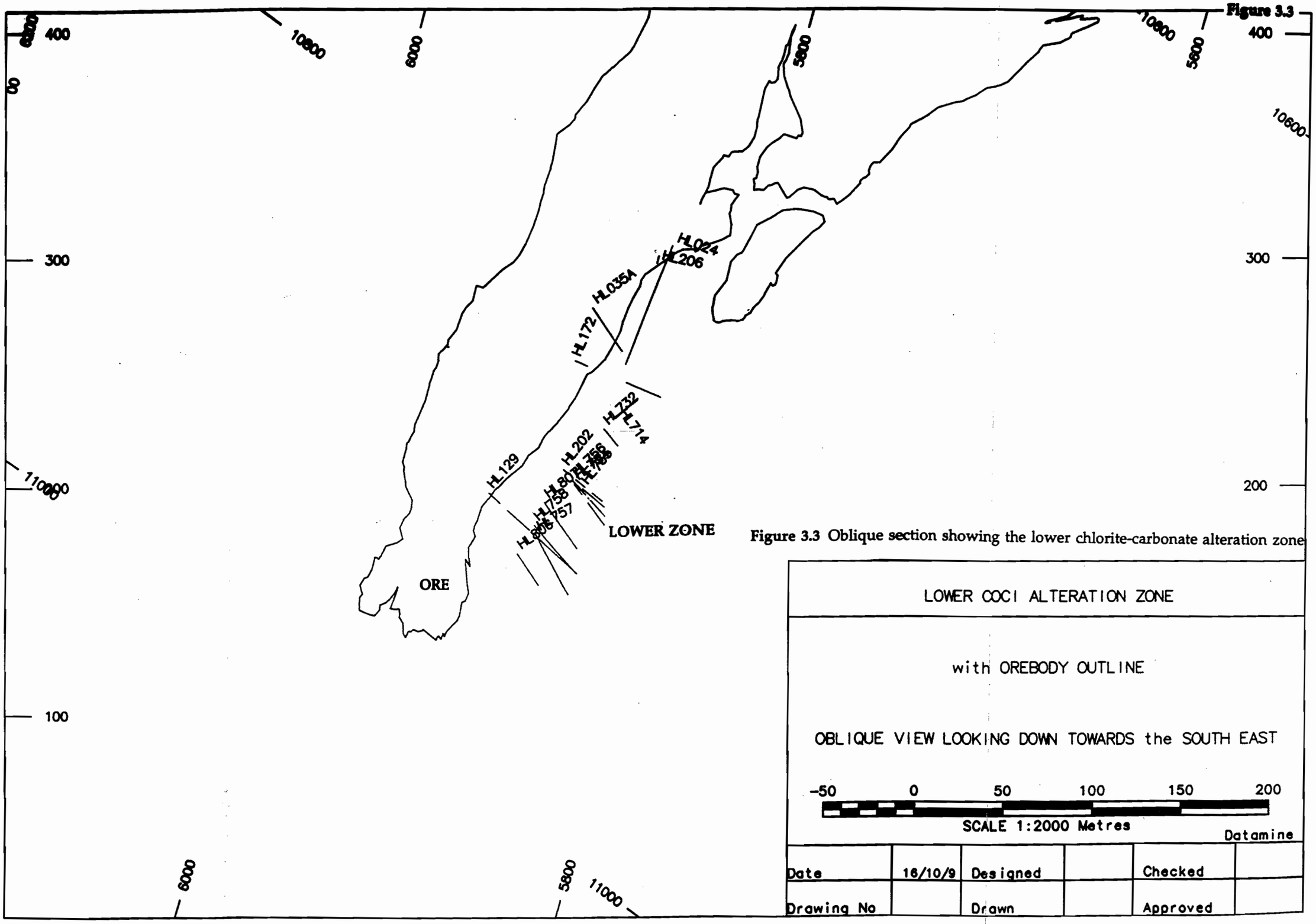

Figure 3.3 Oblique section showing the lower chlorite-carbonate alteration zone

3.3 Vertical Distribution

The chlorite-carbonate contact zone extends for approximately 10-15 metres in small patches, below the ore horizon. Carbonate alteration occurring around the chlorite-carbonate zone on the contact is associated with other alteration minerals; quartz, sericite, pyrite and chlorite.

The chlorite-carbonate lower zone is located approximately 30-50 metres below the ore horizon as illustrated in an oblique section in Figure 3.3. This zone is separated from the contact alteration zone based solely on drill-core data. Underground mapping could not be undertaken to delineate between the two zones. The lower zone is a continuous, well defined lense-like feature and is situated under the thickest part of the ore deposit. This zone is also located close to the Jack Fault occurs only on the west side of the east flank of the ore deposit (refer to Fig. 3.2).

On cross-section 10910N (Fig. 3.4a), the chlorite-carbonate alteration zone is located approximately 10-15 metres below the ore deposit on the western and eastern flanks. The lower chlorite-carbonate alteration zone is located directly below the thickest part of the ore deposit. Carbonate and chlorite alteration assemblages are common in this lower zone.
Cross-section 10947.5N also shows the lower alteration zone and it is located near the Jack fault, approximately 30 metres below the thickest part of the ore deposit (Fig. 3.4b). The thin discontinuous contact zone consists of predominantly quartz, carbonate, sericite and chlorite alteration assemblages. The lower chlorite-carbonate alteration zone are also associated with the Jack Fault on sections 11010N and 11047.5N and the contact zone is patchy and discontinuous (Fig 3.4 c, d). On the most northern cross-section, 11090N, there is no lower alteration zone below the ore, however there is patchy chlorite-carbonate alteration on the contact of the ore deposit (Fig 3.4e).

3.4 Contacts with the massive sulphide deposit.

The chlorite-carbonate alteration zone is intimately associated with the massive sulphide ore deposit as it is situated on the ore-footwall contact and will be referred to as the 'contact zone'. This contact, in most cases, is brecciated or gradational and often carbonate veinlets extend into the ore deposit. Massive sericite, or sericite-quartz-pyrite-carbonate alteration alteration assemblages in 1-2 metre zones can separate the chlorite-carbonate from the ore deposit when it is close to the contact (Fig. 3.5 a, b). However, the chlorite-carbonate zone can be up

Figure 3.4 a)

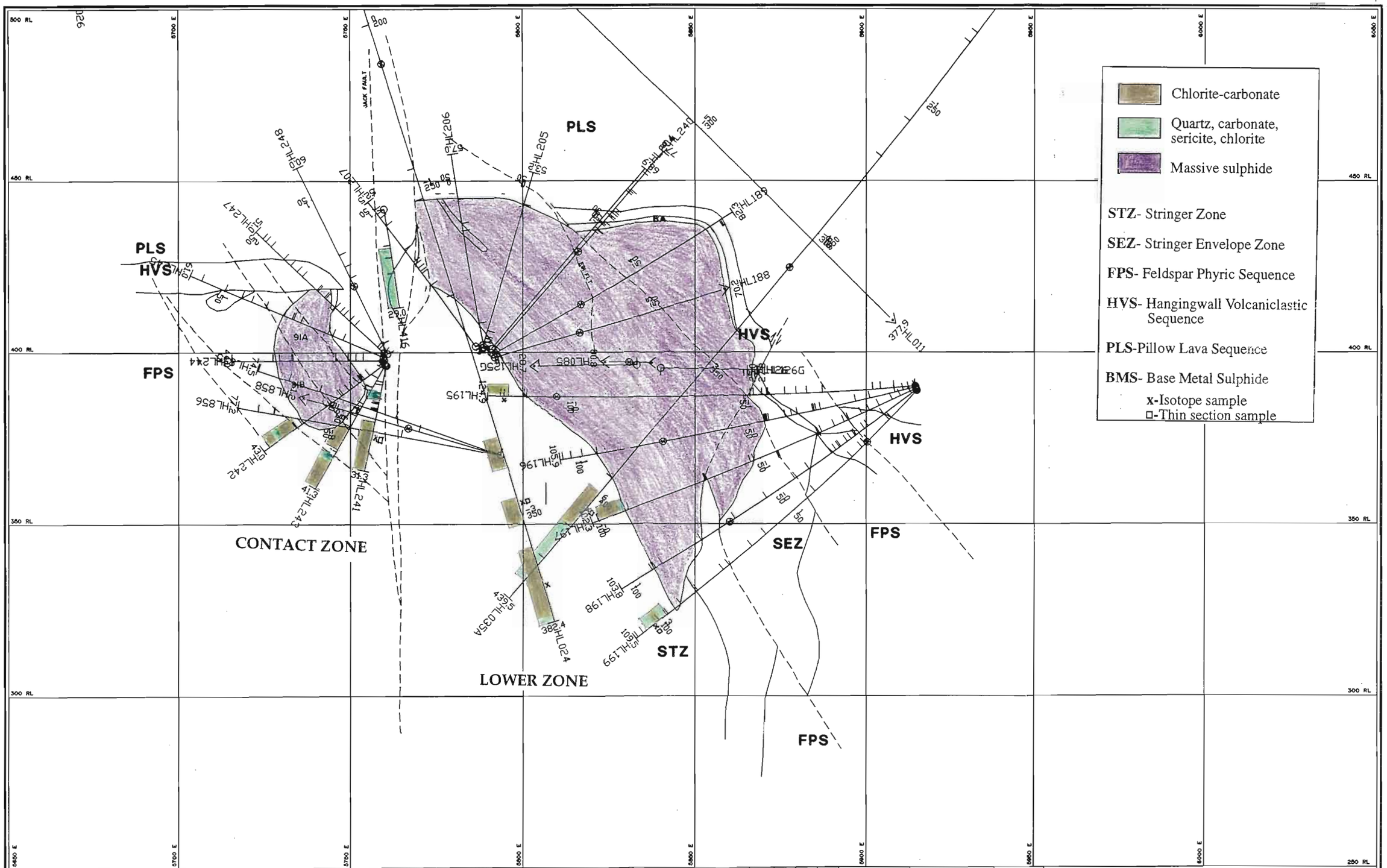

Figure 3.4 a) Cross-section through Hellyer at 10910N. Illustrating the distribution of the chlorite -carbonate alteration assemblages and carbonate alteration associated with chlorite, quartz and sericite alteration minerals. The location of the contact and lower carbonate bearing alteration zones are highlighted

ALTERATION	REV	DATE	REVISION	DRAWN	CKD	APP	APP
Albite	A	22/8/96	REVISED INTERPRETATION	DLL			
Chlorite							
Carbonate							
Epidote							
Feldspar							
Fuchsite							
Hematite							
Mica							
Pyrite							
Sericite							
Silica							
Tremolite							

NORTH

SCALE	1:2000	
DRAWN	SFM	17/09/96
CHECKED	AHM	17/09/96
DESIGNED	CSD/RDH	
DESIGN CKD		
DESIGN APP		
PROJECT APP		

Aberfoyle Resources Limited
HELLYER DIVISION
A.C.N. 004 664 108

GEOLOGY SECTION
10910.0 N
SECTION LIMITS 10900.0 10920.0

DRAWING No. GS-910-01
REVISION

E:\DRAFTED\HELLYER\GEOLOGY\SECTIONS\10910

Figure 3.4 b)

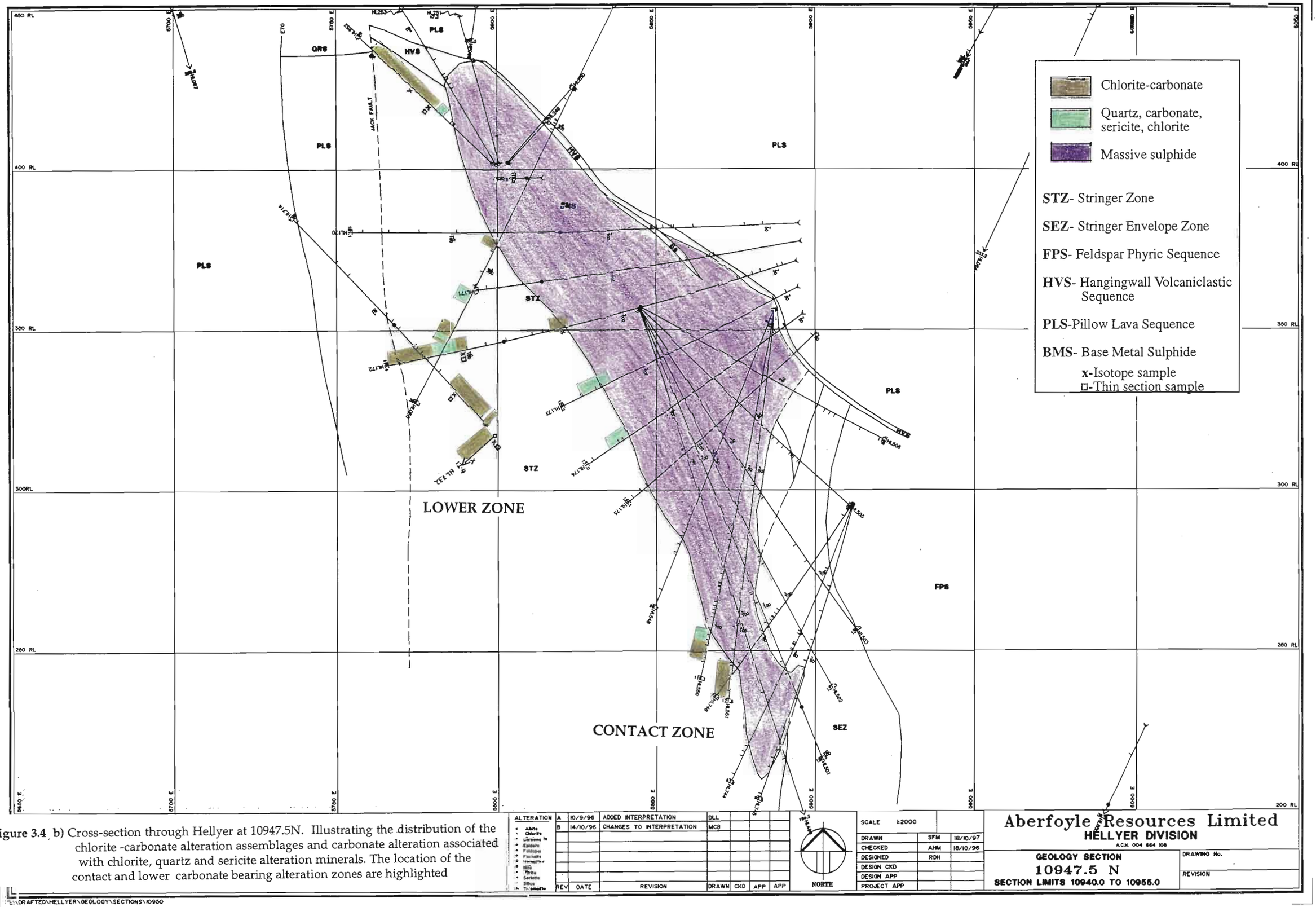

Figure 3.4 b) Cross-section through Hellyer at 10947.5N. Illustrating the distribution of the chlorite -carbonate alteration assemblages and carbonate alteration associated with chlorite, quartz and sericite alteration minerals. The location of the contact and lower carbonate bearing alteration zones are highlighted

Figure 3.4 c)

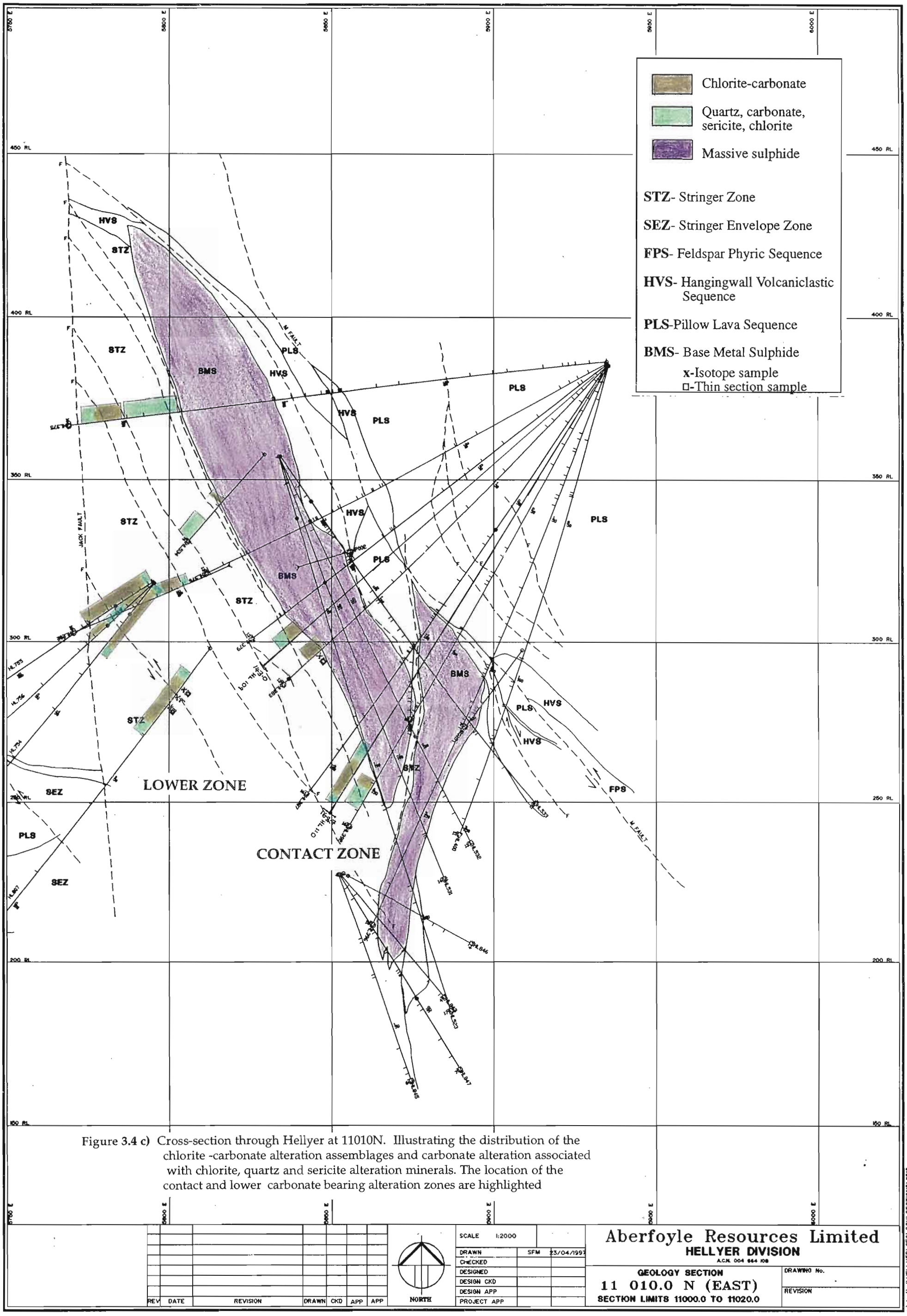

Figure **3.4 c)** Cross-section through Hellyer at 11010N. Illustrating the distribution of the chlorite -carbonate alteration assemblages and carbonate alteration associated with chlorite, quartz and sericite alteration minerals. The location of the contact and lower carbonate bearing alteration zones are highlighted

REV	DATE	REVISION	DRAWN	CKD	APP	APP

NORTH

SCALE	1:2000	
DRAWN	SFM	23/04/1997
CHECKED		
DESIGNED		
DESIGN CKD		
DESIGN APP		
PROJECT APP		

Aberfoyle Resources Limited
HELLYER DIVISION
A.C.N. 004 644 108

GEOLOGY SECTION
11 010.0 N (EAST)
SECTION LIMITS 11000.0 TO 11020.0

DRAWING No.

REVISION

e:\drafted\HELLYER\GEOLOGY\SECTIONS\1000

Figure 3.4 d)

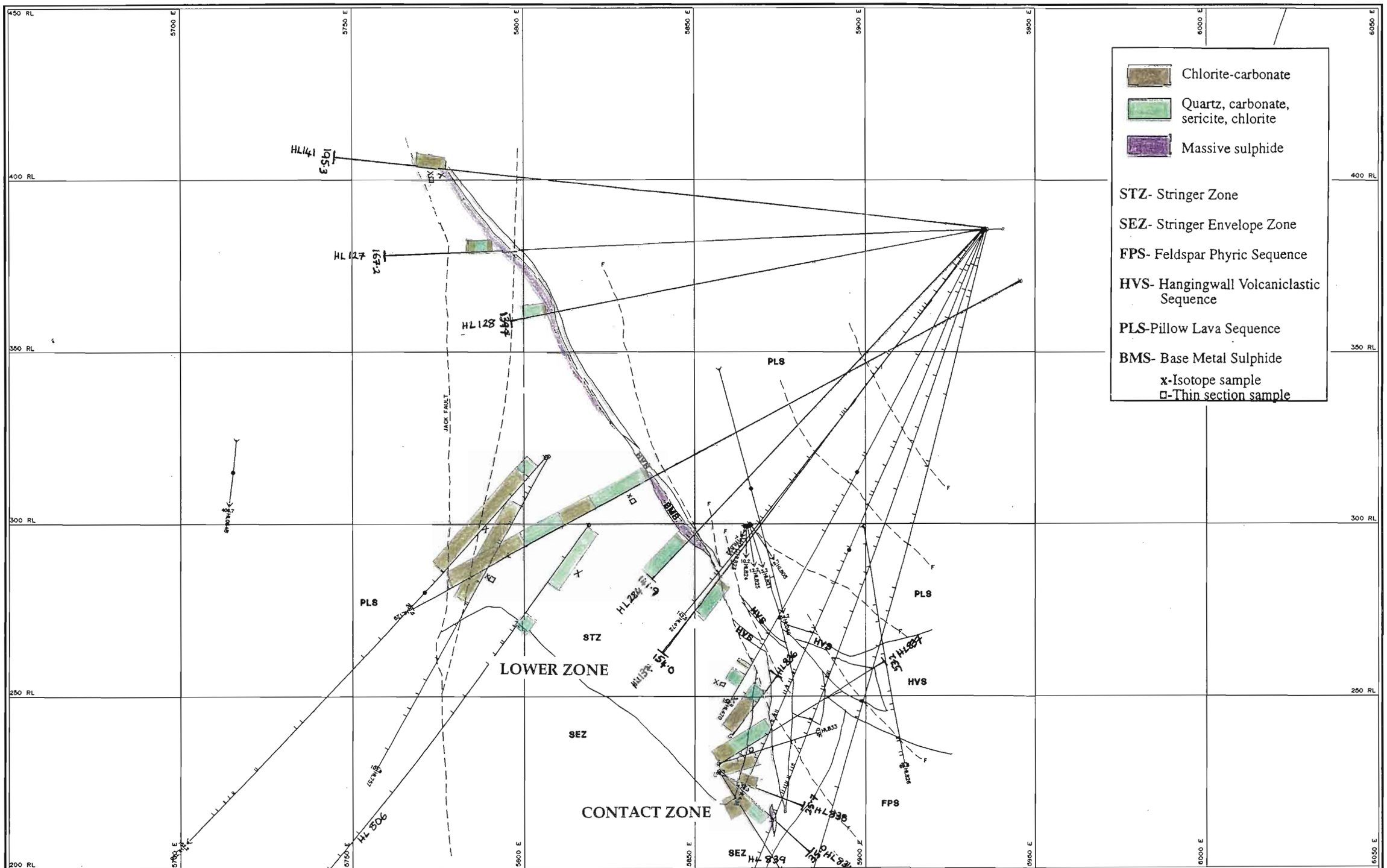

Figure 3.4 d) Cross-section through Hellyer at 11047.5N. Illustrating the distribution of the chlorite -carbonate alteration assemblages and carbonate alteration associated with chlorite, quartz and sericite alteration minerals. The location of the contact and lower carbonate bearing alteration zones are highlighted

E:\DRAFTED\HELLYER\GEOLOGY\SECTIONS\8050

Figure 3.4 e)

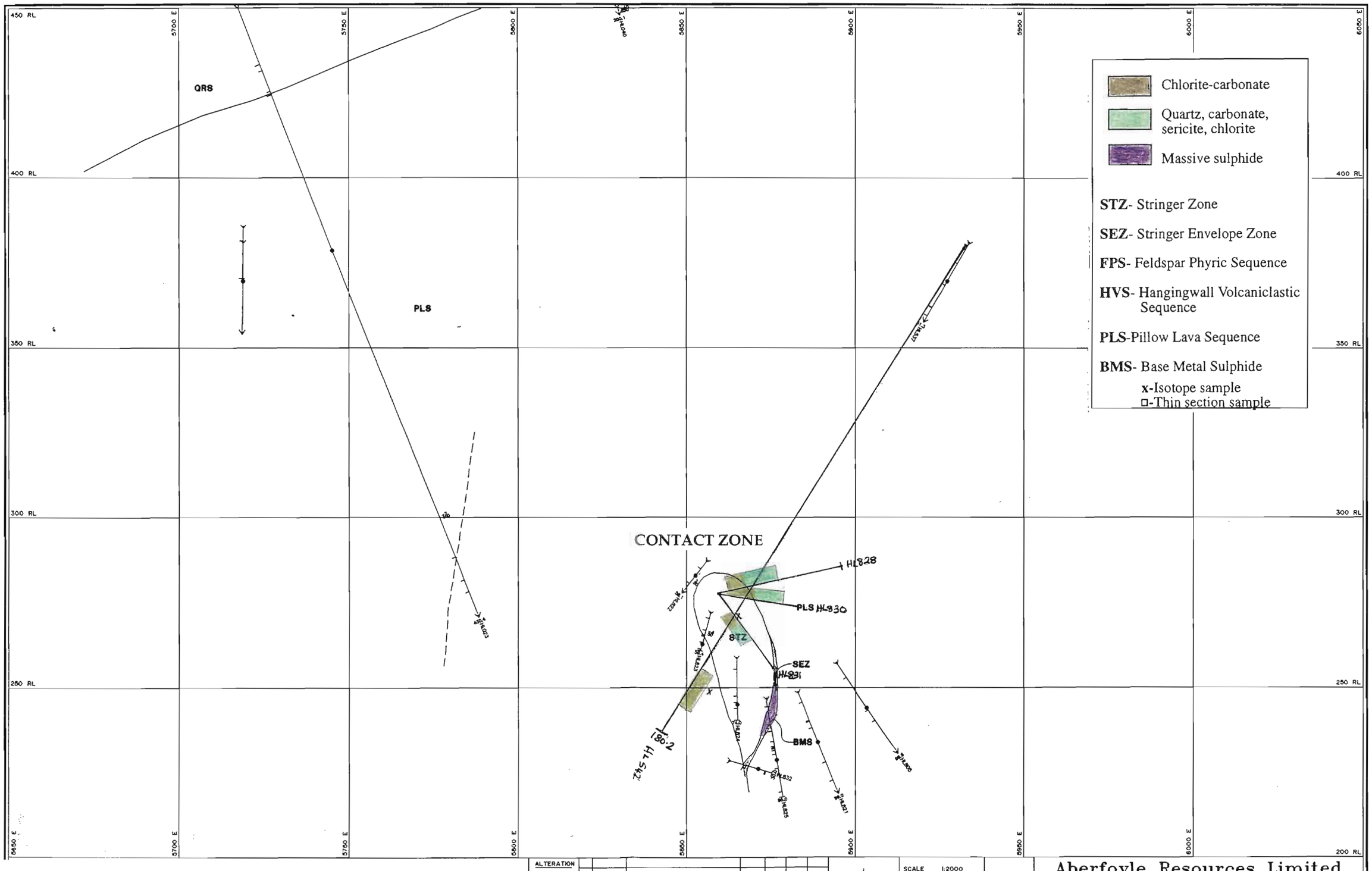

Figure 3.4 e) Cross-section through Hellyer at 11090N. Illustrating the distribution of the chlorite -carbonate alteration assemblages and carbonate alteration associated with chlorite, quartz and sericite alteration minerals. The location of the contact and lower carbonate bearing alteration zones are highlighted

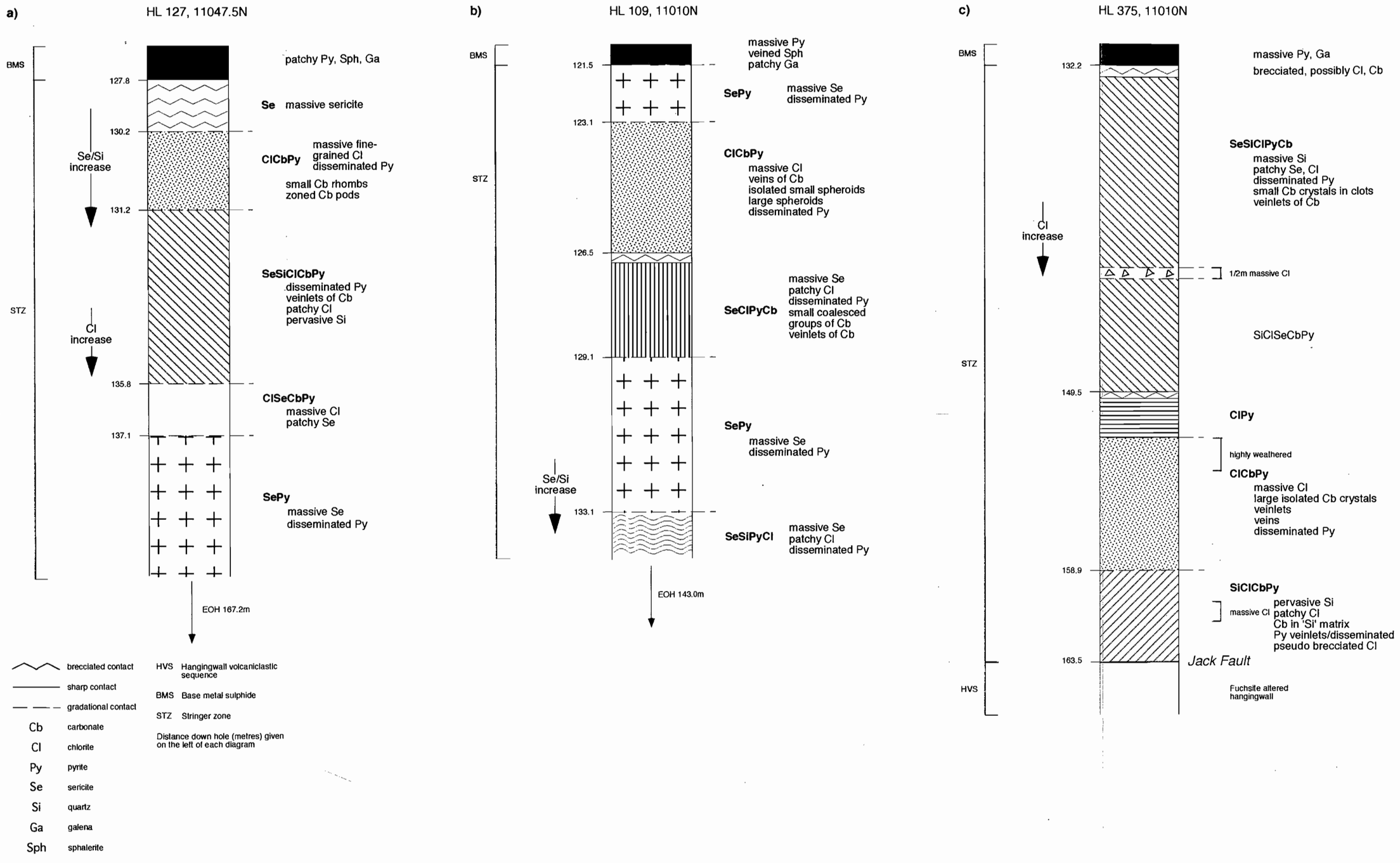

Figure 3.5 Stratigraphy of HL 127 a), HL 109 b), and HL 375 c) showing the styles of contact between the chlorite-carbonate alteration and the massive sulphide

to 15 metres below the ore contact (Fig. 3.5 c). The surrounding alteration zones consist of sericite, quartz, pyrite and carbonate in different proportions. The sericite and quartz alteration assemblages usually overprint the chlorite-carbonate alteration zone.

3.5 Summary

The chlorite-carbonate alteration zone appears on the contact of the Hellyer ore deposit as a patchy, discontinuous horizon. It is not vertically extensive and has an average thickness of 10 metres. The contact chlorite-carbonate alteration zone is overprinted more significantly by quartz and sericite alteration.

Chlorite-carbonate alteration also occurs in a thicker zone approximately 35-45 metres below the contact zone. It is continuous from 10910N to 11010N and below the thickest part of the ore deposit and is only found on the west side of the east flank of the ore deposit. It lies adjacent to the Jack Fault and can be up to 30 metres thick. In plan view, the contact chlorite-carbonate alteration zone is widespread and underneath the ore deposit and the lower alteration zone is only on the western side of the eastern flank.

More detailed investigations into the carbonate and chlorite will be outlined in Chapter Four, Mineralogy, Textures and Paragenesis.

CHAPTER 4

MINERALOGY, TEXTURES AND PARAGENESIS

4.1 Introduction

The major minerals in the chlorite and carbonate alteration zone are massive chlorite and a texturally diverse iron-rich dolomite which have previously been documented as dolomitic spheroids in a fine-grained chlorite matrix (Plate 4.1) (Gemmell and Large, 1992). Carbonate alteration, however, is a more widespread feature in the footwall alteration zone than previously described and is also associated with other alteration minerals such as sericite, quartz and disseminated pyrite. Carbonate occurs as veinlets, pods, coalesced and isolated spheroids and rhombs. A well documented cross-cutting Devonian calcite vein system is also a feature of this alteration zone (Gemmell and Large, 1992). This chapter outlines the textural characteristics of carbonate in and around the chlorite-carbonate alteration zone and its paragenesis. Cathodiluminiscence techniques (CL) were used to investigate carbonate minerals and textures and staining techniques helped determine the type of carbonate.

4.1.1 Methods

Thirty polished thin-sections were produced from rock samples showing distinct carbonate textures, locations of these samples and their textures are outlined in Appendix 2.1 and in Figures 3.4 a, b, c, d, and e. An example of a petrological interpretation sheet can be found in Appendix 2.2.

Rock samples were stained using a technique outlined by Evamy (1962). This uses a mixture of hydrochloric acid, alizarian red S and potassium ferricyanide to distinguish between different types of carbonate and is outlined in Table 4.1.

Cathodoluminescence studies allow a documentation of carbonate paragenesis, however studies on carbonate alteration associated with VHMS deposits using cathodilumunescence has been relatively uncommon (Smith et al., 1992). Cathodoluminesence is the light emitted from a crystal when it is bombarded by electrons (Nickel, 1978; Pierson, 1981 *in* Hill and Orth, 1994). The crystal lattice absorbs energy from the beam and can activate or hinder luminescence.

In carbonates, Mn^{2+} ions can activate luminescence and Fe^{2+} ions can repress luminescence at concentrations of >10,000ppm (Sommer, 1972; Nickel, 1978; Pierson, 1981 *in* Hill and Orth, 1994). The colour seen is dependant on the ratio of luminescent and non-luminescent ions in the crystal. A bright yellow or orange colour indicates that carbonate is Mn^{2+}- rich and a dull orange or red colour indicates that the carbonates are Fe^{2+}- rich.

Polished thin sections were analysed through a binocular microscope on a Nudide ELM-2B Luminoscope at the University of Tasmania. A focussed beam is produced by a cold cathode electron gun with a constant current of 0.6 mA at 6-8kV.

To investigate the textural distribution of the carbonate, select portions of sixty diamond drill holes were logged and particular attention was given to types of carbonate textures, their association with each other and other alteration minerals.

STAINING REAGENTS

Staining reagents	*Calcite*			*Dolomite*		
Compositions are given in weights percent. Critical solution strengths are underlined.	Fe^{2+} free	Fe^{2+} poor	Fe^{2+} rich	Fe^{2+} free	$\frac{Fe^{2+}}{Mg^{2+}} < 1$	$\frac{Fe^{2+}}{Mg^{2+}} > 1$
	calcite *sensu stricto*	ferroan calcite		dolomite *sensu stricto*	ferroan dolomite	ankerite
0.2% hydrochloric acid 0.2% alizarin red S	red	red	red	not stained	not stained	not stained
0.2% hydrochloric acid potassium 0.5–1.0% ferricyanide	not stained	light blue	dark blue	not stained	light blue	dark blue
0.2% hydrochloric acid 0.2% alizarin red S potassium 0.5–1.0% ferricyanide	red	mauve	purple	not stained	light blue	dark blue

Table 4.1 Various staining techniques outlining the different colours obtained from different compositions of calcite and dolomite (after Evamy, 1962)

4.2 Mineralogy

In hand specimen, the dolomite occurs as distinctive cream to white 5-10mm spheroids, 1-2mm spheroids and rhombs, 1-2mm veinlets and massive clots. The results from the staining test indicated that the carbonate was either dolomite or iron- dolomite, as the samples stained light blue or colourless (Table 4.1). In thin section chlorite, sericite, pyrite and minor quartz are also associated with the carbonate. Plate 4.1 is an example of the chlorite-carbonate alteration underground, showing the large dolomite spheroids in a massive chlorite and pyrite matrix.

In hand specimen, chlorite is black, fine-grained, in most cases massive, however it can have a patchy 'pseudo-brecciated' texture when overprinted with massive quartz and sericite (Plate 4.2). In thin section, chlorite is fine-grained and is generally massive and foliated. In some instances remnant volcaniclastic and andesitic fragmental textures can be recognised within the chlorite as light and dark zones that show clast-shapes.

In hand specimen, sericite is lighter grey, massive and is usually associated with chlorite and quartz. It can also occur as a very fine-grained overprinting feature usually associated with fine-grained quartz (Plate 4.2). In thin section, it is fine grained and is white/speckled under crossed-nicols.

In hand specimen, quartz can appear as a pervasive siliceous overprint, or as quartz crystals within remnant volcaniclastic clasts. In thin section, quartz is colourless in plain light, and grey under crossed-nicols.

Disseminated and coalesced euhedral pyrite grains are also common and can be associated with the chlorite or in some instances it is present in the carbonate. Pyrite is fine-grained and disseminated or can occur as 5mm-4cm veins.

4.3 Carbonate Textures

The chlorite-carbonate (dolomite) alteration zone is texturally distinct from the other alteration zones. Based on core logging and thin section observations carbonate textures consist of veinlets, massive carbonate (defined as a mosaic of 100-250μm anhedral crystals) small rhombs and small and large spheroids. The rhombs and small and large spheroids are only associated with massive chlorite in hand specimen. A summary of the carbonate textures is in Table 4.2.

Plate 4.1: Underground development exposure of the chlorite-carbonate alteration, (Photo courtesy of B. Gemmell)

Plate 4.2: Core specimen of pseudo-brecciated patchy chlorite (Cl)-dolomite (Do) alteration with a quartz (Qtz)-sericite (Se) overprint (Sample 1, HL 807; scale bar in cms).

Plate 4.3: Core specimen of isolated, zoned, large dolomite spheroids (Do) in a fine-grained chlorite (Cl) matrix (Sample 5, HL 755; scale bar in cms).

Plate 4.4: Core specimen showing large spheroids (Do) interlocking to form a vein structure composed in a matrix of fine-grained chlorite (Cl) (Sample 4, HL 756; scale bar in cms).

Plate 4.5: Photomicrograph of part of an isolated, dolomite spheroid with euhedral boundaries and light and dark banded overgrowths. (Sample 5, HL 755; scale bar=250μm; plain light; scale bar=500μm)

Plate 4.6: Photomicrograph of an isolated large spheroid, taken under cathodiluminescence highlighting radial overgrowths. The bright orange bands are indicative of a Mn-rich carbonate and the dull orange, a Fe-rich carbonate (Sample 5, HL 755; scale bar=1mm)

Plate 4.7: Void in the centre of a large carbonate spheroid. Finer-grained dolomite (1) occupying most of the photomicrograph, the cleaner dog-tooth carbonate (2) towards the centre and the twinned carbonate in the centre (3) (Sample 5, HL 755; scale bar=500μm; plain light).

Plate 4.8: Photomicrograph taken under cathodiluminescence illustrating three generations of carbonate 1) the dull dolomite on the periphery 2) the reddish dolomite towards the centre and 3) the bright yellow calcite in the centre twinned and dog-toothed carbonate (Sample 5, HL 755; scale bar=500μm).


4.1


4.2
Do
Se
Cl
Qtz
HL 807 | 9.40m


4.3
Cl
Do
HL 755 15.50m


4.4
Cl
Do
HL 828 8.80m

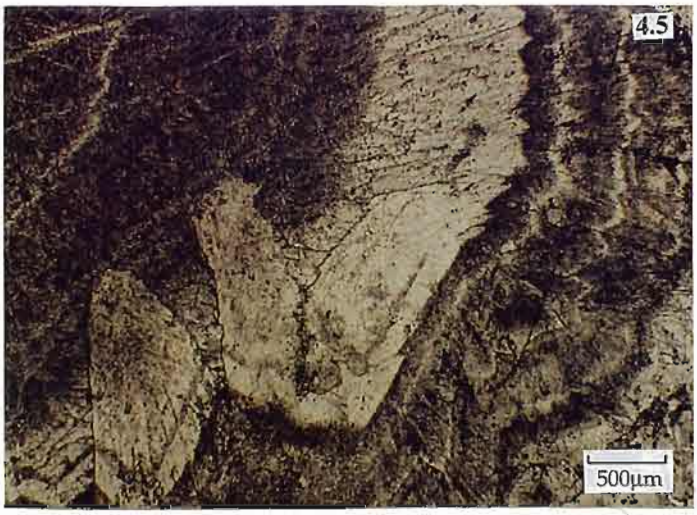
4.5
500µm

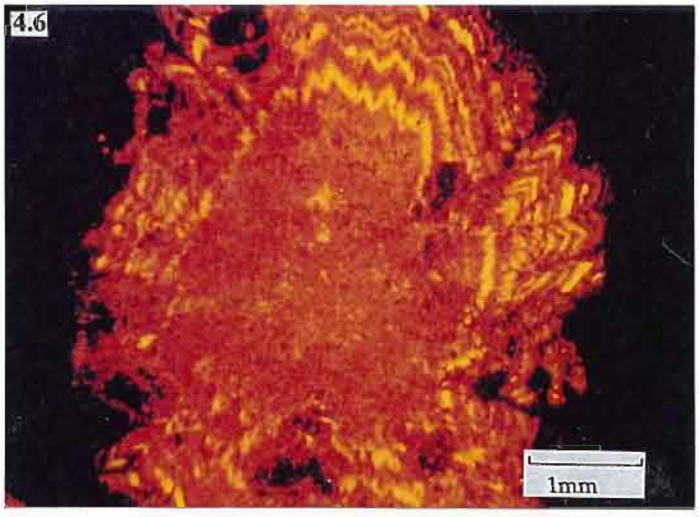
4.6
1mm

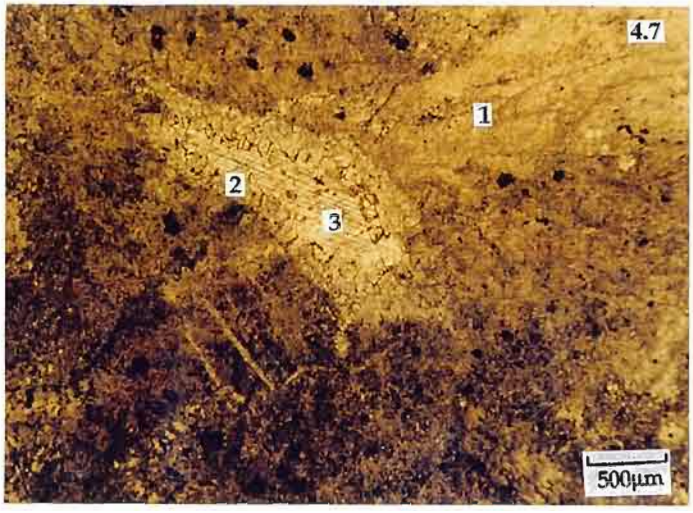
4.7
1
2
3
500µm

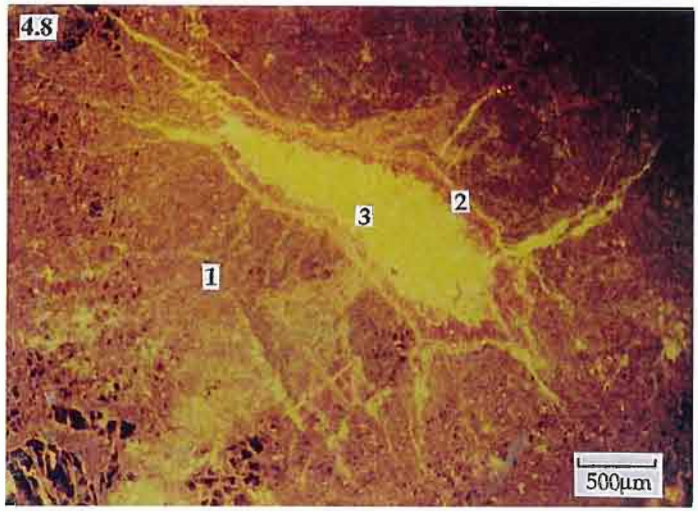
4.8
3
2
1
500µm

4.3.1 Large Spheroids

In hand specimen, spheroids are cream coloured, approximately 5-15mm in diameter and occur in a fine-grained chloritic matrix (Plate 4.3). The spheroids are commonly isolated but can coalesce to form vein-like structures (Plate 4.4). They can also in a matrix of other alteration minerals sericite, quartz and pyrite.

In thin section, the 5-15mm dolomitic spheroids are euhedral, have a finer-grained core which is surrounded by successive overgrowths of light and dark coloured banded dolomite (Plate 4.5). These radial overgrowths (0.1-0.5mm width) are zoned, radiate from the centre of the crystal and exhibit sector and undulose extinction. They are enhanced by cathodiluminescence (Plate 4.6).

The cores of the spheroids are fine-grained. Sometimes the centres of the spheroids have been dissolved out, leaving voids. In Plate 4.7 there are three different generations of carbonate growing into the void, followed by a later stage calcite precipitation. These are enhanced by the cathodoluminesence (Plate 4.8). This shows the dull orange dolomite on the periphery grading into a light red carbonate towards the centre. There is also bright yellow dog-tooth calcite growing into the centre, which also contains calcite. The CL data indicates that the different generations of carbonate precipitates contained variable proportions of mangansese and iron. The brighter Devonian calcite in the centre of the spheroid is Mn^{2+} - rich. The fluids that precipitated the dolomite overgrowths have lower Mn-concentrations.

Coarse-grained sericite can grow on the rim of the spheroids (Plate 4.9). The dolomite spheroids contain chlorite inclusions and they envelope the chlorite matrix (Plate 4.10). Disseminated euhedral pyrite is also a common feature in the chloritic matrix and in the spheroids.

Plate 4.9: Photomicrograph of sericite (Se) rimming the large spheroids (Do) in a chlorite (Cl) matrix (Sample 5, HL 755; scale bar=250μm; under crossed polars).

Plate 4.10: Photomicrograph of chlorite inclusions (Cl) within a large spheroid. The carbonate spheroid (Do) is enveloping the chlorite matrix (Sample 5, HL 755; under crossed polars; scale bar=100μm55)

Plate 4.11: Core specimen of small spheroids (Ss) and rhombs (Rm) in a matrix of fine-grained chlorite (Cl) (Sample 8, HL 202; scale bar in cms).

Plate 4.12: Core specimen showing the small spheroids (Ss) forming in distinct zones within the chlorite (Cl) matrix (Sample 2, HL 137; scale bar in cms)

Plate 4.13: Core specimen showing coalesced small spheroids (Ss) preferentially forming in the chlorite (Cl) matrix not in the sericite (Se) - quartz (Qtz) matrix (Sample 5, HL 202; scale bar in cms)

Plate 4.14: Photomicrograph of anhedral spheroids (Do) in a chlorite (Cl)-pyrite (Py) matrix. Some crystals show radial crystal growth (Sample 8, HL 202; scale bar=500μm; plain light)

Plate 4.15: Photomicrograph of the spheroids (Do) nucleating off quartz grains (Qtz). Pyrite (Py) is also associated with the centre of the spheroids. (Sample 8C, HL 202; scale bar=100μm; plain light)

Plate 4.16: Core specimen of carbonate rhombs coalescing and forming a pod (Sample 5, HL 757; scale in cms).

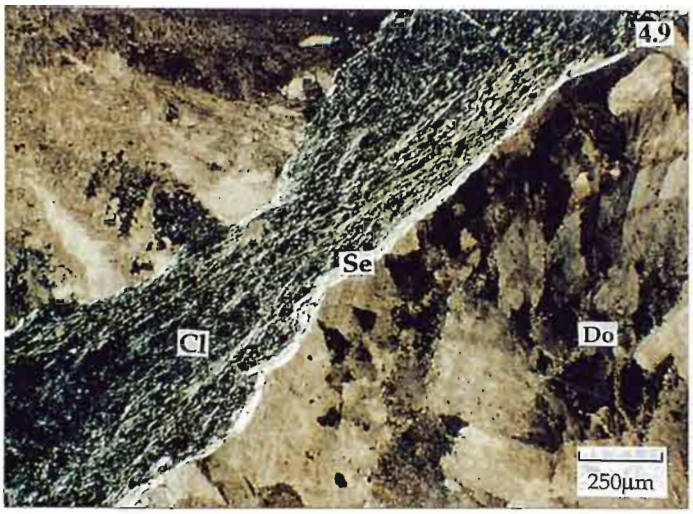
4.9
Se
Cl
Do
250µm

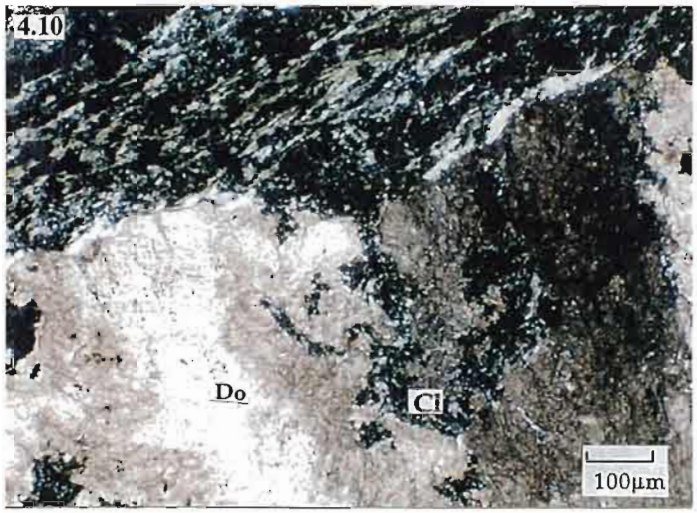
4.10
Do
Cl
100µm

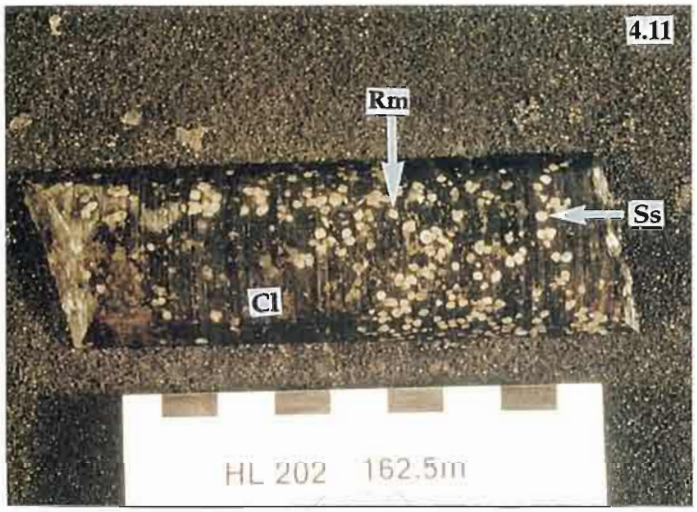
4.11
Rm
Ss
Cl
HL 202 162.5m


4.12
Ss
Cl
HL 137 132.8m

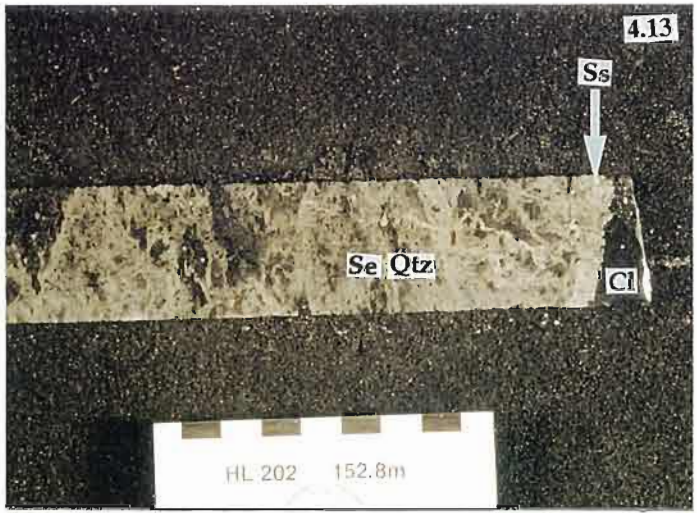
4.13
Ss
Se Qtz
Cl
HL 202 152.8m

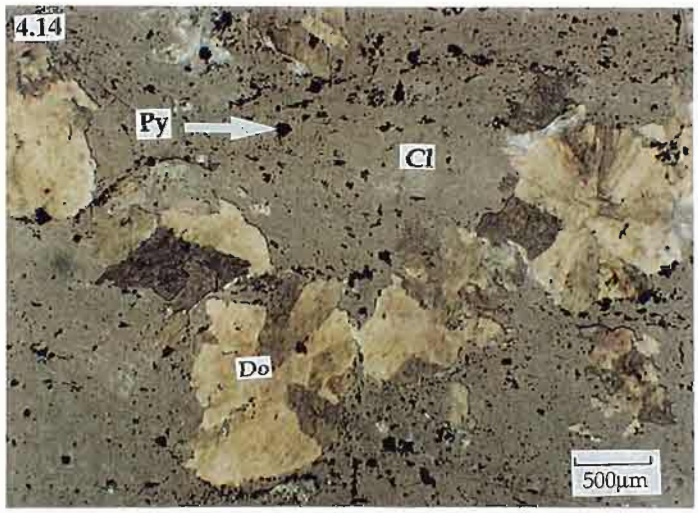
4.14
Py
Cl
Do
500µm

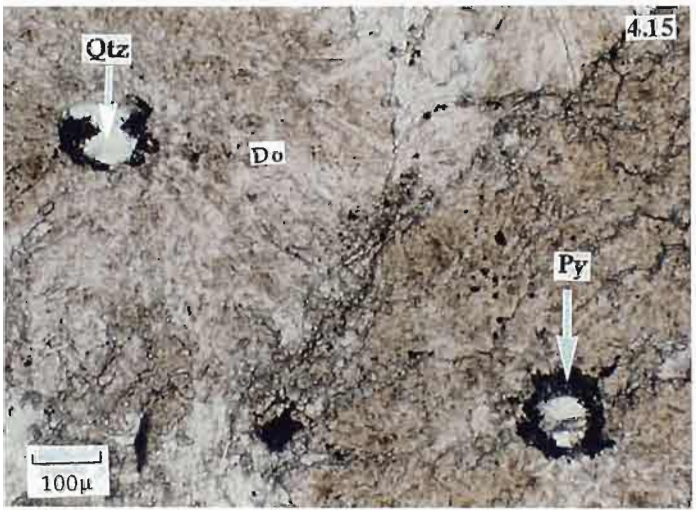
4.15
Qtz
Do
Py
100µ


4.16
HL 757 41.90m

4.3.2 Small Spheroids

The small dolomite spheroids range from 1-2 mm diameter and in hand specimen are a smaller version of the large spheroids however there are certain differences between the two. The small spheroids occur as disseminated crystals in a chlorite matrix (Plate 4.11) and in distinct coalesced zones (Plate 4.12).

The small spheroids can group together on the boundary between chlorite alteration and sericite/quartz alteration (Plate 4.13).

In thin-section they grow radially with undulose extinction (Plate 4.14) and in some instances the spheroids nucleate off quartz crystals associated with pyrite (Plate 4.15). They do not, however, exhibit compositional zonation like the large spheroids and their crystal boundaries are not as well defined.

Table 4.2 A summary of carbonate textures in the footwall of Hellyer

Carbonate Texture	**Description**	**Associations**	**CL**
Spheroidal: **i) Large Spheroids, from 5-15mm** **-Dolomites** **-Dolomites with minor Fe.** **(Stain colourless and light blue)**	Macroscopic: Cream-coloured radiating spheroids that can be isolated or coalesced into veins Found mostly in a black, fine grained chlorite matrix. Microscopic: Core:- - very fine-grained carbonate Periphery carbonate:- - coarser-grained - compositionally zoned - radiates from the centre. - Undulose and sector extinction - No evidence of growth by nucleation.	Microscopic: Sometimes rimmed with coarse-grained sericite. Present in a fine-grained chlorite, pyrite and sericite matrix. Can contain voids in their centres filled with clean, twinned calcite. Chlorite is foliated and fine-grained.	Growth rings on the periphery of the carbonate spherules show alternate luminescence from dull to light orange. Central calcite filling the voids is a bright yellow.
ii) Small Spheroids 1-2mm diameter **-Dolomites minor Fe,** **-Dolomites (stain light blue and colourless)**	Macroscopic: -Isolated and coalesced (sometimes in small zones) in fine-grained chlorite matrix. Microscopic: -Anhedral -Undulose extinction -Zoned	Can be close-packed, disseminated or coalesced into clumps. Associated with fine-grained foliated chlorite, sericite, quartz and euhedral pyrite. Some spheroids radiate off quartz and pyrite crystals.	Dull to non-luminescent

Rhombs, 1-1.5mm diameter -Dolomite -Dolomite with minor Fe (stain light blue and colourless).	Macroscopic: Isolated crystals in a fine-grained chlorite matrix. Microscopic: - Rhombic shape - Zoned - Euhedral	Can be close-packed to form large pods	Dull to non-luminescent
Veinlets, <5mm width - Dolomite with minor Fe - dolomite (stain light blue and colourless)	Macroscopic: Anastomosing or isolated in fine grained chlorite, sericite and quartz matrix Microscopic: -Well defined boundaries	Can lead to massive carbonate clots or be associated with massive, pervasive carbonate.	Dull to non-luminescent
Massive Carbonate, Clots -Dolomite with minor Fe -Dolomite (stain light blue and colourless)	Macroscopic: Occurs as a clot-shaped texture in a fine-grained chlorite, sericite quartz and pyrite matrix Microscopic: -Anhedral - Fine and coarse-grained - Sometimes undulose extinction	Associated with fine veinlets, small and large spheroids and rhombs.	Dull to non-luminescent.
Devonian Veins 50mm -1/2m -Fe-poor calcite (stain mauve)	Macroscopic: - Bright white - Cross-cut the chlorite-carbonate alteration. - Anastomosing Microscopic: -Twinned - Cleaner than the earlier carbonate. -Undulose extinction	Can fill voids in old carbonate crystals. Cross-cuts Cambrian alteration.	Bright orange to bright yellow

4.3.3 Rhombs

Zoned rhombs are also a distinctive carbonate texture and are more common that the small spheroids. In hand specimen they are cream to white and range from 1-1.5mm in diameter and occur in a chlorite matrix. They can be isolated (Plate 4.11) or form pods (Plate 4.16) in a chlorite matrix. In thin section, the rhombs are euhedral and is some instances their shape is distorted. The rhombs are also radially zoned, these zones appear as light and dark bands and are approximately 0.25-0.5mm thick (Plate 4.17). The rhombs also coalesce to form pods (Plate 4.18).

Plate 4.17: Photomicrograph of isolated rhombs (Rm) in a chlorite (Cl) matrix. Note the zoning within the rhombs (Sample 5, HL 757; scale bar=500μm; plain light)

Plate 4.18: Photomicrograph of coalesced rhombs (Rm) in a chlorite matrix (Cl). The shape of the rhombs becomes distorted when they coalesce. (Sample 5, HL 757; scale bar=500μm; under crossed polars)

Plate 4.19: Core sample of massive dolomite clots (Ma) associated with anastomosing veinlets (Vlt) in a chloritic matrix (Cl) (Sample 2, HL 141; scale bar in cms).

Plate 4.20: Hand sample of an isolated massive dolomite pod in a chorite (Cl) matrix (Sample 2, HL 202; scale bar in cms).

Plate 4.21: Photomicrograph of massive dolomite (Ma) associated with contorted veinlets. The massive dolomite consists of aggregates of 100-250μm anhedral crystals (Sample 3, HL 807; scale bar=500μm; under crossed polars)

Plate 4.22: Photomicrograph of massive dolomite (Ma) enveloping small coalesced zoned rhombs (Rms) (Sample 3, HL 141; scale bar = 500μm; plain light)

Plate 4.23: Photomicrograph of massive dolomite, which consist of coarse (Cs) and fine (Fn)-grained anhedral crystal aggregates. (Sample 1, HL 35A; scale bar=500μm, under crossed polars)

Plate 4.24: Photomicrograph of a volcaniclastic fragment (Qtz) enveloped massive carbonate (Ma) in a fine-grained chlorite (Cl) and sericite (Se) matrix (Sample 5, HL 757; scale bar=500μm; under crossed polars).

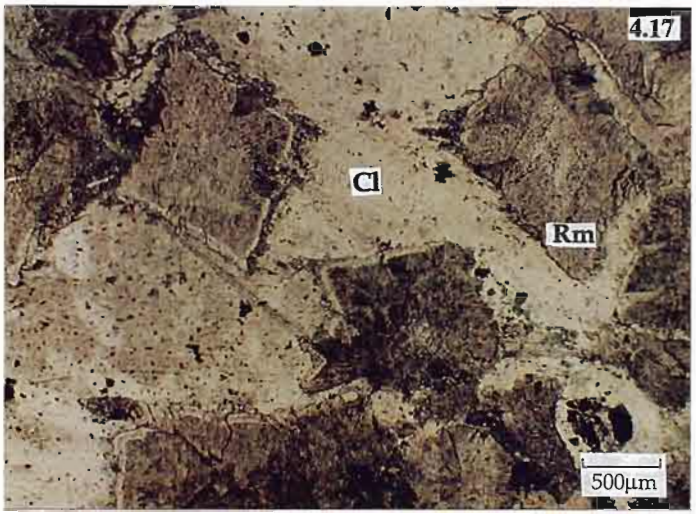
4.17
Cl
Rm
500µm

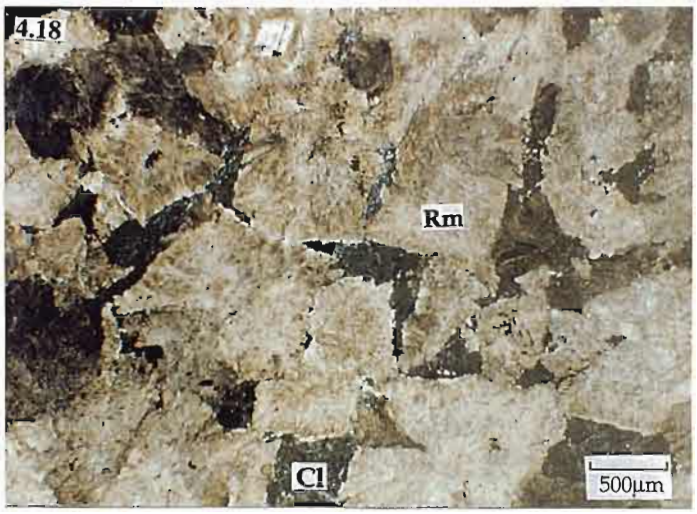
4.18
Rm
Cl
500µm

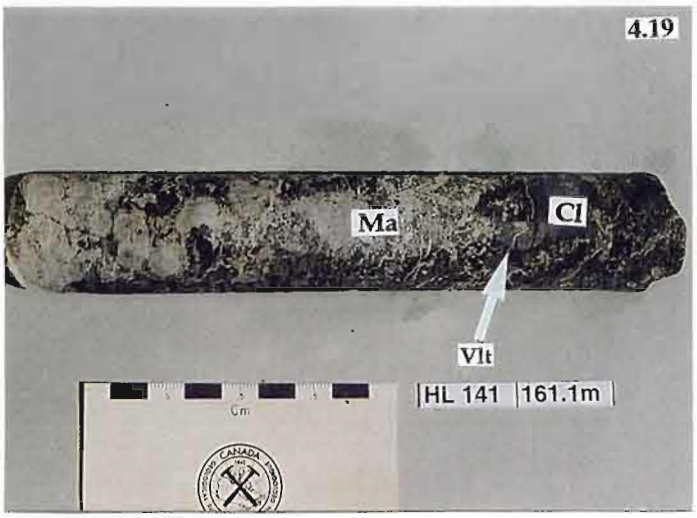
4.19
Ma
Cl
Vlt
HL 141 161.1m


4.20
Cl
HL 202 149.3m

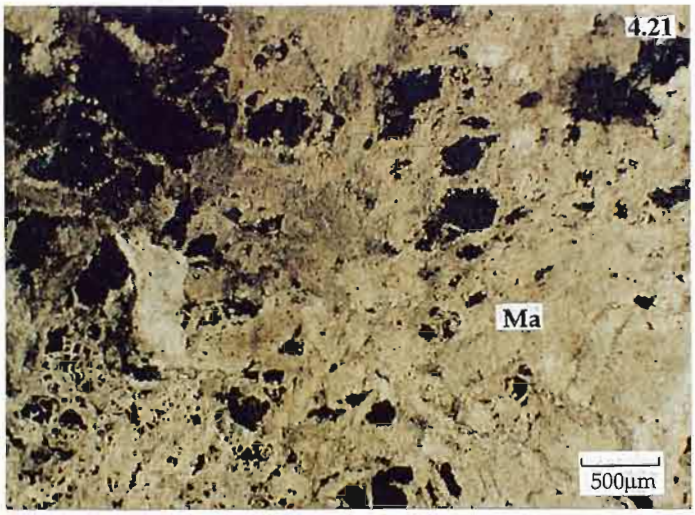
4.21
Ma
500µm

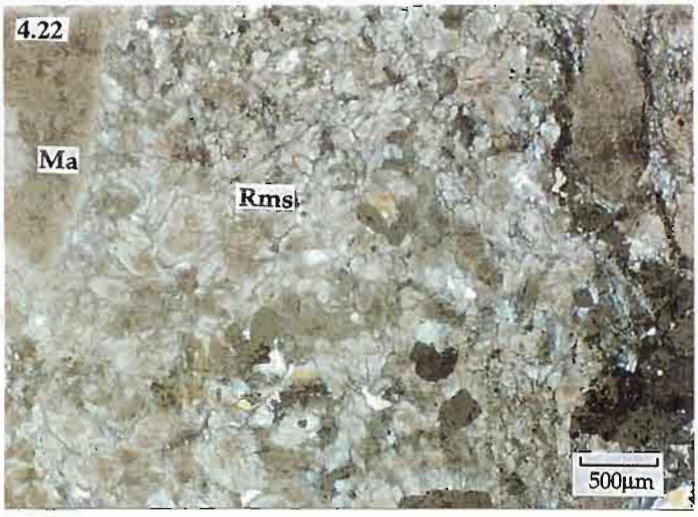
4.22
Ma
Rms
500µm

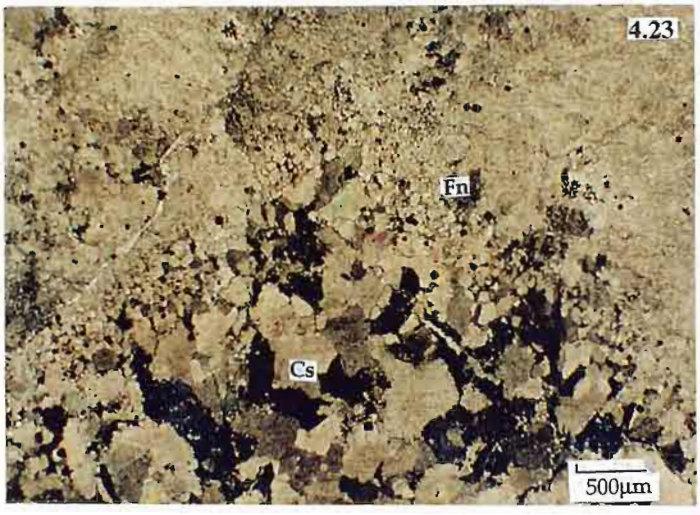
4.23
Fn
Cs
500µm

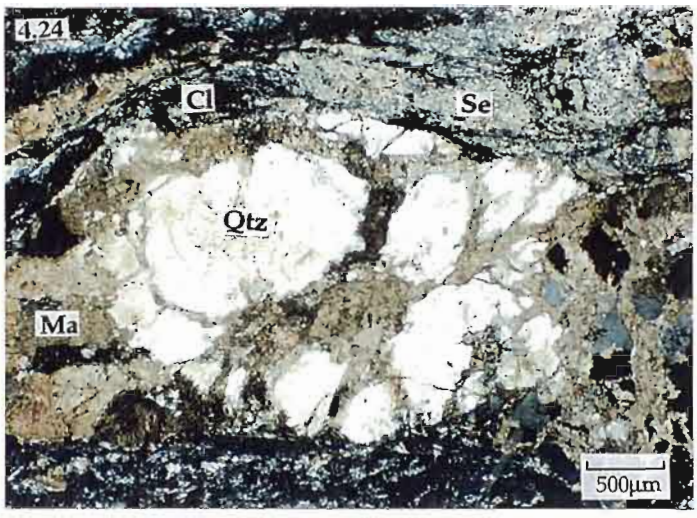
4.24
Cl
Se
Qtz
Ma
500µm

The dolomite rhombs coexist with small spheroids and are associated with a chlorite, sericite and pyrite matrix. There is no evidence in the cores of the rhombs that indicates they grew by nucleation off a pre-existing mineral in the matrix.

4.3.4 Massive carbonate

Massive dolomite is associated with fine-grained chlorite, sericite, pyrite and quartz. In hand specimen the massive dolomite is a cream to white and can form pods up to 3cm in diameter (Plate 4.19, 4.20). In thin section it consists of aggregates of fine-grained anhedral dolomite crystals ranging from 100-250μm in diameter. These pods can have anastomosing veinlets branching off them (Plate 4.21). Occasionally the massive dolomite envelopes rhombic carbonate and can envelope it (Plate 4.22).

The massive dolomite can also form clumps of fine and coarse-grained dolomite (Plate 4.23). The massive carbonate can also grow on the rims of relict volcano-sedimentary clasts (Plate 4.24). Massive dolomite also occur as circular shapes consisting of aggregates of finer grained dolomite crystals (Plate 4.25). Under cathodiluminescence there is a void in the centre of this massive pod of carbonate filled with later stage calcite (bright yellow) which also appears on the rims (Plate 4.26).

4.3.5 Veinlets

In hand sample, 1-2mm veinlets of dolomite coexist with massive dolomite, small/large spheroids and rhombs (Plate 4.19). In thin section the veinlets are contorted, anastomosing and in some cases, cross-cut the spheroidal carbonate, (Plate 4.27) and can also pass around them (Plate 4.28).

4.3.6 Devonian Calcite Veins

In core samples, large calcite veins can be distinguished as they are white, react with cold hydrochloric acid, range from 20mm-1/2cm thick and cross-cut the chlorite-carbonate alteration (Plate 4.29). In thin section, the calcite can be distinguished from the dolomite as it is cleaner, twinned and has high birefringence (Plate 4.30). In this study, this carbonate is not investigated as it is a later stage Devonian feature and not associated with earlier Cambrian carbonate alteration (Gemmell and Large, 1992).

Plate 4.25: Photomicrograph of a massive carbonate (Ma) pod surronded by Devonian calcite (Ca). Note intergrowths of calcite towards the centre and on the rim of the pod. All in a chlorite (Cl)-pyrite (Py) matrix (Sample 5, HL 757; scale bar= 500μm; plain light).

Plate 4.26: Photomicrograph of Plate 4.25 taken under cathodiluminescence. Showing the later stage bright yellow calcite (Ca) precipitation in the pod and rimming the dull orange pod (Do) (Sample 5, HL 757; scale bar=500μm).

Plate 4.27: Photomicrograph of a dolomite veinlet (Vlt) cross-cutting a small spheroid (Ss) in a chlorite, pyrite, quartz and sericite matrix (Sample 8C, HL 202; scale bar=500μm plain light).

Plate 4.28: Photomicrograph of carbonate veinlets (Vlt) passing around a spheroid (Ls) in a chlorite (Cl) matrix. (Sample 1, HL 241; scale bar = 500μm; plain/reflected light).

Plate 4.29: Core sample showing the Devonian calcite veins cross-cutting quartz (Qtz)-chlorite (Cl) alteration they can reach up 1/2m thickness. (Sample 5, HL 758)

Plate 4.30: Photomicrograph showing the Devonian calcite (Ca). Note it appears cleaner and twinned compared to the Cambrian dolomite alteration (Do). (Sample 6, HL 807; scale bar= 500μm; under crossed polars).

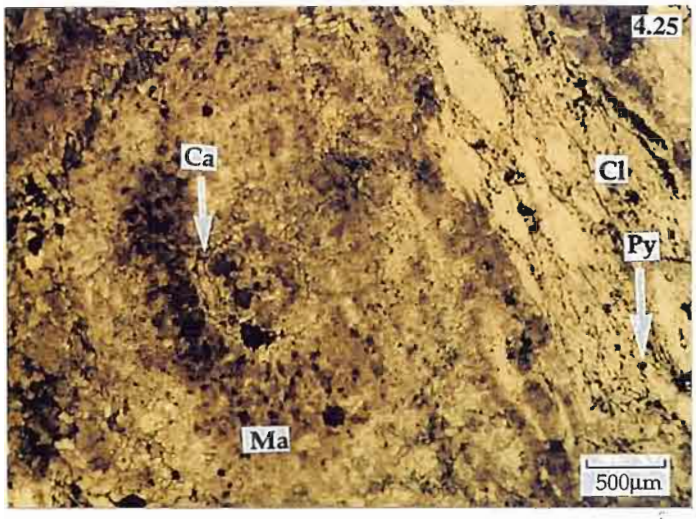
4.25
Ca
Cl
Py
Ma
500µm

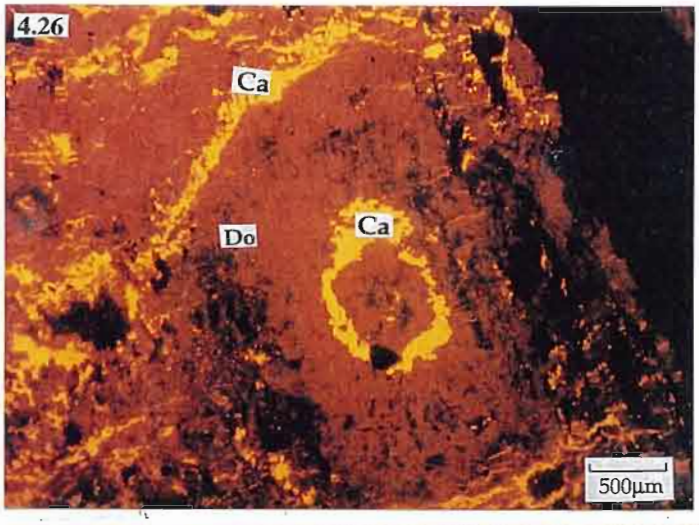
4.26
Ca
Do
Ca
500µm

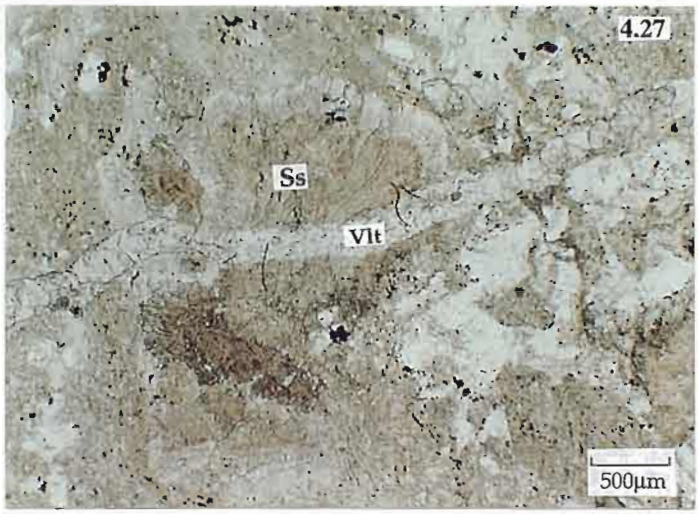
4.27
Ss
Vlt
500µm


4.28
Cl
Ls
Vlt
500µm


4.29
Qtz
Cl
Ca
Cm
HL 758 35.2m

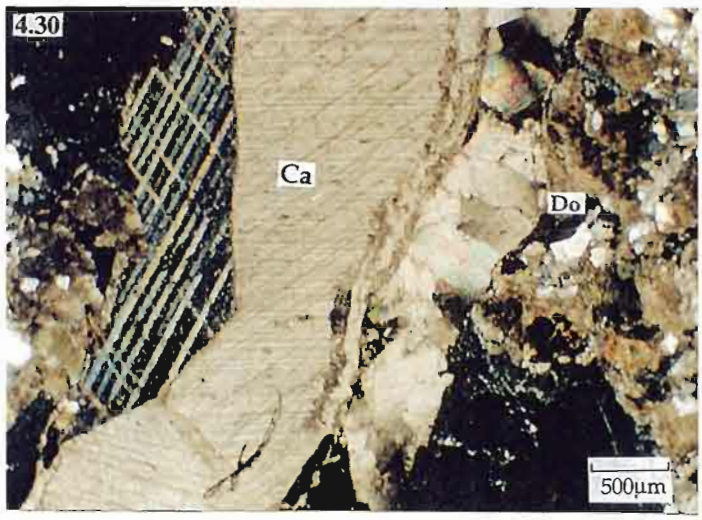
4.30
Ca
Do
500µm

4.4 Paragenesis of the carbonate

4.4.1 Results

Cathodiluminescence studies on the large carbonate spheroids indicate that several pulses of fluid precipitated compositionally variable carbonates in the footwall at Hellyer. In Plate 4.6 the central core of the spherule is dark orange indicating a high iron content, towards the edges, the euhedral carbonate overgrowths show a number of alternating dark orange and bright yellow bands, indicating alternating Fe-rich and Mn-rich dolomite precipitation, respectively (Plate 4.14).

The rhombs, smaller spheroids, massive and veined carbonate were all dull to non-luminescent under CL indicating the high iron content.

4.4.2 Metamorphic features

There are several features that indicate the effect of the Devonian metamorphism on the chlorite-carbonate alteration at the Hellyer ore-deposit. The large spheroids have coarser-grained sericite on their rims. The rhombs have commonly been distorted and the pyrites commonly have pressure shadows the contain quartz, indicating shearing and rotation.

4.4.3 Textural and mineral paragenesis

From a hand sample and petrographic investigation of the dolomite textures a paragenesis is proposed. Only a few cross-cutting relationships are observed such as veinlets cross-cutting spheroids and massive carbonate enveloping rhombs. It is proposed that most of the textures were formed synchronously (Fig. 4.1).

Petrographic investigations show that the dolomite was a secondary alteration phase after chloritisation of the original host volcanic. Evidence that supports this argument is inclusions of chlorite inside the dolomite spheroids, indicating the spheroids enveloped the chlorite matrix as they grew (Plate 4.6). Pyrite is also in the chloritic matrix and in most instances it is only associated with the chlorite rather than the dolomite.

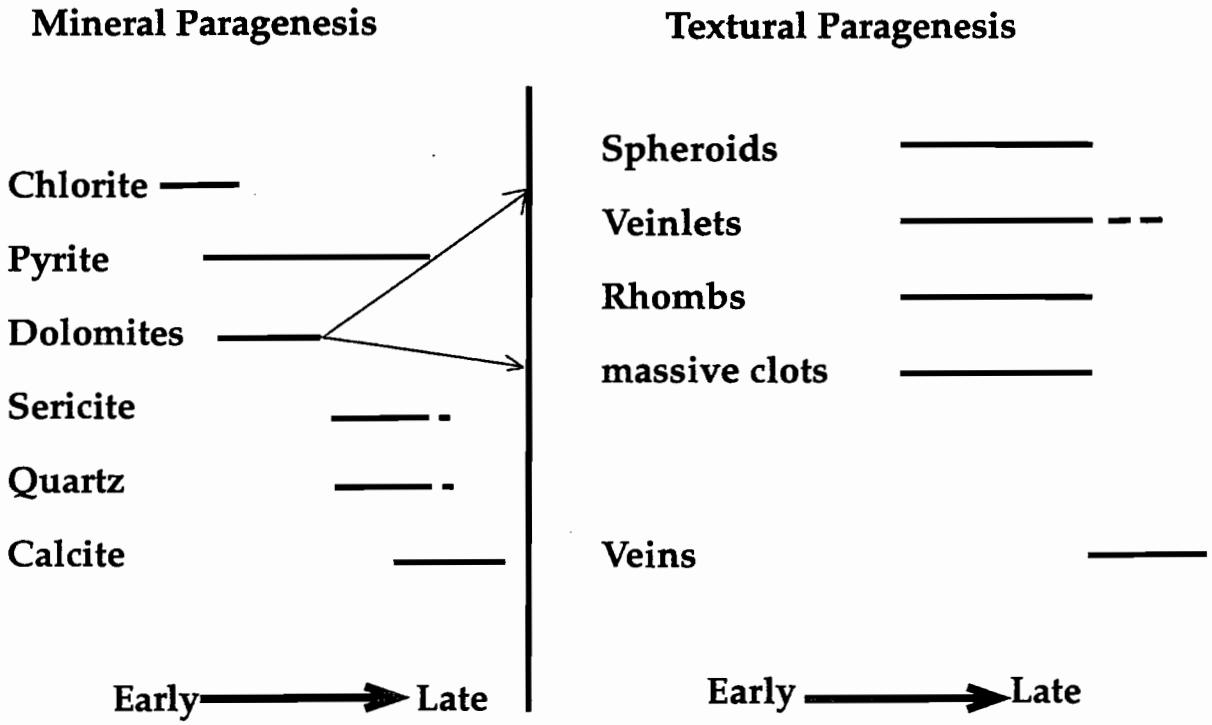

Figure 4.1 Mineral and textural paragenesis of the chlorite-carbonate alteration zone. Note: only represents the Cambrian hydrothermal precipitates, not the younger metamorphic or deformational events

Sericite and quartz then overprinted the chlorite, pyrite and dolomite as in many slides, these assemblages cross-cut the chlorite and carbonate pervasively.

The small and large spheroids can be grouped together as they are texturally similar and usually occur together. The large spheroids are more mineralogically zoned than the small spheroids, reflecting variable physico-chemical conditions while the crystals were growing. There is also evidence that the small spheroids nucleated off quartz crystals in the chloritic matrix. Small and large spheroids grow preferentially in chlorite, this is shown when small spheroids coalesce at the boundary between chlorite and quartz-sericite alteration. The carbonate clearly is preferentially existing in the chlorite and this could be a function of the space available and the competency of the matrix. The quartz/sericite alteration probably lacks space for the carbonates to grow, whereas the chlorite is more ductile, allowing the growth of the spheroids.

The cores of the large spheroids are very fine-grained and therefore difficult to identify any nucleation sites. The rhombs have a euhedral shape and are usually associated with the small spheroids and possible grew in an open space as they crystal shape has been preserved. The veinlets indicate several generations of dolomite. In some slides the veinlets cross-cut the spheroids and in others they pass around them.

The massive dolomite can be associated with rhombs and veinlets. It can be pervasive, enveloping slow-growing zoned rhombs. A possible interpretation could be, initially small carbonates grew off a number of closely-packed nucleation sites and their growth was hindered by an influx of massive pervasive carbonate. Massive carbonate is also fine and coarse grained which could be a function of growth rate. Rapid growth produced fine-grained carbonate and slow growth produced coarse-grained carbonate. Contorted veinlets branch off the massive dolomite in a contorted fashion and could indicate fracture or cavity precipitation.

Finally, it has been the matrix and physico-chemical environment that the dolomites have been subject to while they were precipitated that has controlled the different textures formed. Even though there are several types and styles of dolomite precipitated they appear to have formed synchronously.

4.5 Textural distribution in the carbonates

Analysis of cross sections 10910N, 10947.5N, 11010N, 11047.5N and 11090N indicate that the carbonate textures in the footwall of Hellyer are evenly distributed with no zonation within in the lower and contact zones.

However, the large dolomite spheroids and massive dolomite are more abundant in the lower alteration zone compared to the contact zone. The distribution of carbonate textures on each cross-section are:

10910N, Figure 4.2a - The carbonate textures on the contact with the massive sulphide are predominantly small spheroids, veinlets and large Devonian calcite veins. In the lower zone, the carbonate textures consist of large spheroids, massive carbonate in the form of clots, small spheroids, veinlets and calcite veins.

10947.5N, Figure 4.2b - The textures in the contact zone are variable and consist of massive carbonate in the form of clots, veinlets, small spheroids, and Devonian calcite veins. There is an increase in large spheroids on the contact from 10910N compared to Figure 4.2 a). In the lower zone the carbonate textures are identical o those of the contact zone.

11010N, Figure 4.2c - Large spheroids are on the contact with the ore deposit along with small spheroids, veinlets and Devonian calcite. In the lower zone large spheroids are more prominent than in the contact zone. Carbonate textures in the lower zone are more diverse than the textures in the contact zone

11047.5N, Figure 4.2d - There are large spheroidal carbonate textures on the contact as well as the lower zone, intermingled with Devonian veins, clots and small spheroids.

11090N, Figure 4.2e - In the contact zone there are small spheroids, clots, veinlets and Devonian veins. There is no lower zone chlorite-carbonate alteration present.

Figure 4.3 shows the distribution of dolomite textures down three drill-holes, all from lower alteration zone. The textures vary considerably and a range of textures can be seen at a single locality.

Figure 4.2 a)

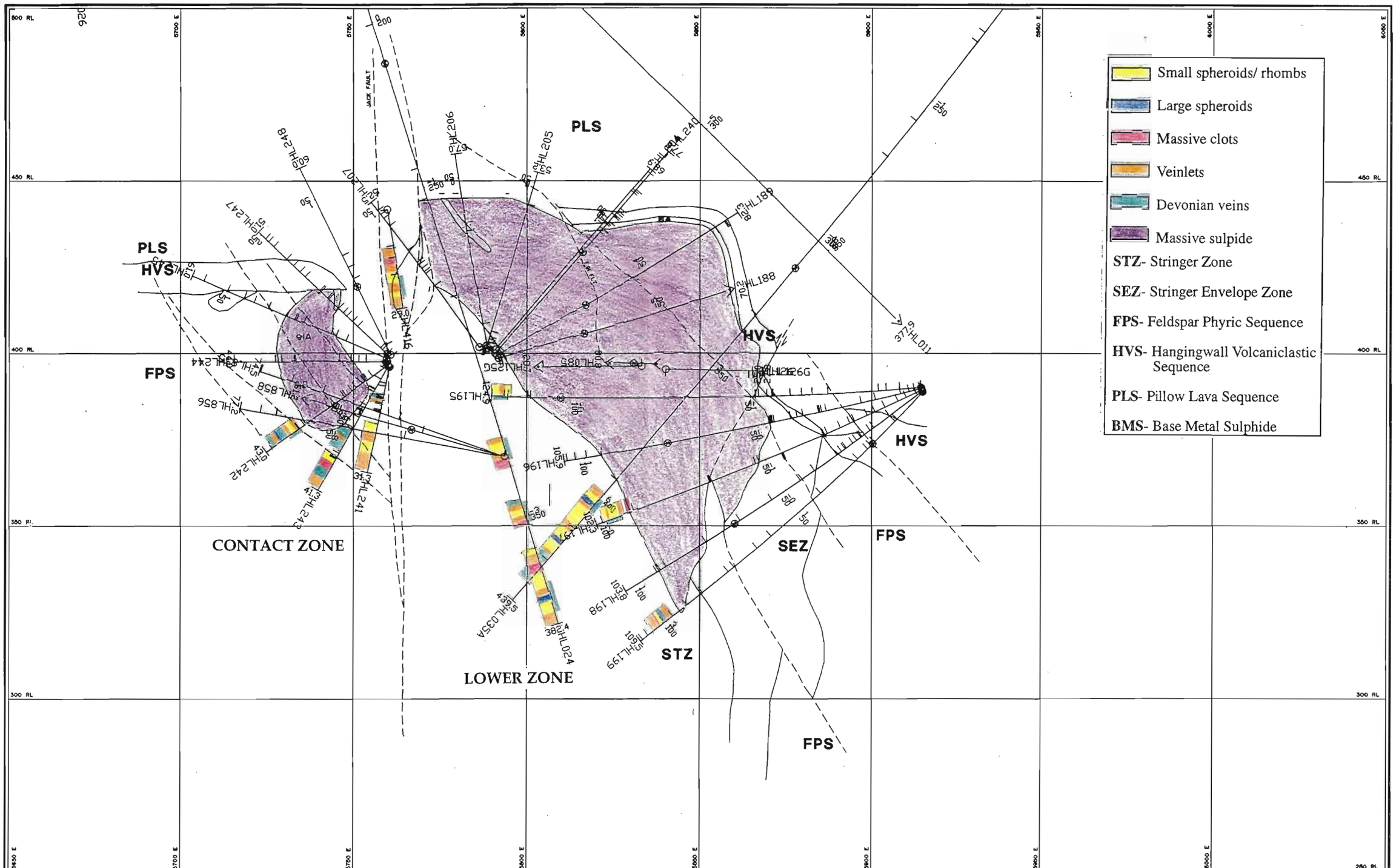

Figure 4.2 a) Cross-section through Hellyer at 10910N showing the distribution of dolomite textures in the contact and lower alteration zones

Figure 4.2 b)

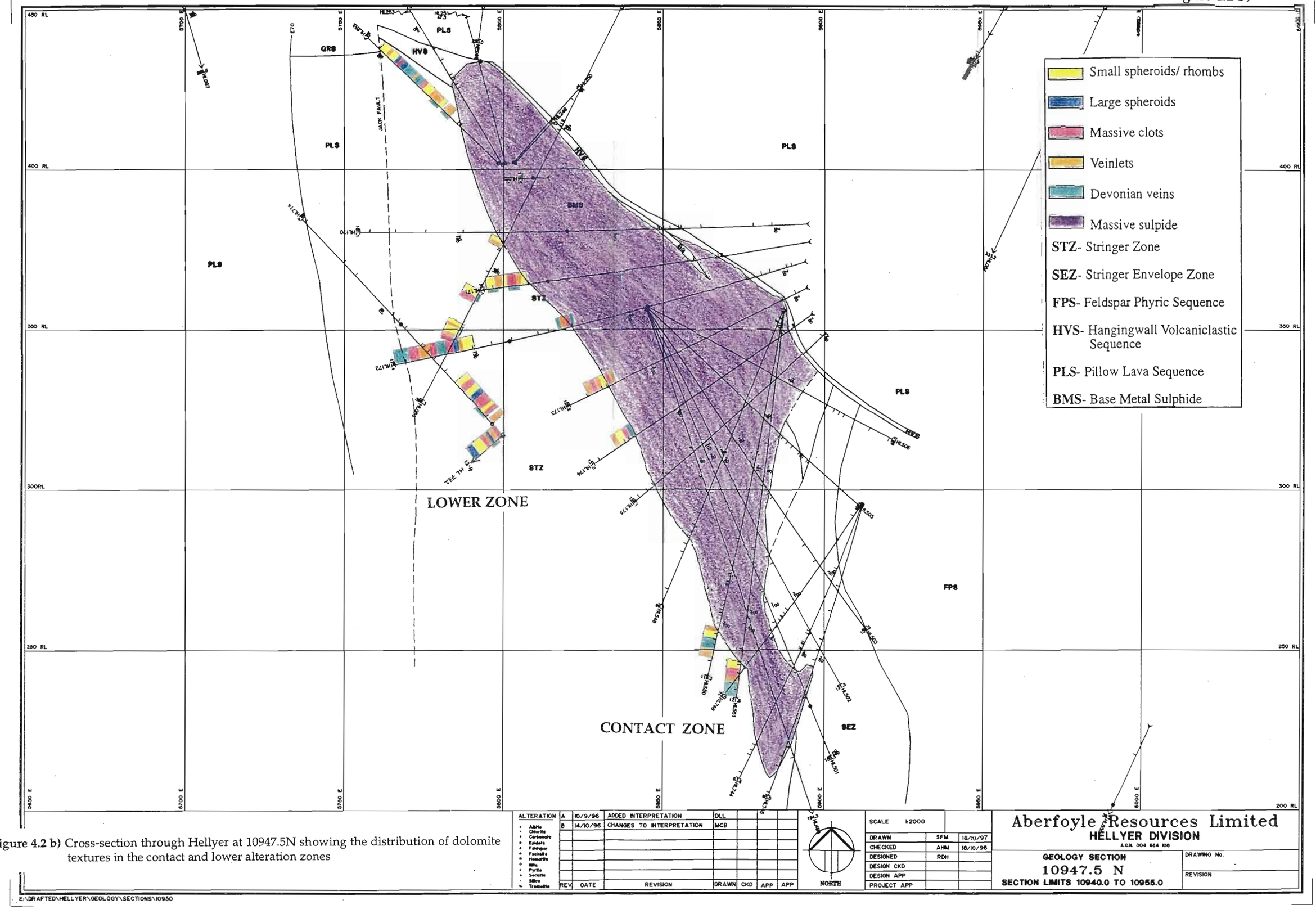

Figure 4.2 b) Cross-section through Hellyer at 10947.5N showing the distribution of dolomite textures in the contact and lower alteration zones

Figure 4.2 c)

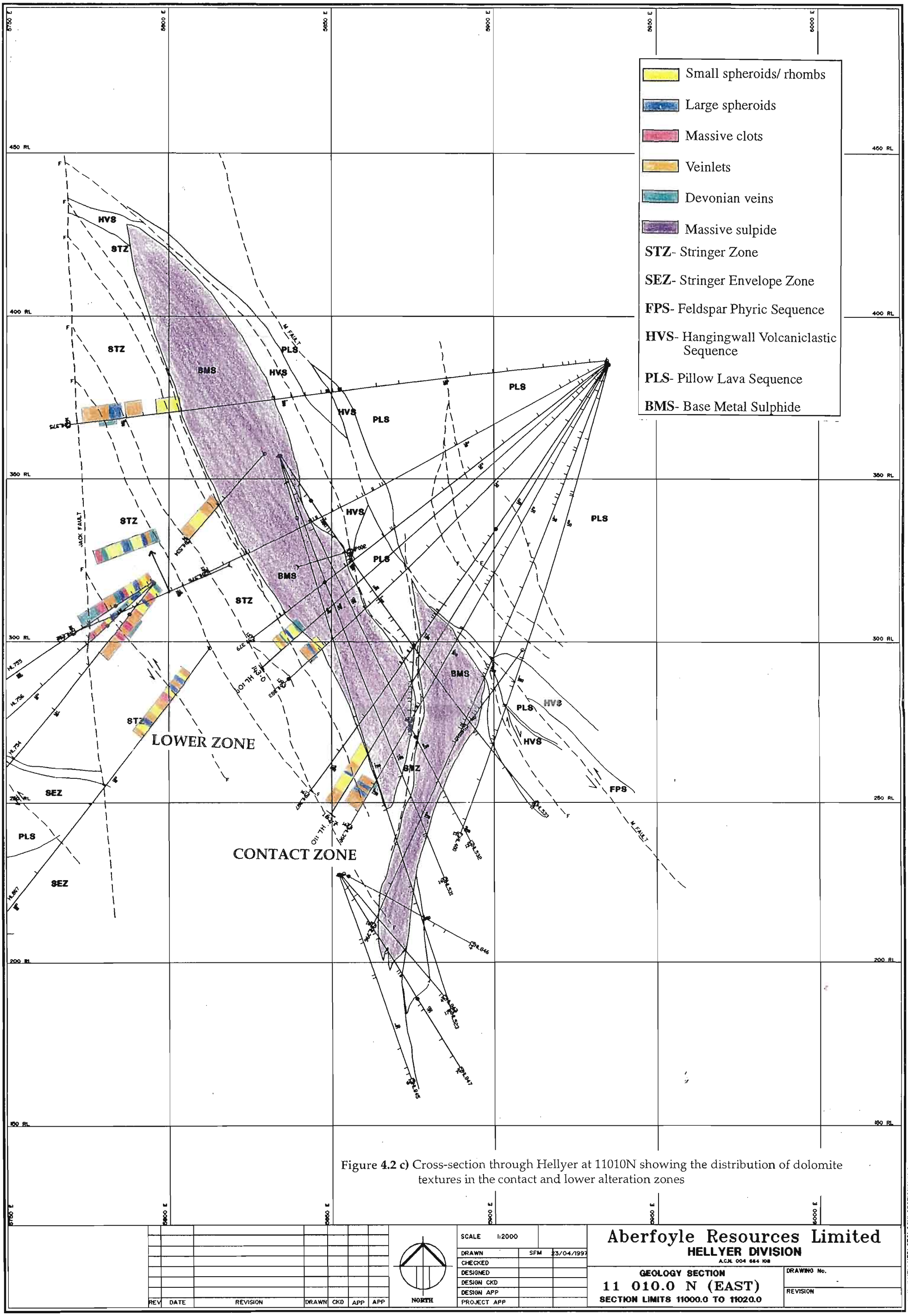

Figure 4.2 c) Cross-section through Hellyer at 11010N showing the distribution of dolomite textures in the contact and lower alteration zones

Figure 4.2 d)

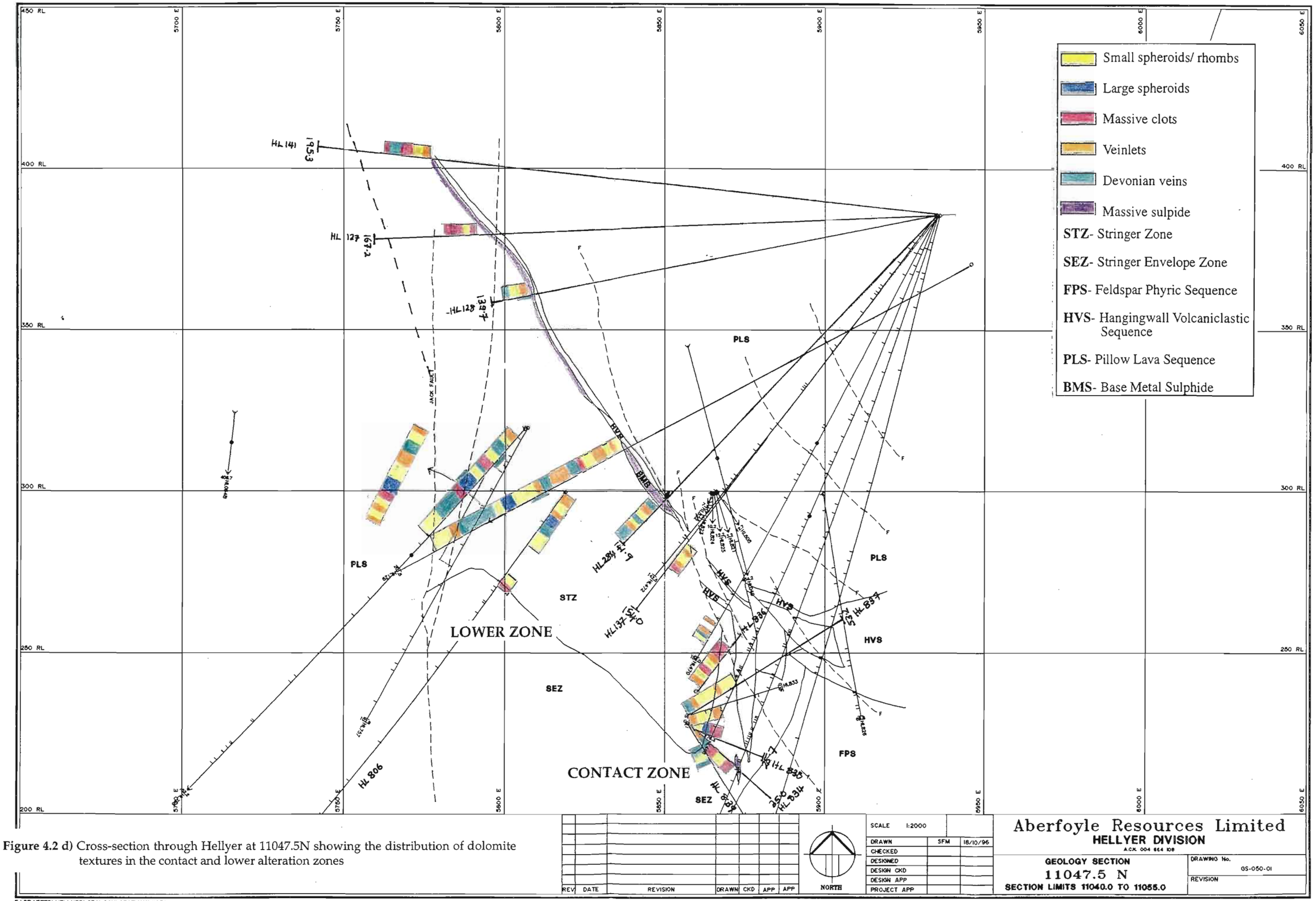

Figure 4.2 d) Cross-section through Hellyer at 11047.5N showing the distribution of dolomite textures in the contact and lower alteration zones

Figure 4.2 e)

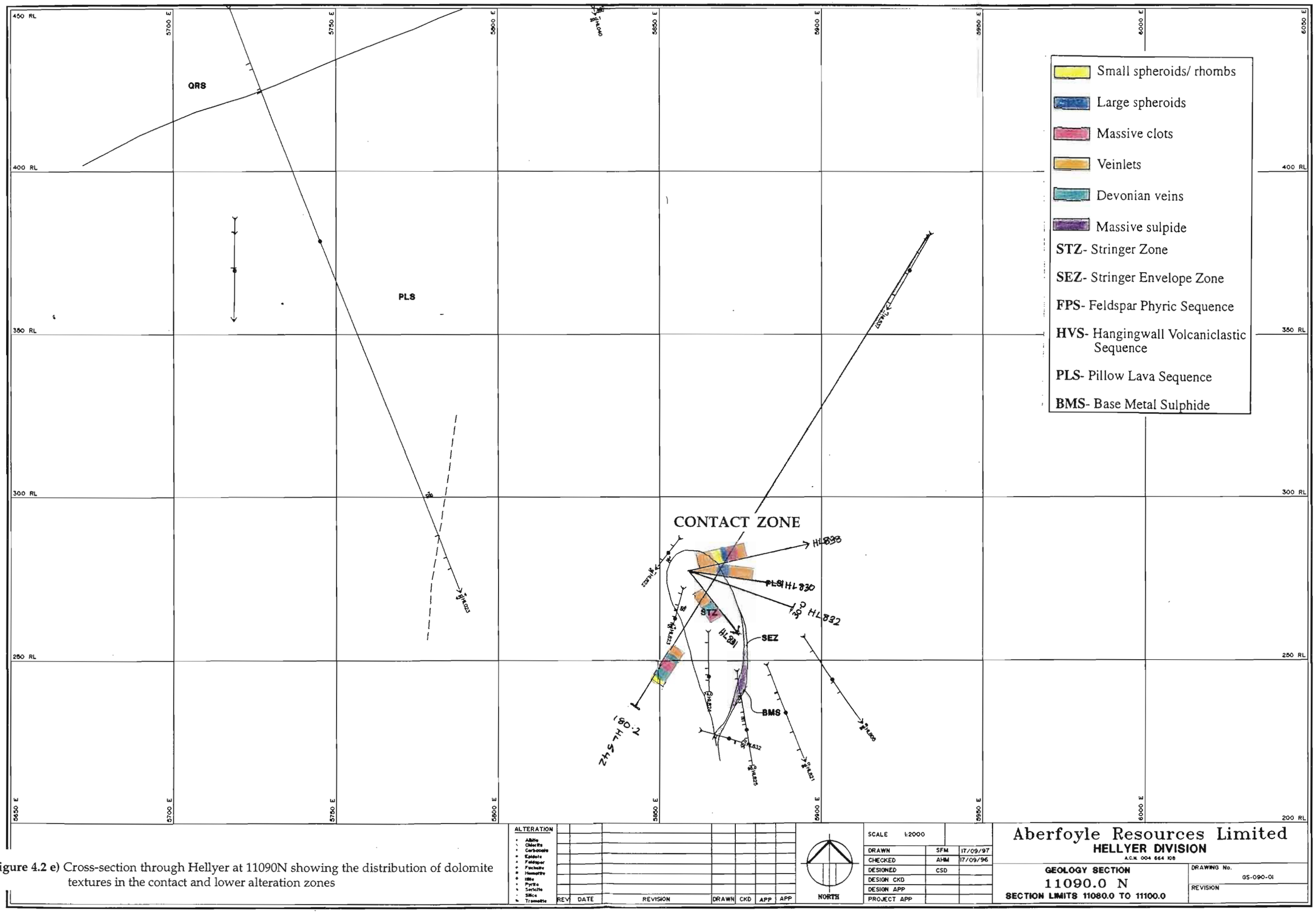

Figure 4.2 e) Cross-section through Hellyer at 11090N showing the distribution of dolomite textures in the contact and lower alteration zones

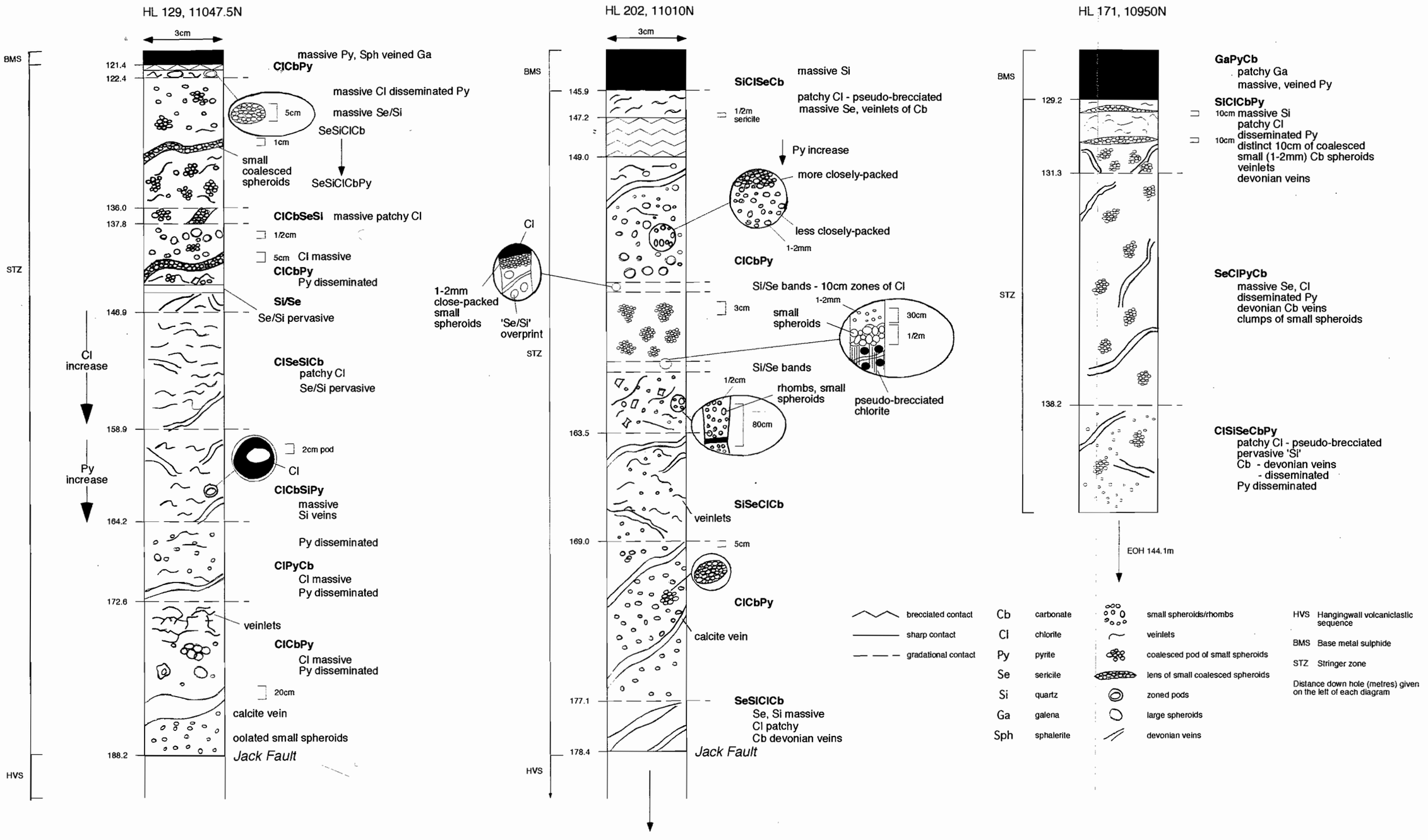

Figure 4.3 Illustrating the distribution of dolomite textures down drill holes HL 129, HL 202 and HL 171

4.6 Interpretation

In general the carbonate textures in the footwall of the Hellyer deposit display no obvious zonation. However with closer examination it is concluded that veinlets and small spheroids are the most common carbonate textures in the contact zone. These textures are commonly associated with quartz, sericite, chlorite and pyrite. Large spheroidal textures only appear in the contact zone between 11010N and 11047.5N and are associated with massive chlorite.
The lower alteration zone shows no textural zonation, however it does contain more patches of large spheroids and massive dolomite than the contact zone. The abundance of large spheroids in the lower zone could be proportional to the increase in chlorite associated with carbonate alteration at greater depths in the footwall, as carbonate spheroids are only in areas of massive chlorite alteration.

4.7 Summary

The dolomite textures in the footwall of the Hellyer ore deposit are diverse and are primarily associated with chlorite, however they also occur with sericite, quartz and pyrite. These textures consist of large and small spheroids, massive clots and veinlets. The spheroids have radial overgrowths indicating several generations of compositionally variable fluid passed through the footwall alteration zone. In some cases quartz crystals occur in the cores of small spheroids as nucleation sites. The small and large spheroids and rhombs grow preferentially in chlorite which is possibly a function of porosity and competency of the matrix in which they are growing. The rhombs textures could be indicative of growth in an open space. Massive carbonate envelopes volcaniclastic fragments and is associated with veinlets.

The dolomite textures show no obvious zonation, however there are a significant increase in the occurrence of large spheroidal textures at greater depths in the footwall. This is possibly related to the increased massive chlorite alteration away from the contact zone. Textures such as veinlets and small spheroids are common in the contact zone. Overall, there is a greater diversity of alteration assemblages in the contact zone as compared to the lower alteration zone.

CHAPTER 5

WHOLE-ROCK GEOCHEMISTRY

5.1 Introduction

This chapter concerns the use of X-Ray Fluorescence (XRF) analyses to determine the major oxide and trace element distribution within the chlorite-carbonate alteration, their changes with respect to spatial distribution and mineralogy in the alteration pipe of the Hellyer ore deposit.

Mass changes within hydrothermal alteration zones associated with volcanic-massive sulphide deposits offer an insight into fluid-rock interaction and are useful in exploring for sulphide mineralisation. In addition, the study of immobile element geochemistry can determine fractionation trends within volcanic rocks and are useful in determining the precursor unaltered rock composition (Barrett and MacLean, 1994).
This chapter will use the whole-rock geochemistry of the chlorite-carbonate alteration zone to:
1) Compare its chemistry to a typical precursor volcanic host rock in the footwall and examine chemical variations, with respect to mass loss and gain, spatially.
2) Compare these chemical changes to those in other alteration zones in the footwall of Hellyer.

5.2 XRF Preparation and analytical techniques

In this study 11 diamond drill core samples from the chlorite-carbonate alteration zone were selected from the contact and lower zone areas in the stringer zone. The initial preparation involved crushing the rock sample with the jaw-crusher into 1-3mm pieces. This was followed by grinding 50g samples in the tungsten-carbide mill. Ignition loss was calculated by heating 1-2 grams of the sample to 1000°C overnight. In these 11 samples the ignition loss was not a true indication of volatiles due the recombination of sulphur dioxide in the ignition furnace with the samples. Duplicate analyses were carried out on some samples to check some low totals. Pressed powder pills were then prepared by Katie McGoldrick for the trace element analysis using samples that did not ignite.
Both major oxides (Al, Ti, Fe, Ca, Mg, Na, K and P) and trace elements were analysed by Phil Robinson at the University of Tasmania using a Phillips 1410

automated XRF. Trace elements analysed were Nb, Zr, Sr, Ba, Y, Rb, As, Cu, Pb and Zn.

5.3 Whole-rock geochemistry of the chlorite-carbonate alteration zone

5.3.1 Methods

In this study, the elemental changes and mass loss/gain in the footwall rocks during alteration to a chlorite-carbonate rock, will be studied in more detail. A broader study on the whole footwall alteration pipe was carried out by Jack (1989) and Gemmell and Large (1992).

This study will enhance the understanding of how the chlorite-carbonate alteration may be significant as a lithogeochemical indicator towards a VHMS ore deposit. Gemmell and Large (1992) used the method of mass balance between unaltered and altered rocks to calculate compositional changes through alteration by hydrothermal fluids. This method was originally devised by Gresens (1967) and was modified by Grant (1986) and uses the graphical method of isocon diagrams to determine the elemental mass change. Element mobility is controlled by 1) the stability and composition of the minerals in the unaltered precursor 2) the stability and composition of the minerals in the alteration product and 3) the temperature and volume of the fluid phase (Rollinson, 1993).

Immobile elements are those that do not gain or lose mass under alteration. The isocon is the line that is made up of immobile elements and passes through the origin on a graph of elements versus n(i) altered/unaltered values (where n(i) is an integer assigned to each element and is dependant on its position along the x-axis). These calculations are carried out under the assumption that alteration is at constant volume, constant mass during the alteration process (Barrett and Maclean, 1994). Gemmell and Large (1992) found that for footwall alteration at the Hellyer deposit immobile elements were TiO_2, Al_2O_3, Zr and Nb.

Grant (1996) devised a method to calculate the absolute mass gain of an element by using the slope of the isocon diagram and the altered and unaltered chemical analysis outlined in the equation below

$C^{A}_{i}(\%) = 100\{ [C^{A}_{i}/mC_{i}^{0})]-1\}$ where ΔC^{A}_{i}= the gain or loss of an element

C^{A}_{i} = the concentration of the element in the altered sample

C_{i}^{0}= The concentration of the element in the unaltered sample

m = the slope of the isocon

and the equation $\Delta C^{A}_{i} = \Delta C^{A}_{i}(\%)/100 * C_i^0$ is applied to convert this value to g/100g. Absolute mass gain and loss measured in g/100g can also be calculated using the method employed by Barrett and Maclean (1993) which uses Zr as the immobile monitor. The total mass change and mass changes are calculated as below:

Mass Change=$Zr_{precursor}/Zr_{altered}$ x $\%element_{altered}$ - precursor composition (Barrett and Maclean, 1993)

- where a positive result indicates mass gain and a negative result indicates mass loss
- Immobile elements do not lose mass, they are only diluted by added mobile mass, therefore must be readjusted to their precursor composition (Barrett and Maclean, 1993).

Both of these methods were employed in this study, however the Barrett and Maclean (1994) method has proved to be much more practical. This method forces the user to look for the an accurate precursor volcanic composition and does not assume element immobility.

5.3.2 Data

Eleven samples from the chlorite-carbonate altered zones were analysed for XRF. They were sampled at various positions laterally across the contact of the ore deposit and also laterally across the lower zone. In all of the samples analysed SiO_2 was characteristically low (between 13.2% and 31.6 %, with one erroneous sample containing 57% Si) and also Na_2O was between 0.0025% and 0.03%. CaO, MgO and FeO were all high, with CaO between 6.1% and 17.8%, MgO between 5% and 22.9% and FeO between 4.1% and 19.3%. Sulphur contents were also high in these samples. XRF results can be found in Appendix 3.1.

Four samples of a relatively unaltered precursor andesite composition were chosen for a comparative mass balance study, these are displayed in Appendix 3.2. The unaltered samples were selected by their high silica and sodium content and low chrome content (indicative of an andesite). As Ti and Zr are assumed immobile elements at Hellyer, the Ti/Zr ratio of the precursor volcanic had to be similar to the altered samples.

5.4 Alteration Indices

In this study, the intensity of the chlorite-carbonate alteration is established by calculating the Ishikawa Alteration Index and the Chlorite/Carbonate/Pyrite Index. These indices give a lithogeochemical indicator of the changing alteration intensities associated with a volcanic-hosted massive sulphide deposits (Large et al., 1996).

The Ishikawa alteration Index (AI) measures the degree of plagioclase alteration to sericite or chlorite and is calculated by the formula (Ishikawa et al., 1976):

$$\frac{100(K_2O+MgO)}{(K_2O+MgO+Na_2O+CaO)}$$

The Chlorite/Carbonate/Pyrite index (CCPI), calculated as

$$\frac{100(MgO+FeO)}{(MgO+FeO+Na_2O+K_2O)}$$

measures the degree of chlorite, carbonate and/or pyrite alteration in volcanic rocks and when plotted against the Alteration Index, indicates the relative abundance of Mg-Fe bearing phases. The major alteration end-members minerals are separated (Large et al., 1996).

5.4.1 Results

On a plot of AI versus CCPI all of the samples in the contact and lower zones are located between the chlorite and dolomite end members (Fig. 5.1a, b). The CCPI ranges from 79-100 and the AI ranges from 47-70. The unaltered samples have also been plotted and have a lower AI and higher CCPI, an indication of a more ferro-magnesian precursor. The samples taken from the contact zone trend towards dolomite/ankerite alteration (Fig. 5.1a). The samples from the lower alteration zone (Fig. 5.1b) trend more towards the chlorite end member, indicating a higher proportion of chlorite in the samples further in the footwall of the ore deposit. This is also supported by logging data in the lower zone. Both plots in Fig 5.1a,b only serve the purpose of identifying the minerals in a highly altered rock.

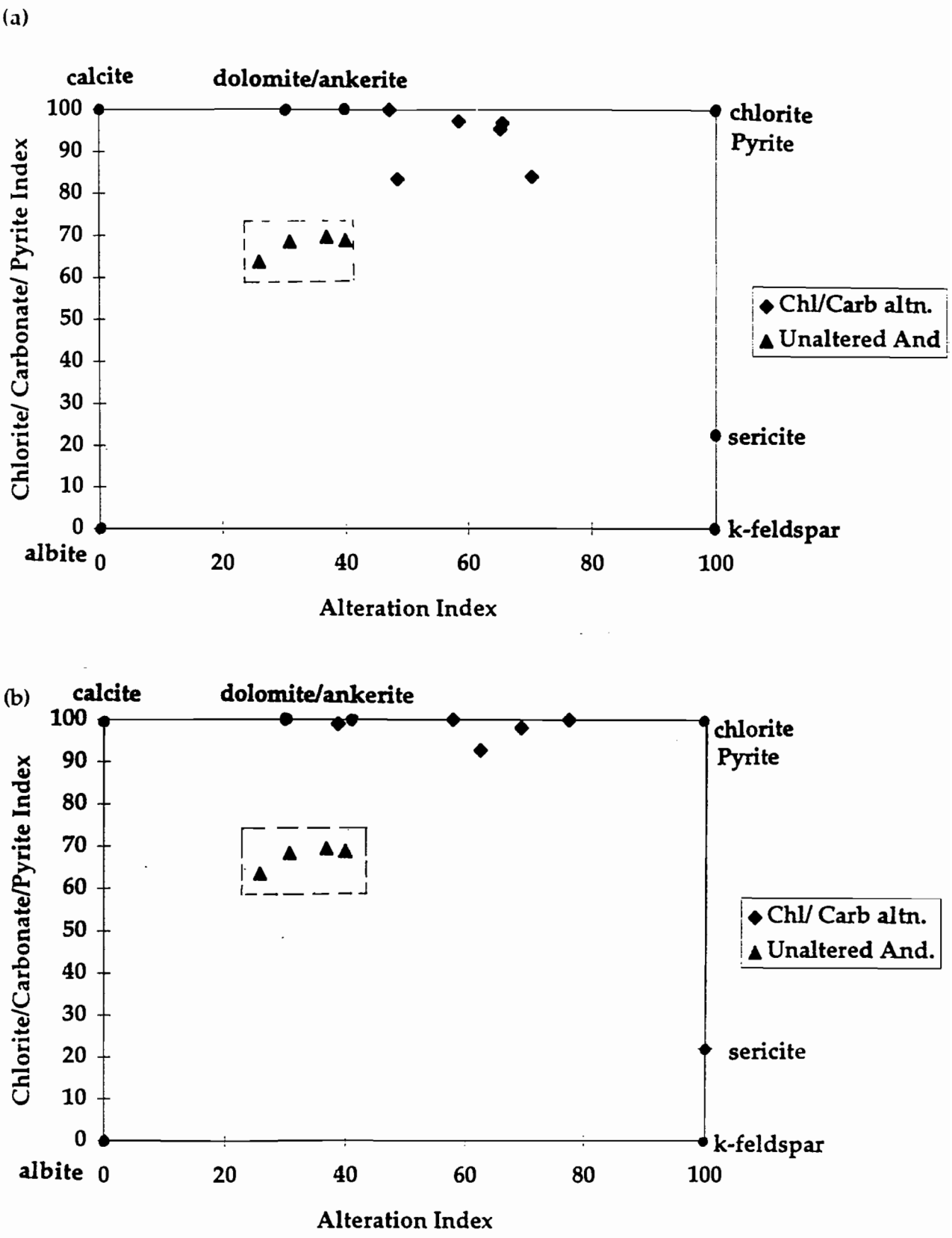

Figure 5.1 Chlorite-Carbonate-Pyrite Index versus Alteration Index for the contact (a) and lower alteration zones (b).

5.4.1.1 Spatial Distribution

Figures 5.2 a and b indicate the relative change in Alteration Index and Chlorite-Carbonate-Pyrite Index with respect to vertical distance below the ore deposit. There is no clear change in either alteration indices with vertical distance into the footwall.

5.5 Mass change analysis of altered volcanics

5.5.1 Establishing a precursor and calculating the overall mass change

Gemmell and Large (1992) analysed five samples from the chlorite-carbonate alteration zone and with these analyses and others from other alteration zones in the footwall of Hellyer, they concentrated on elemental changes laterally across the alteration pipe. An unaltered precursor andesite was used in their study.

In the present study, eleven samples from the lateral and vertical extent of the contact and lower zone alteration zones were collected. As Ti and Zr are known immobile elements in the footwall of Hellyer (Gemmell and Large, 1992), a plot of TiO_2 versus Zr can indicate the overall mass loss or gain of an altered volcanic relative to the precursor (Barrett and MacLean, 1993).

Figure 5.3 is a plot of TiO_2 versus Zr for the contact and lower alteration zones and includes data from the chlorite-carbonate alteration zone collected by Gemmell and Large (1992). Data from their study is in Appendix 3.3. According to Barrett and MacLean (1993), a plot of the immobile element pairs of variably altered samples from a single precursor unit will produce a linear array that will pass through the origin, the point of infinite mass gain. Points that plot further away from the origin than the unaltered, chemically distinct, precursor rock unit are those which have undergone mass loss. Figure 5.3 illustrates that the samples in both the contact and lower zones have undergone an overall mass gain. It also indicates that the samples were typically andestic in composition as they plot between the dacitic and basaltic fields (the dacites and basalts selected for this plot are in Appendix 3.4).

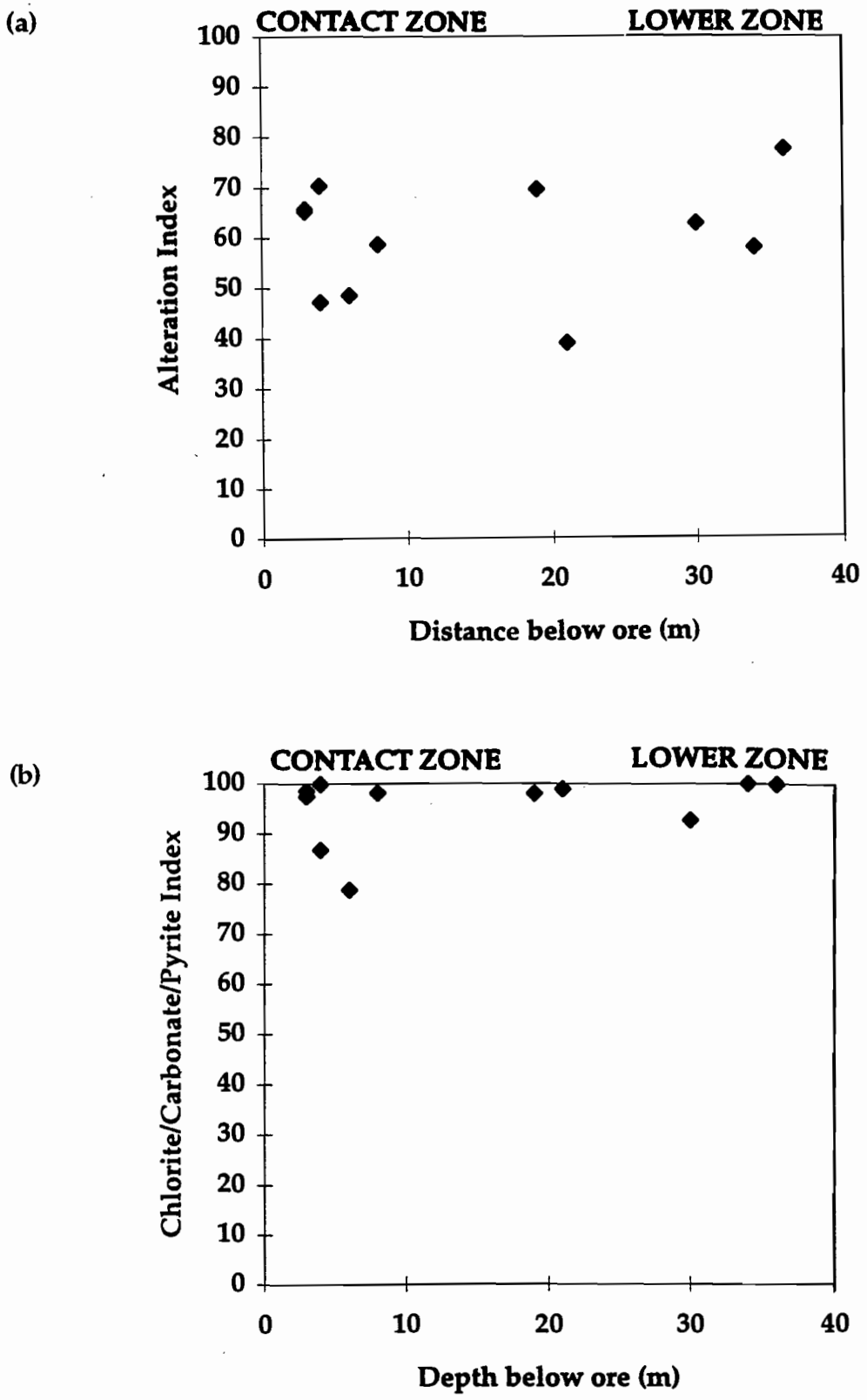

Figure 5.2 Alteration Index versus distance from the ore (a) and Chlorite-Carbonate-Pyrite-Index versus distance from the ore (b).

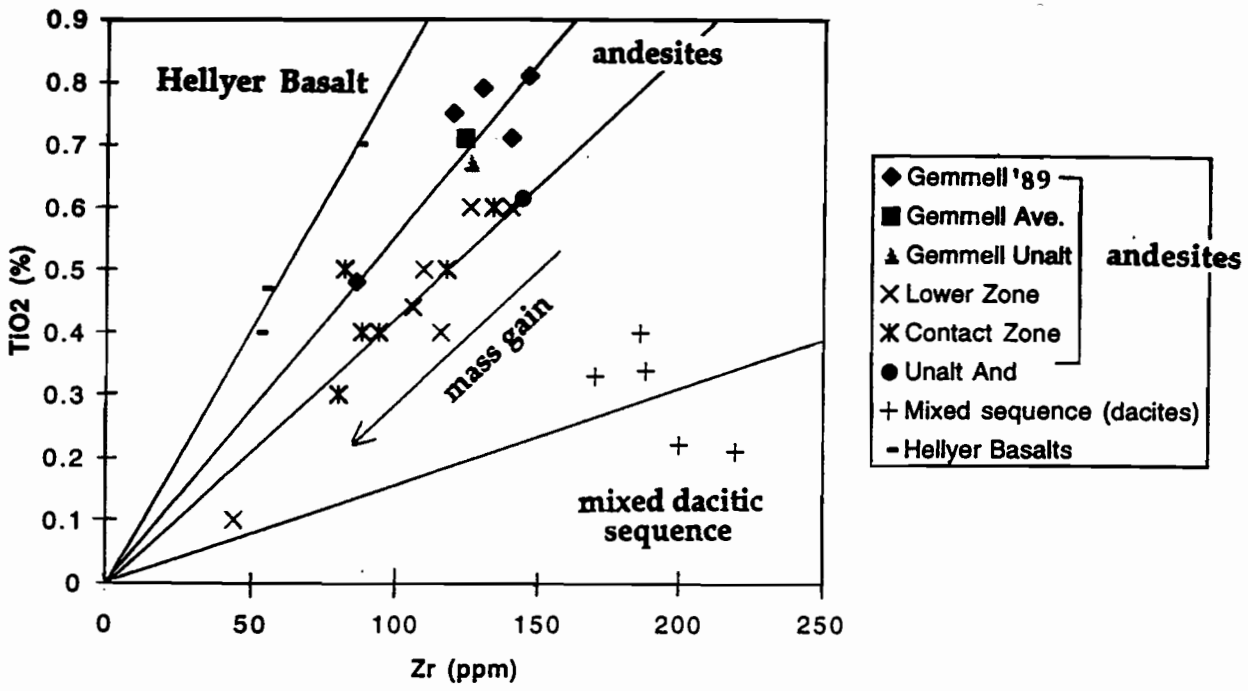

Figure 5.3 Immobile element plot of TiO_2 versus Zr, note the slight compositional differences between the contact and lower alteration zones.

5.5.2 Mass-gains and losses

Using the correct unaltered precursor samples is important in recognising the mineralogical and geochemical changes in hydrothermally altered rocks (Jack, 1989) For all of the samples a precursor andesite was selected to fit the data (Fig 5.3) on the assumption that the original footwall rocks were predominantly of andesitic composition.

5.5.2.1 Contact and Lower alteration zones

Isocon diagrams will be used, in part, to determine the mass gain or loss in elements from a typical unaltered host volcanic. For the contact zone an average of all of the data in this area was used and Figure 5.4a shows Ti, Al, P and Zr lie on the isocon. This indicates that these elements are immobile, correlating with the elements found as immobile in the Hellyer footwall by Gemmell and Large

(1992). An average was also taken from the lower zone and an isocon plot is in Figure 5.4 b showing similar results to the contact alteration zone. An average of both zones is displayed in Figure 5.4 c. Figure 5.5 is a histogram that has been produced to represent the absolute elemental mass gain and loss using Grants (1996) method (refer to 5.3.1). This uses the average elemental data from the contact and lower alteration zones.

The lower alteration zone has a higher Fe and Mg gain than the contact zone and also has a higher Si loss. An average of both zones show that Zr, Ti, and Al remain stable. S, Fe, Mn, K, Mg, and Ca increase and Si and Na are lost under the alteration process. Both the contact and lower zones geochemistry show only slight differences, however anything less than 5g/100g is to be neglected. Overall, converting an andesite to a chlorite-carbonate altered rock involves a net mass gain of 18g /100g (calculated using the Barrett and Maclean (1993) method in 5.3.1).

5.6 Comparison with other alteration zones

Gemmell and Large (1992) studied the elemental mass loss and gain in the various alteration zones in the Hellyer footwall. Their histogram of absolute mass gain and loss laterally across the stringer system including the chlorite-carbonate alteration zone is shown in Figure 5.5 b.

Sulphur- Shows a general decrease from the sericite zone to the chlorite-carbonate zone, to a sharp increase in the siliceous core.

Iron-Compared to the chlorite zone the Fe contents in the chlorite-carbonate zone are lower and could be attributed to the decrease in sulphides (pyrite).

Magnesium- Magnesium content appears to increase dramatically from the sericite zone to the chlorite-carbonate zone and indicates the presence of dolomite and Mg in the chlorite.

Calcium- Also a dramatic increase in the chlorite-carbonate zone, indicating the presence of dolomite.

Silica and Sodium-Both decreased in the chlorite and chlorite-carbonate zones due to conversion of plagioclase to chlorite.

(a)

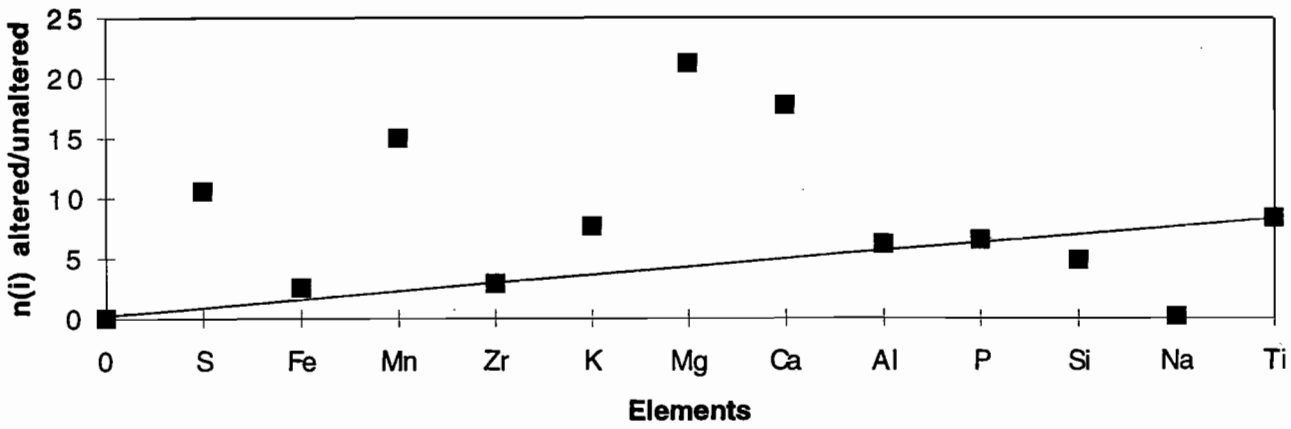

(b)

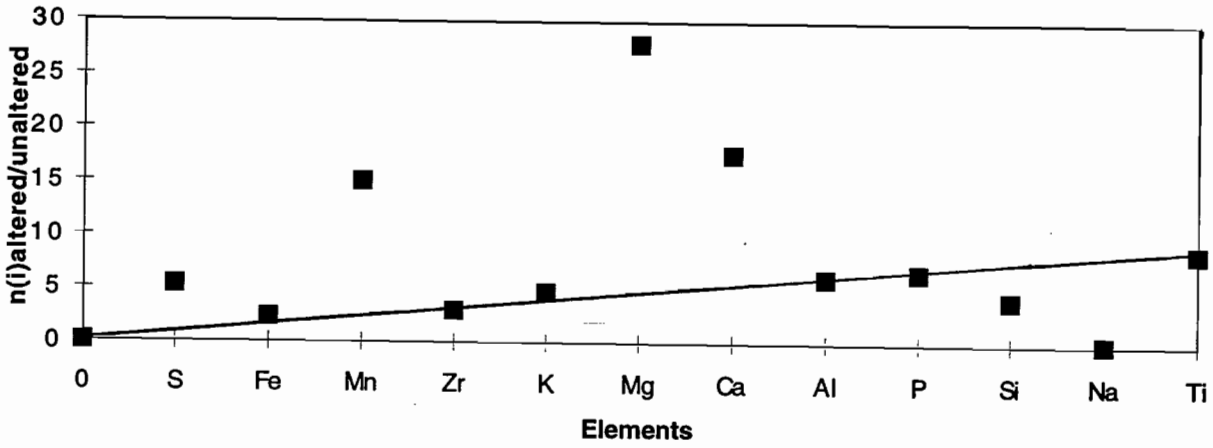

(c)

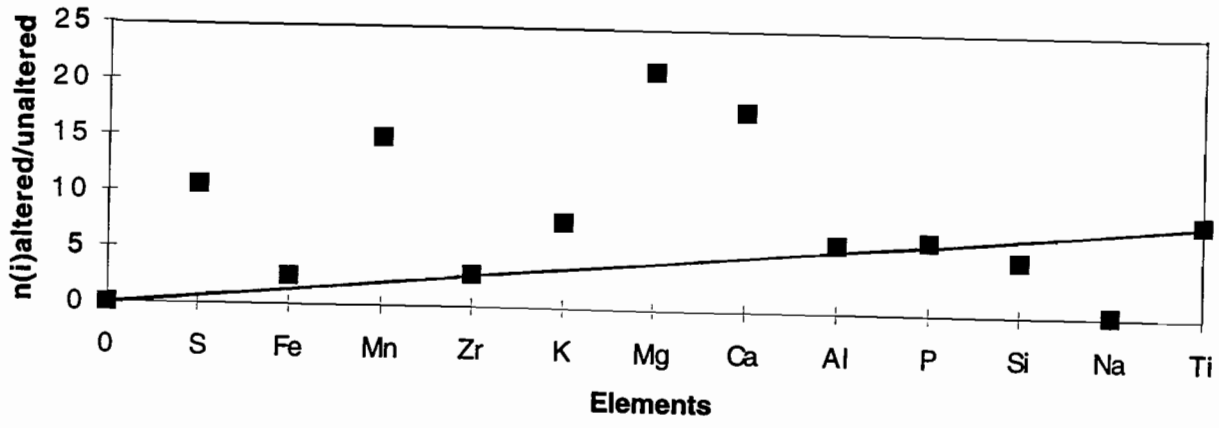

Figure 5.4 Isocon diagrams illustrating the elemental gains and losses for the chlorite-carbonate alteration in (a) the contact zone (b) the lower zone and (c) an average of both zones

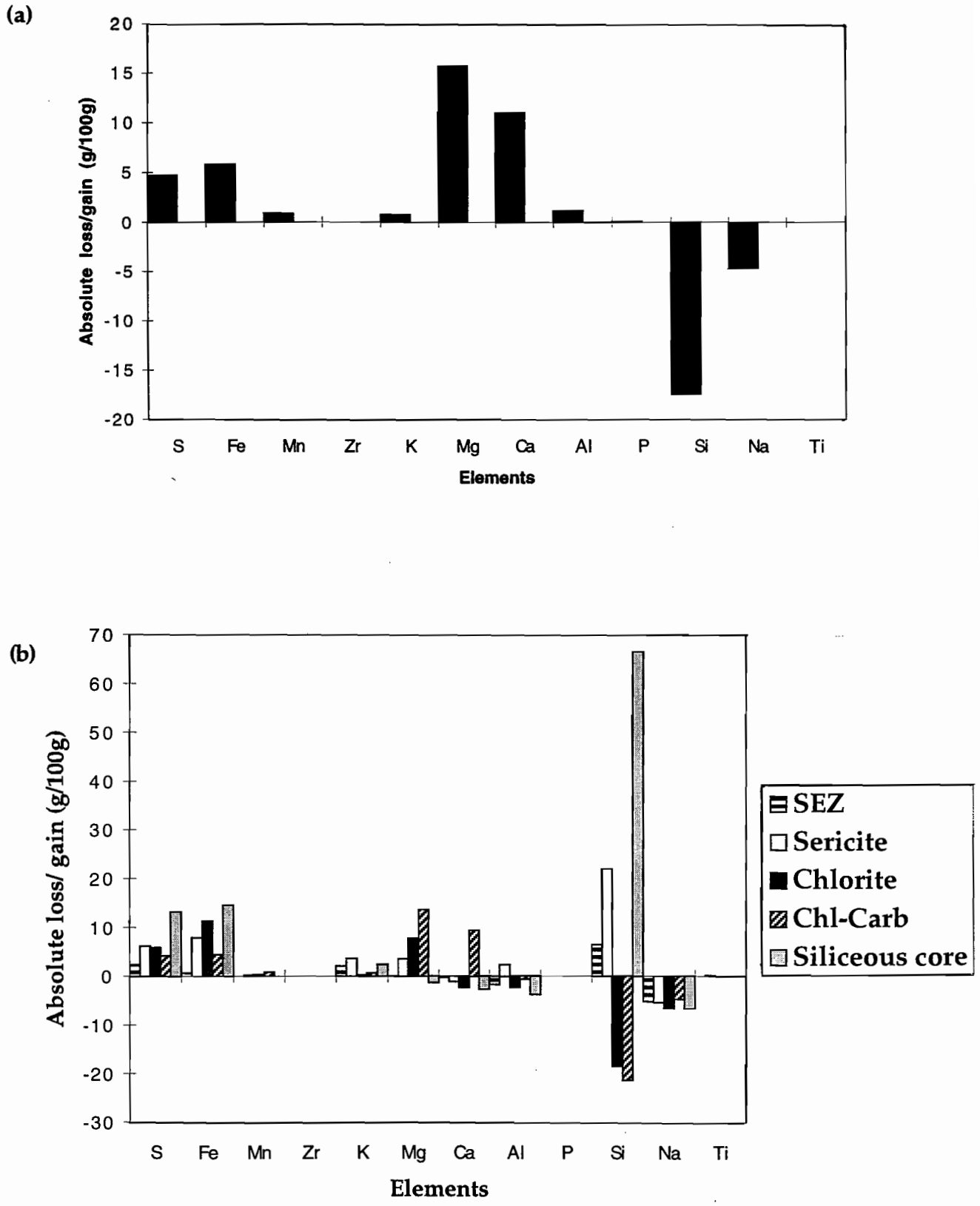

Figure 5.5 A histogram representing the absolute elemental mass gains and losses for the chlorite-carbonate alteration zone (a) and comparing this to other alteration zones in the footwall alteration pipe at Hellyer (b)

5.7 Discussion

5.7.1 Summary and interpretation

The chlorite-carbonate alteration shows has similar whole-rock geochemistry on the contact and in the lower alteration zones. The lower zone has a higher proportion of chlorite than the contact zone because of its closer association with the venting fluids lower in the footwall. The hydrothermal process of transforming an unaltered footwall andesite into a chlorite-carbonate assemblage involves a nett mass gain of 18g/100g .

Its major gains are S, CaO, FeO and MgO which are related to the dolomite, chlorite and pyrite content. The Mg was probably derived from seawater. SiO_2 and Na_2O have been lost from the chlorite-carbonate zones probably from the destruction of feldspars. Other oxides such as Al, K and P have remained relatively stable.

CHAPTER 6

CARBON AND OXYGEN STABLE ISOTOPE STUDIES ON THE CARBONATES

6.1 Introduction

Carbon and oxygen isotope data can be used to give the physico-chemical constraints on the depositional environment of an ore deposit (Taylor, 1987). The variables that control the isotopic composition of hydrothermal carbonates are, the initial composition of the fluid, temperature and the dissolved carbon species (Zheng and Hoeffs, 1993). Carbon isotopes, in particular, give an insight into the source of carbon in hydrothermal fluids and hydrothermal depositional processes (Davidson, 1993). This study concentrates on establishing the composition of the initial fluid that precipitated the Cambrian hydrothermal dolomites in the footwall of Hellyer. From this information, a model will be proposed for genesis of the chlorite-carbonate alteration zone.

6.2 Previous Work

Isotopic data was initially obtained from the chlorite-carbonate alteration zone and the 2A, 2B, 2C syn-mineralisation veins and 4,5 and 6 post-mineralisation stockwork veins on the footwall of Hellyer by Gemmell (1988); Appendix 4.1. Four samples taken from the chlorite-carbonate alteration zone close to the contact with the massive sulphide and in a zone below the contact at 10850N.

Gemmell (1988) concluded that the carbon and oxygen isotope signature from the chlorite-carbonate alteration zone was similar to the stage 2A syn-mineralisation carbonate veins. He interpreted the results to indicate a similar source of carbon and oxygen from either seawater or modified seawater for the dolomite in 2A veins and in the chlorite-carbonate alteration. Similar isotopic studies on the hydrothermal carbonates in VHMS deposits in Tasmania have been conducted by Dixon (1980), Khin Zaw et al. (1996), Khin Zaw and Large (1992).

6.3 Methods

Forty samples were selected from the lateral and vertical extent of the contact and the lower chlorite-carbonate alteration zones. The samples are texturally diverse and taken from a wide area in the footwall from 10250N to 11090N. These samples were analysed at the Central Science Laboratory using the Micromass 602D spectrometer at the University of Tasmania. The samples were heated at 25°C for 24 hours and reacted with H_3PO_4 so that carbon dioxide was given off, according to the method of McCrea (1950).

The results are expressed relative to the Standard Pee Dee Belemnite (PDB) for carbon and Standard Mean Ocean Water (SMOW) for oxygen, measured in per mil (‰)

6.4 Results

6.4.1 Oxygen and carbon isotopes

The $\delta^{18}O$ values of the Cambrian hydrothermal carbonates at Hellyer range from +10.29 to +18.29‰, with an average value of +15.25‰. The $\delta^{13}C$ values range from +0.31 to +2.8‰, with and average value of +1.55‰. Isotope values and locations are in Appendix 4.2 and Figures 3.4 a, b, c, d and e.
Figures 6.1a and b indicate that there are two separate isotopic populations. The data indicate that the contact carbonate alteration zone has carbon and oxygen isotopes lighter than in the lower alteration zone.

6.4.2 Variations in $\delta^{18}O$ and $\delta^{13}C$ in different textural types of carbonate

The dolomites at Hellyer are primary and show no evidence of recrystallisation (refer to chapter 4). Growth bands on the carbonate spheroids have been well preserved and indicate that they have not been disrupted by the later Devonian metamorphism. Figure 6.2a indicates that there is an isotopic distinction between the textures in the carbonates in the contact zone. The shows that $\delta^{18}O$ and $\delta^{13}C$ values decrease from large spheroids to massive clots to small spheroids to veinlets, which indicates that these various textures are precipitating on a cooling trend. The isotopic data from the lower zone shows no differences between textural types (Fig 6.2 b).

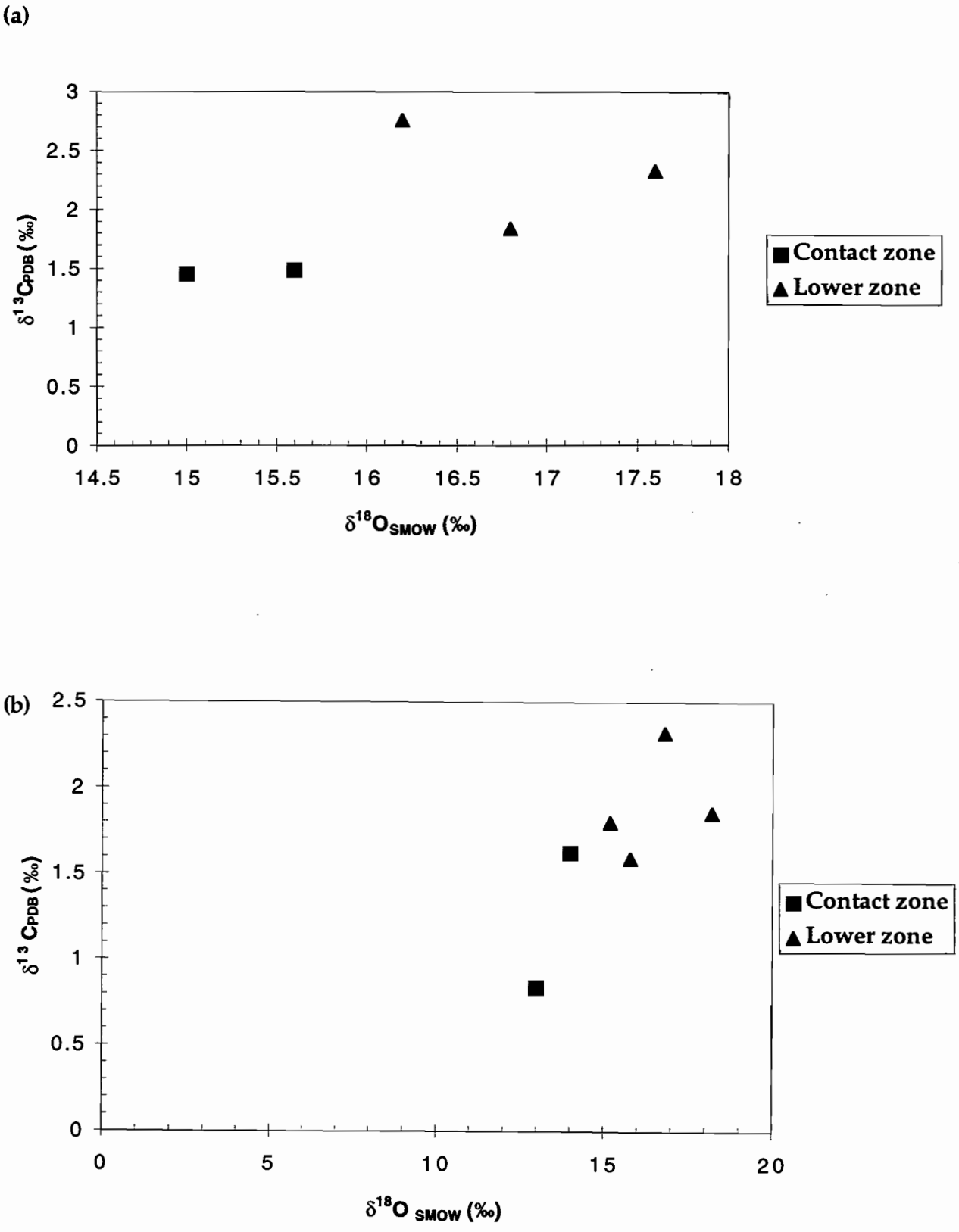

Figure 6.1 Distinguishing the two isotopic populations of the contact and lower alteration zones at 10950N (a) and 11047.5N (b).

6.4.3 Equilibrium Isotopic Fractionation

Fractionation refers to the difference in the isotopic composition of a fluid and the mineral that precipitated from that fluid. It is controlled by mass differences between atoms (Davidson, 1993). The isotopic fractionation factor, or how much fractionation there has been, between a mineral and its fluid is given by the equation:

Oxygen isotopes

$$\Delta AB = \delta_A - \delta_B \sim A(10^6 T^{-2}) + B$$

Δ=change
δ=difference in the ratio of the isotope in the sample relative to a standard.
A=sample
B=fluid
T=Temperature of the fluid (Davidson, 1993)
The experimental oxygen isotope fractionation factor for dolomite-H_2O in H_2CO_3 dominated fluids was calculated by Matthews and Katz (1977) as:

$$\Delta^{18}O\ (AB) = 3.06(10^6/T^2) - 3.24$$

and the experimental carbon isotope fractionation factor for dolomite-H_2O was calculated by Ohmoto and Rye (1979) and Deines et al. (1974) as:

$\Delta^{13}C\ (AB) = 7.53 - 18.11*10^3/T + 8.7307*10^6/T^2 - 8.914*10^8/T^3$ (where H_2CO_3 is the dominant carbon species in the fluid).

A Cambrian seawater isotopic value of $\delta^{18}O$=0‰ and $\delta^{13}C$=0‰ is assumed to create the equilibrium isotopic cooling curve for a fluid of constant composition at $X(H_2CO_3)$=0.01 (Khin Zaw, 1991), (Fig 6.3). The cooling curve represents carbon and oxygen isotopic fractionation at fixed temperatures. It is assumed that H_2CO_3 is the dominant CO_2 bearing species in this system because HCO_3^- decreases with increasing temperatures and is virtually absent at or above 150°C (Bischoff and Seyfried, 1978). The prescence of chlorite indicates that fluid conditions were weakly acidic/alkaline (neutral). Figure 6.4 shows that the stability field of H_2CO_3 encroaches into the alkaline field at higher temperatures.

(a)

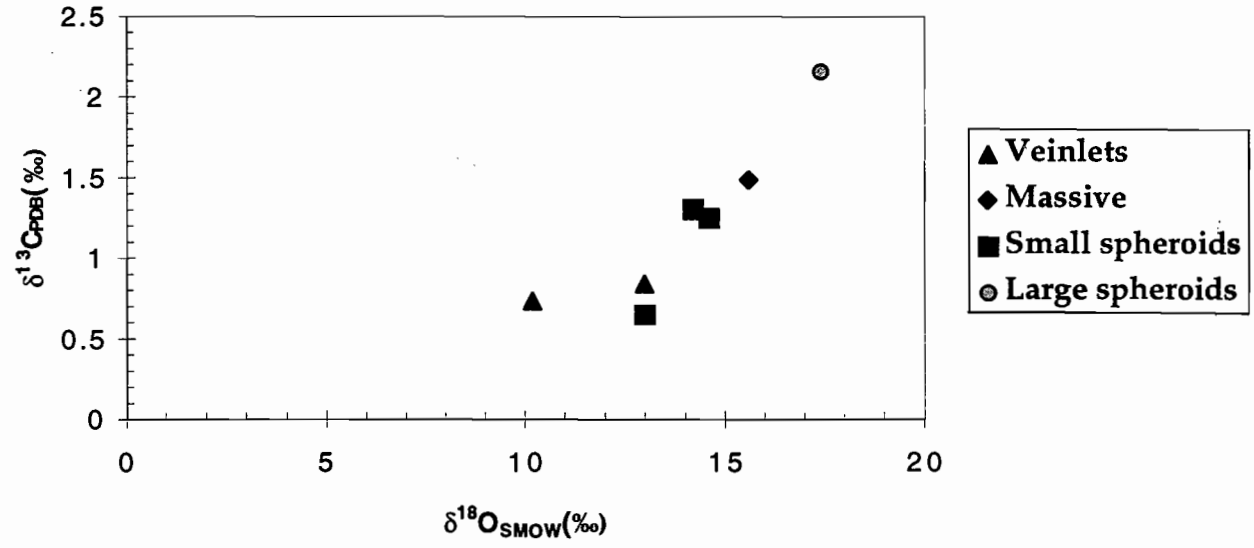

(b)

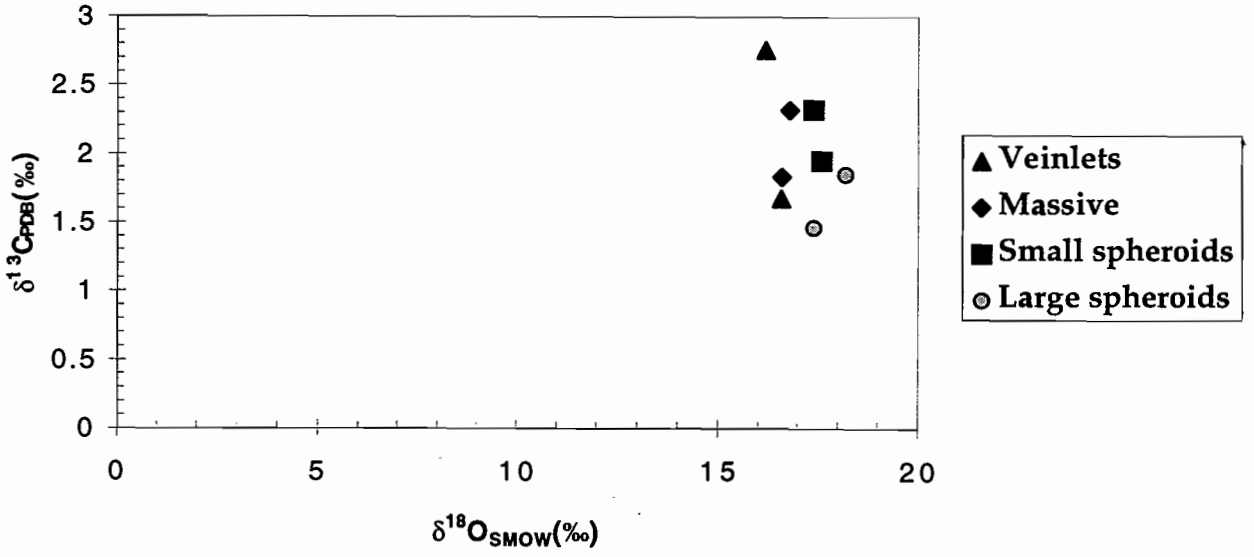

Figure 6.2 Isotopic variation in the textures in the contact alteration zone (a) and the lower alteration zone (b)

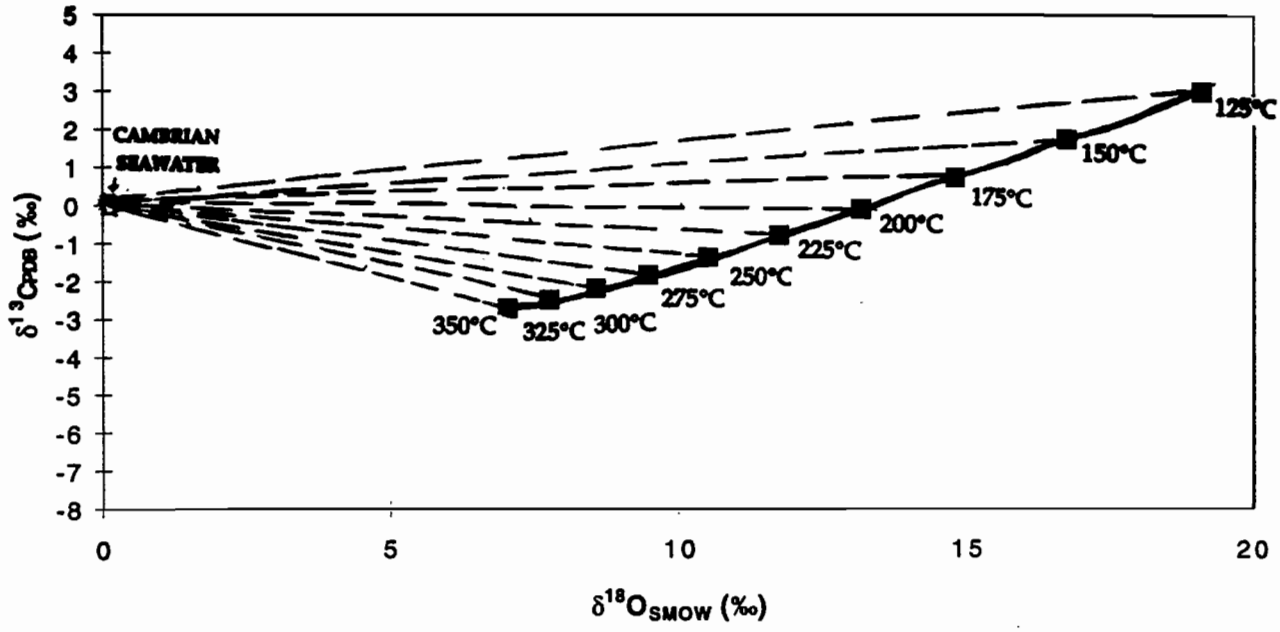

Figure 6.3 Isotopic fractionation curve for Dolomite-H_2O precipitating on a temperature gradient within a H_2CO_3 dominated fluid. Fractionation curves were calculated for carbon from the data of Ohmoto and Rye (1979) and for oxygen from the data of Matthews and Katz (1977).

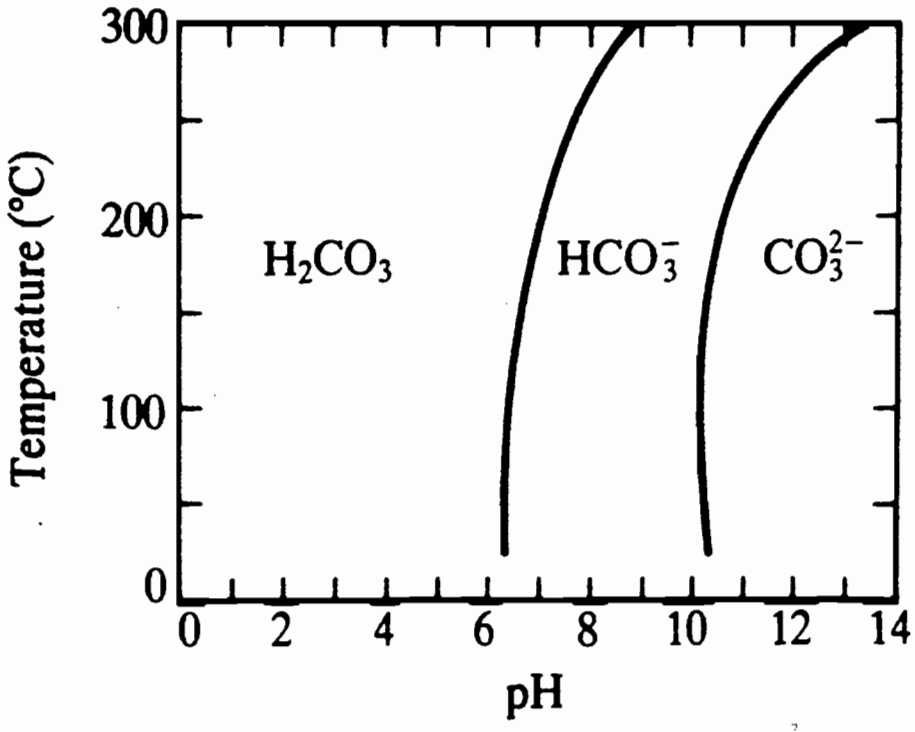

Figure 6.4 The temperature dependance of pH, the concentration of the carbon species are equal (after Krauskopf and Bird, 1969)

6.5 Composition of the hydrothermal fluids

Khin Zaw et al. (1996) report temperature constraints on the formation of stringer veins in the Hellyer footwall. They determined fluid inclusion homogenisation temperatures from the 2A (170°-220°C), 2B (165°-322°C) and 2C (190°-256°C) syn-mineralisation veins through the siliceous core. This data gives a rough temperature range at which the chlorite-carbonate alteration may have formed and indicates that the temperatures in the footwall fluctuated over time. Figure 6.5 illustrates that the temperature stability range for chlorite in volcanic-hosted geothermal systems is broad, between 100° and 250°C (Henley and Ellis, 1983). From this, a temperature of 200°C is applied to the chlorite-carbonate alteration zone on the contact and a temperature of 250°C is applied to the lower zone assuming there were cooler temperatures on the contact (from infiltrating seawater).

Figures 6.6 a and b show the initial composition of the fluid that the dolomites precipitated from and was calculated by overlaying the theoretical curve onto the contact and lower alteration zone data at 200° and 250°C, respectively.

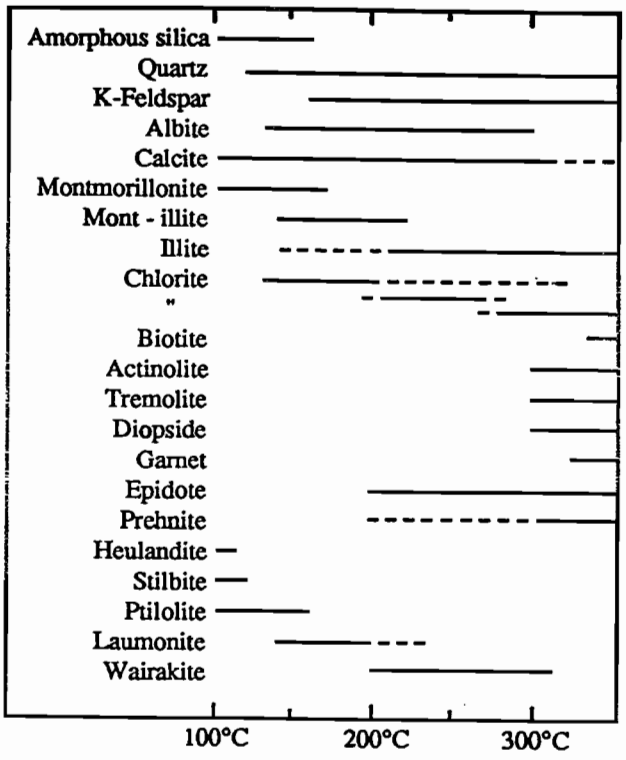

Figure 6.5 Stabilities of minerals in volcanic-hosted geothermal systems (after Henley and Ellis, 1983)

(a)

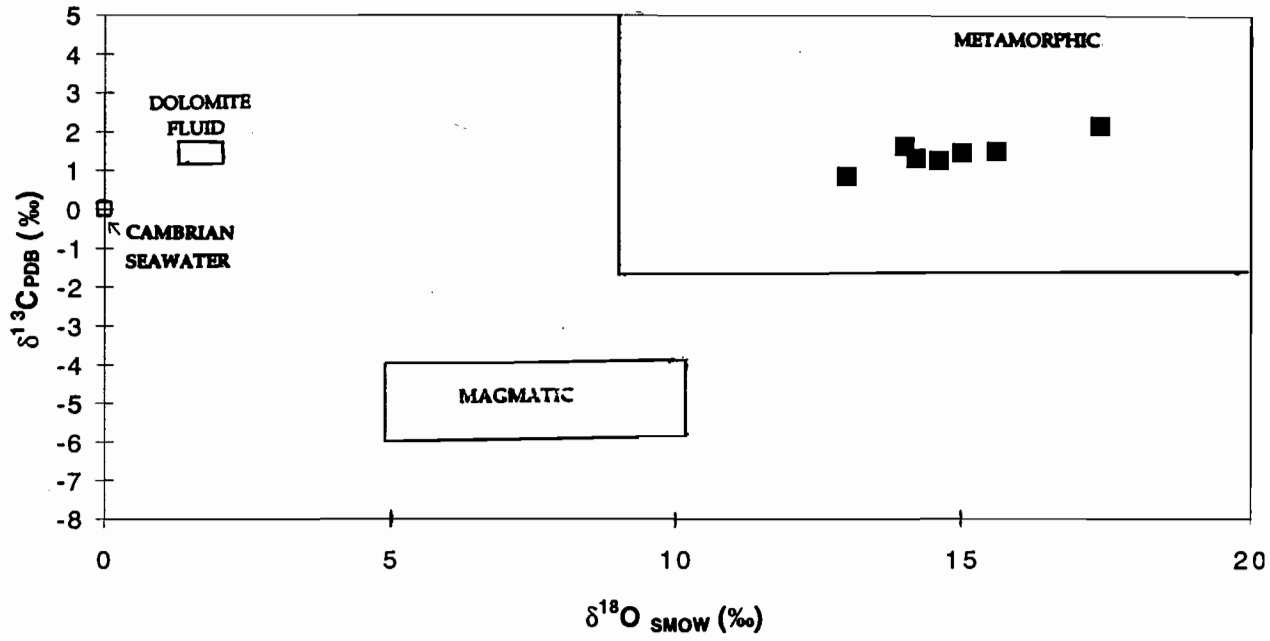

(b)

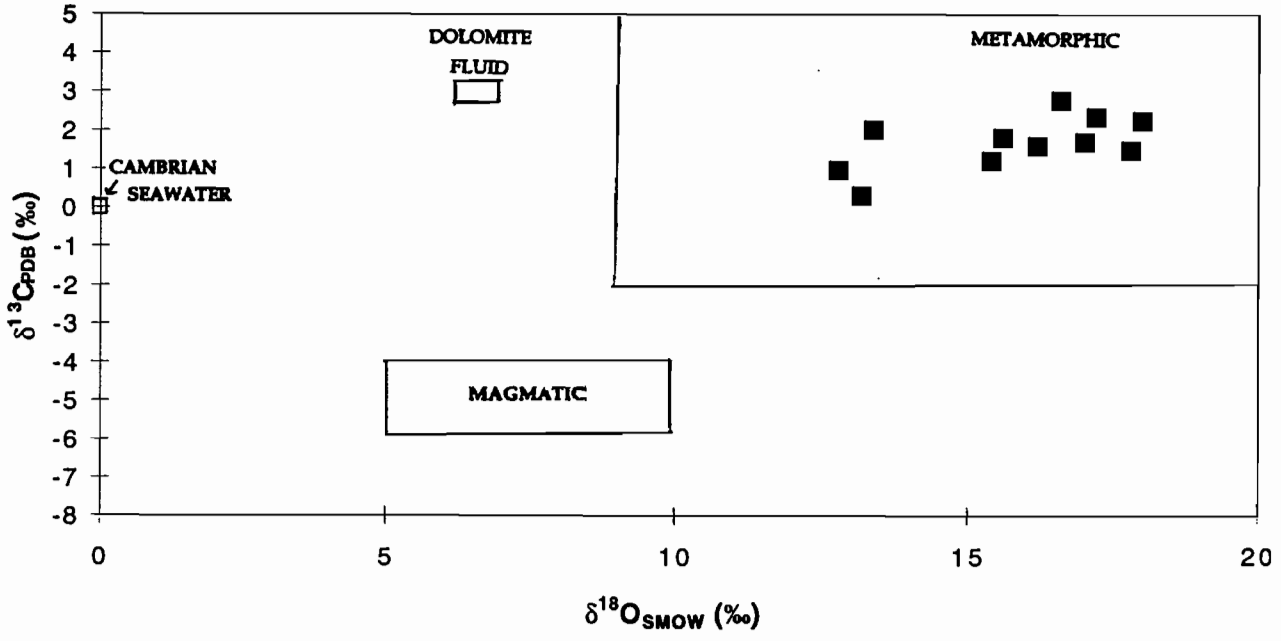

Figure 6.6 The initial fluid composition for the contact (a) and lower chlorite-carbonate alteration zones (b).

The initial fluid composition for the contact zone has $\delta^{18}O$ values between +2 and +4‰ and $\delta^{13}C$ values between +0.8 and +1.2‰. The fluid composition for the lower zone has $\delta^{18}0$ values between +4‰ and +6‰ and $\delta^{13}C$ values between +1.4 and +1.8‰. The contact zone isotope composition is close to the seawater isotopic field. The lower alteration zone has an isotopic composition further removed from the seawater field and closer to the metamorphic field.

Figure 6.7 compares the isotopic signatures of the pre-mineralisation contact and lower chlorite-carbonate alteration zones with the syn- and post- mineralisation stringer veins (from Gemmell, 1988; Appendix 4.2). The data illustrates that the carbonate signatures can be used to distinguish different events of carbonate precipitation in the Hellyer footwall. The post-mineralisation veins are related to the Devonian Tabberabberan Orogeny (Gemmell and Large, 1992) and have significantly lower $\delta^{13}C$ values than the syn- and pre-mineralisation dolomite alteration. The $\delta^{13}C$ values of the syn-mineralisation veins have similar carbon values to the chlorite-carbonate alteration but lower $\delta^{18}O$ values. These varying isotopic values between the alteration zone and the syn- and pre-mineralisation veins could possibly be related to different physico-chemical (temperature, pressure and water/rock ratios) conditions in the footwall over time. According to Taylor (1987) magmatic fluids have $\delta^{18}O$ values in the range of +5 to +10‰ and $\delta^{13}C$ values of -4 to -6‰. Metamorphic fluids have $\delta^{18}O$ values that range from +10 to +25‰ and $\delta^{13}C$ values that range from -2 to +6‰ with temperatures between 200°C and 400°C and CO_2/CH_4 ratios>>1 (Taylor, 1987).

6.6 Interpretation

The different isotopic signatures of the contact and lower zones reflect the fluid conditions during the initial stages of hydrothermal alteration. McArthur (1996) proposes the alteration pipe in the footwall was initiated by the weak circulation of seawater through the sea-floor rocks. He argued that in the later stages of evolution of the alteration pipe, sulphides and metals were leached from the basement rocks.

The contact and the lower chlorite-carbonate alteration zones have higher $\delta^{13}C$ and $\delta^{18}0$ values than Cambrian seawater. Davidson (1993) argued that the when H_2CO_3 is the dominant carbon species in the fluid, cooling will cause $\delta^{13}C$ and $\delta^{18}O$ values of carbonates precipitated from that fluid to be more positive at lower temperatures. Khin Zaw (1991) argued that the increased $\delta^{13}C$ and $\delta^{18}O$ values at the South Hercules deposit was a result of cooling during the later stages of Cambrian mineralisation. This theory could be applied to the pre-mineralisation

chlorite-dolomite alteration zone at Hellyer as it is found in what was the mixing zone between hydrothermal fluids and cooler seawater.

It is argued that $\delta^{13}C$ values could also be increased by the contribution of CO_2 from another source. Golding et al. (1993) interpret the high $\delta^{13}C$ values at the Mount Morgan VHMS deposit (refer to Table 6.1) to be derived from dissolution of marine carbonate in the footwall volcanic succession. There is no evidence of any carbonate rocks in the proximal footwall of Hellyer. There are marine carbonates in Neoproterozoic rocks in western Tasmania, however it is undetermined whether these can be found deeper in the footwall of the Hellyer deposit. Calver (1996) showed that the $\delta^{13}C$ values for carbonate horizons in the Success Creek Group were between -4 and +7‰, and carbonates in the upper Oonah formation were between -6 and +4‰. The carbon values from Hellyer are in these ranges and could indicate incorporation of higher $\delta^{13}C$ values into

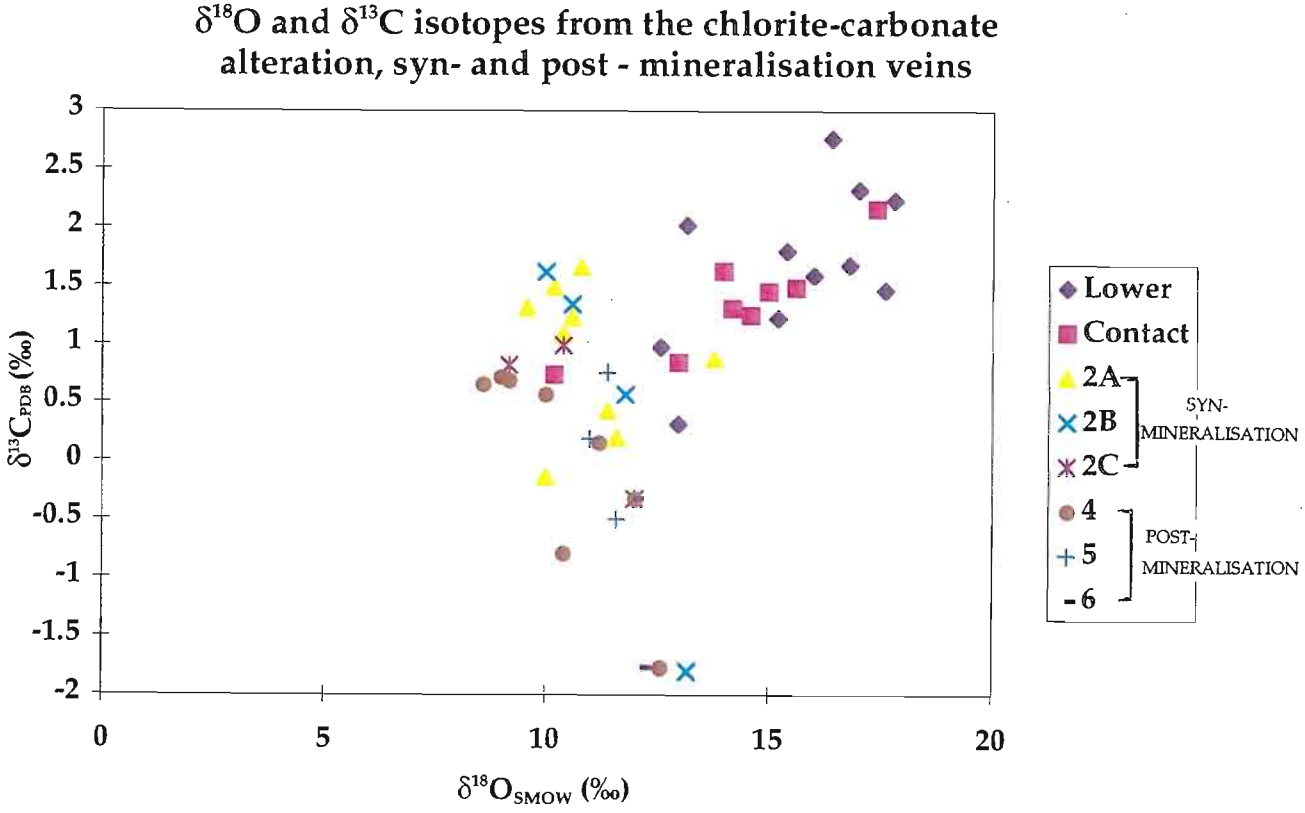

Figure 6.7 $\delta^{13}C$ versus $\delta^{18}O$ for the chlorite-dolomite alteration, syn- and post-mineralisation veins (data from Gemmell, 1988).

deep-seated hydrothermal fluids which then could have travelled up through the footwall to Hellyer. The source of CO_2 in the 2B syn-mineralisation veins is interpreted to be from degassing of a distal magmatic source (Khin Zaw et al., 1996), however the source of CO_2 for the pre-mineralisation dolomite alteration is unknown.

The increase in $\delta^{18}O$ values from Cambrian seawater could be due to a number of factors. $\delta^{18}O$ isotopic modification can be achieved by changes in temperature, pH (Davidson, 1993) and interaction with the wall-rocks over a wide-temperature range. This is ultimately controlled by the water/rock ratio (Taylor, 1987; Huston, 1997). The chlorite-carbonate alteration at Hellyer formed where the water-rock ratios were high. Studies on wall-rock interaction and its influence on isotopic fractionation were not undertaken in this study because no accurate data was available on the initial $\delta^{18}O$ value of the altered rock.

Comparing the two alteration zones indicates that the contact alteration zone has an initial fluid composition of seawater and resulted from the mixing of infiltrating seawater and hydrothermal fluid (modified seawater). The lower alteration zone has a signature suggesting that the hydrothermal fluid was primarily modified seawater with a minor magmatic input (the $\delta^{18}O$ values are in the magmatic range). This difference between the two zones could be due to their relative position and the effect of infiltrating seawater. It is concluded that the original hydrothermal fluid may have been similar for both zones however the infiltrating seawater in the contact may have diluted the original signature (modified seawater±minor magmatic fluid) to cause this zone to have an isotopic signature closer to Cambrian seawater. This greater influence of seawater in the contact zone explains the cooling trend seen in the precipitation of different carbonate textures in the contact zone. The isotopic signature for the fluid in the lower alteration zone is close to the metamorphic field, however, as there is no evidence of metamorphic recrystallisation in the dolomites (refer to chapter 4), therefore metamorphic fluids can be excluded as an influence on the fractionation of the carbon and oxygen isotopes.

6.7 Comparison with other VHMS deposits

Carbon and oxygen isotopic values from the dolomites at Hellyer are considerably heavier than Rosebery North ($\delta^{18}O$=+10.6 to +12.4‰ and $\delta^{13}C$= -8.8‰ to -0.6‰; Dixon, 1980) and South Hercules hydrothermal carbonates ($\delta^{18}O$= +9.8 to +16.7‰ and $\delta^{13}C$= -3.5‰ to 0.6‰ (Khin Zaw and Large, 1992). Khin Zaw (1991) argues

that the isotopic composition of the volcanogenenic fluid from Rosebery is consistent of evolved seawater.

Huston (1997) outlined the carbon and oxygen isotopic fields from various VHMS deposits (Table 6.1). He found that, of the eight deposits studied, the $\delta^{13}C$ range was from 0‰ to -5‰ and the $\delta^{18}O$ values ranged from +6‰ to over +20‰. For some of the VHMS deposits he reviewed, the $\delta^{13}C$ ranges indicated a source of dissolved bicarbonate in seawater and the range of $\delta^{18}O$ values indicated deposition from a hydrothermal fluid at temperatures between 100°C and 300°C. The $\delta^{13}C$ values at Hellyer are higher than the VHMS deposits that Huston (1997) reviewed (Fig. 6.8).

6.8 Conclusions

The $\delta^{13}C$ and $\delta^{18}O$ isotopic signatures of dolomites in the chlorite-carbonate alteration zones at Hellyer indicate that the fluids were predominantly hydrothermal fluid with a minor component of magmatic fluid. It is argued that the positions of the contact and lower alteration zone influenced their isotopic signatures. The isotopic signature in the contact zone indicates that the fluids contained more seawater. It is possible that infiltrating seawater may have diluted the original signature.

The increased carbon values of both zones from original Cambrian seawater may possibly be analogous of cooling by mixing of seawater and hydrothermal fluids. This increase may have possibly been influenced by a distal carbonate source in the footwall. There is no conclusive evidence of any carbonate rocks in the footwall of Hellyer that may have influenced its isotopic signature. The increased oxygen values were possible influenced by changes in temperature and fluid interaction with the wall-rocks. The lower alteration zone has oxygen isotopic values that indicate a magmatic component, however the source of CO_2 for the pre-mineralisation dolomites is undetermined.

Deposit	Age	Range in $\delta^{13}C$ (‰) (mean, n)	Range in $\delta^{18}O$ (‰) (mean, n)	Comments	Reference
East Shasta district, California	Late Permian	-6.8 to -0.9 (-4.6, 6) -12.7 to -1.7 (-6.9, 5) -3.1 to 3.8 (-0.2, 3)	15.9-18.9 (17.1, 6) 13.5-16.9 (14.9, 5) 17.1-19.0 (17.8, 3)	Calcite and dolmite from Afterthought deposit. Calcite from regional alteration halo. Limestone units.	Eastoe and Nelson (1988)
Mt. Chalmers, Queensland	Permian	-4.4 to -1.1 (-3.5, 5)	12.0-18.5 (14.8, 5)	Calcite and dolomite in late stage veins.	D. Huston, unpublished data
Mt. Morgan, Queensland	Devonian	-1.1 to 1.4 (0.5, 23)	8.4-14.6 (9.6, 23)	Limestone lenses in Banded Mine Sequence.	Golding et al. (1993)
Buchans, Newfoundland	Late Ordovician-Early Silurian	-1.6 to -0.5 (-1.3, 5) -4.2 to -1.5 (-3.2, 11)	9.814.2 (12.1, 5) 10.4-20.0 (15.0, 11)	Calcite from mineralized veins. Calcite from metamorphic veins	Kowalik et al. (1981)
South Hercules, Tasmania	Cambrian	-3.5 to 0.6 (-2.1, 12)	9.8-16.7 (12.9, 12)	Carbonate with a large variety of occurrences. Strong correlation between $\delta^{13}C$ and $\delta^{18}O$.	Khin Zaw and Large (1992)
Ducktown, Tennessee	Late Proterozoic	-17.4 to -13.9 (-15.6, 19) -20.2 to -15.2 (-18.8, 5)	7.6-10.2 (8.8, 19) 7.5-9.6 (8.5, 5)	Calcite gangue to ore. Calcite in wall rocks.	Addy and Ypma (1977)
West Bergslagen, Sweden	Middle Proterozoic	-1.8 to 0.1 (-0.6, 8)	13.1-20.2 (16.2, 8)	Calcite and dolomite associated with base metal occurrences.	de Groot and Sheppard (1988)
Horne, Quebec	Archean	-4.5 to -2.0 (-3.2, 3)	7.2-9.5 (8.3, 3)	Calcite from quartz-calcite±chlorite and Remnor Au veins.	MacLean and Hoy (1991)
Hellyer, Tasmania	Cambrian	+0.31 to +2.8 (+1.55, 36)	+10.29 to +18.29 (+15.25, 36)	Dolomite from a pre-mineralisation alteration zone	Gemmell and Large (1992), this study

Table 6.1 Carbon and isotope data from various VHMS deposits, Huston (1997) in comparison to values from the Hellyer deposit.

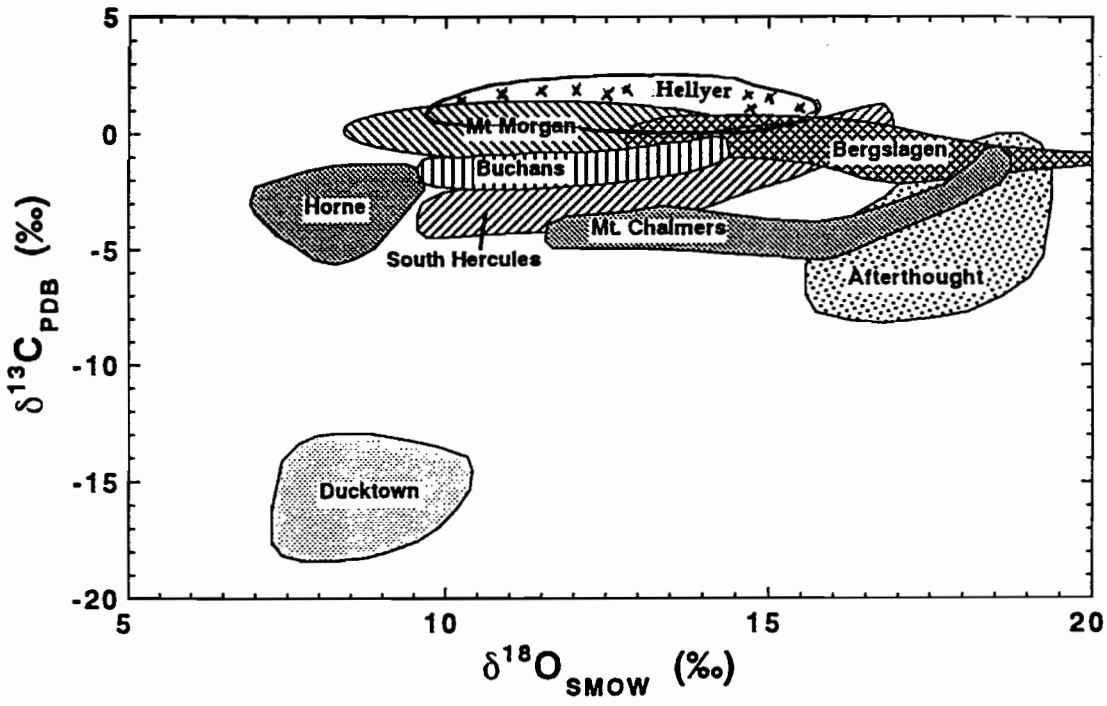

Figure 6.8 Graphical representation comparing the $\delta^{13}C$ and $\delta^{18}O$ values from Hellyer to other VHMS deposits studied by Huston (1997).

CHAPTER 7

FORMATION OF THE CHLORITE-CARBONATE ALTERATION ZONE

7.1 Introduction

This chapter discusses the genesis of the chlorite-carbonate alteration zone beneath the Hellyer VHMS deposit and proposes a model for dolomite precipitation.

The alteration pipe in the footwall of the Hellyer ore deposit formed when circulating hydrothermal fluids interacted with and metasomatised the volcanic host rocks. The same fluids were then responsible for the deposition of the massive-sulphide deposit (Gemmell and Large, 1992). During ore deposition, the intensity of hydrothermal convection was at or near its peak. (Gemmell and Large, 1992).

7.2 Controls on the distribution of the chlorite-carbonate alteration zone

Chlorite-carbonate alteration zones are found in the northern part of the Hellyer ore deposit, on the east flank. This characteristic alteration assemblage can also be found on the west flank, and as small discontinuous patches in the southern part of the ore deposit (Fig. 3.2).

On the ore contact, the chlorite-carbonate alteration assemblage occurs as thin discontinuous lenses centred around the northern and central hydrothermal discharge sites identified by Gemmell and Large (1992); (Fig. 3.1 b). There is also a lower stratiform chlorite-carbonate alteration zone approximately 40 metres below the contact zone. This zone is more laterally continuous than the chlorite-carbonate alteration adjacent to the ore deposit and is only found on the west side of the east flank of the ore deposit, up to 11050N (Fig. 3.2).

The spatial association of both chlorite-carbonate zones to the ore body implies a close genetic association with mineralisation, as carbonate-chlorite assemblages have not been documented at greater depths within the footwall alteration pipe, or distal to the deposit. The carbonates have formed primarily in intense zones of chlorite alteration within the footwall, on the edges of the main hydrothermal vent.

The distribution of the chlorite-carbonate alteration assemblages along the contact of the ore deposit is discontinuous and contains sericite and quartz alteration assemblages. The lower chlorite-carbonate zone with only minor sericite and quartz alteration assemblages. The localisation of the chlorite-carbonate alteration assemblages in the northern end of the ore deposit could be due to intense hydrothermal activity and (consequently) higher water/rock ratios. Gemmell and Large (1992) argued that there are three sites of hydrothermal discharge at Hellyer (Fig. 3.1b). Within the footwall alteration pipe, chlorite, sericite and quartz-rich alteration zones are present in the north, whereas and sericite and quartz alteration assemblages are predominant in the south. Their study concluded that the northern and central feeders were the hottest sites of hydrothermal discharge.

The carbonate alteration on assemblage formed below the base of the ore deposit probably formed at the same time as the alteration assemblage in the lower zone because there are no textural or geochemical differences between the zones (refer to Chapters 4 and 5). It is possible that the two separate zones signify pre-existing seafloors and precipitated at different times, however there is no substantial evidence to support this theory. The lower alteration zone is situated near the Jack Fault, which was once a topographic low on the sea floor when the alteration pipe was forming (McArthur, 1996). The chlorite-carbonate alteration assemblage in the lower zone only occurs on the western side of the east flank (Fig. 3.2) and ends abruptly, inferring that this zone could be lithologically or structurally controlled.

7.3 Textural interpretations in the genesis of the chlorite-carbonate alteration zone

Carbonate textures within the chlorite-carbonate alteration zone have been well preserved and show little or no evidence of metamorphic recrystallisation. The most distinguishing carbonate textures are large and small zoned spheroids (Plates 4.3 and 4.11), and rhombs that occur in a matrix of massive chlorite (Plate 4.17). The spheroids and rhombs have preserved growth bands and rhombic crystal shapes. Chlorite occurs as inclusions within some carbonate spheroids.

Textural evidence that the carbonate spheroid nucleation on quartz crystals associated with clusters of pyrite (Plate 4.15). Most of the primary volcanic textures have been obliterated during metasomatism, although many samples contain relict clast shapes in the chlorite matrix. In some instances, massive carbonate has altered volcaniclastic clasts (Plate 4.24).

Small and large spheroids grew preferentially in chlorite rather than quartz and sericite alteration, this could be related to the low competency of chlorite as compared to sericite and quartz (Plate 4.13). Chlorite also has a high Mg-content and this could supply the Mg required for dolomite precipitation. Offler and Whitford (1992) argued that Mg-chlorite-rich assemblages are formed when unmodified seawater and hydrothermal fluids mix. Magnesium is partly leached from the chlorite and is precipitated as dolomite.

Massive carbonate is also associated with contorted veinlets (Plate 4.19), which, according to Whitford and Craven (1983) is evidence of precipitation in a cavity. Sericite and quartz are also present in the rocks and have overprinted the chlorite-carbonate alteration zone.

7.4 Geochemical controls

An andesitic precursor from the footwall of the Hellyer deposit would gain significant mass when altered to a chlorite-carbonate assemblage. Elements lost in this process are Na and Si (feldspar destruction) and elements gained are Mg, Ca and Fe (chloritisation and dolomitisation of the host rock). This large mass gain in the rock could generate voids for carbonates to grow. At Hellyer the chlorite-carbonate alteration whole-rock geochemistry does not change between the contact and lower alteration zones.

7.5 Carbon and oxygen stable isotopes

In Chapter 6, carbon and oxygen isotopic data from the carbonates was used to conclude that the fluids responsible for footwall alteration at Hellyer were a combination of seawater and hydrothermal fluids (modified seawater±some magmatic input). The isotopic data indicates that the contact and lower alteration zones were precipitated from fluids with different isotopic compositions.

The contact carbonates have an isotopic signature consistent with modified Cambrian seawater (hydrothermal fluid) mixed with infiltrating seawater. The lower zone signature suggests the hydrothermal fluid was predominantly modified seawater (with a small component of magmatic fluids). The magmatic $\delta^{18}O$ signature may be from the input of CO_2-rich volatiles degassed from a deep-seated magma. There is no textural evidence of metamorphic recrystallisation on the carbonates so their isotopic signature have not been influenced by metamorphic fluids.

Clearly, both alteration zones formed from a single hydrothermal fluid that changed as it interacted with footwall rocks and mixed with infiltrating seawater.

7.6 Conditions for the precipitation of hydrothermal dolomites

7.6.1 Previous work

Khin Zaw et al. (1996) proposed some temperature, pressure, salinity and pH constraints on the depositional environment of the chlorite-carbonate alteration zone. They concentrated on the syn- and post-mineralisation veins passing through the alteration pipe. Fluid inclusion studies on the 2B syn-mineralisation veins indicated that the ore fluid had a high salinity of 11 eq. wt% NaCl, approximately 2-3 times higher than modern-day seawater).

Khin Zaw et al. (1996) illustrated that the compositions of the ore fluids fluctuated over time as CO_2 was only present in the 2B syn-mineralisation ore fluids. They argued that CO_2 may have been incorporated into the hydrothermal fluids as a volatile phase exolved off a distal magma source. These fluctuations could be characterised by increased CO_2 concentrations in the pre-mineralisation fluids (dolomite precipitation). Temperatures in the footwall of Hellyer also fluctuated dramatically, this is shown by the temperature differences between the 2A (170°-220°C), 2B (165°-322°C) and 2C (190°-256°C) syn-mineralisation veins (Khin Zaw et al., 1996). These temperature ranges bracket the possible temperatures at which the chlorite-carbonate alteration could have formed. It is assumed, based on alteration rank (Fig. 6.4), that the temperatures of formation of the chlorite-carbonate alteration zone were between 200° and 250°C. There has been no fluid inclusion studies on the dolomites to substantiate this.

7.6.2 Physico-chemical conditions of carbonate deposition

Precipitation of carbonate is proportional to temperature, calcium ion activity, the amount of CO_2 in the solution (or the pH) and the partial pressure of the CO_2 above the system (Krauskopf and Bird, 1995). Calcite has retrograde solubility, so that its solubility decreases with increasing temperature (Ellis, 1963). The pH of the solution also influences the solubility of calcite, such that a decrease favours an increase in the solubility of calcite, (the forward reaction in equation (1)), similarly an increase in pH favours precipitation of calcite. A CO_2 increase in the solution causes more calcite to dissolve and a decrease in CO_2 in the solution favours an the precipitation of calcite (Krauskopf and Bird, 1995).

$CaCO_3 + 2H^+ \longrightarrow Ca^{2+} + H_2CO_3$ (aq) **(1)**

7.6.2.1 Carbonate deposition in subaerial geothermal systems

Simmons and Christenson (1994) studied the origin of hydrothermal calcites forming in the Broadlands-Ohaaki goethermal system in the North Island of New Zealand. They argued that for most geothermal systems, temperature, fCO_2 boiling, mixing, water/rock interaction and pH are the limiting factors that control the precipitation of calcite.

(Browne, 1987) compared the alteration mineral assemblages at the carbonate-rich Broadlands and the carbonate deficient, calc-silicate-rich Wairakei geothermal fields. He related the abundance of calcite at Broadlands to high concentrations of CO_2 in the hydrothermal solutions. This analogy could be used for the precipitation of dolomites at Hellyer. Figure 7.1 is an stability diagram for calcium and magnesium minerals at 260°C. For a particular molality of CO_2 the carbonate field can be plotted as a horizontal line at a specific value of log $(a_{Ca^{2+}}/a2_{H^+})$, (Fig. 7.1).

Above this horizontal line the solution is saturated with respect to calcite and it precipitates, below this line kaolinite and chlorite are stable and will precipitate. Therefore calcite will precipitate when the molality of CO_2 and the activity of Ca^{2+} increases and pH of the fluid increases (hydrogen activity decreases).

Reed and Spycher (1985) discussed boiling as a mechanism for precipitating calcite. They argue that boiling of fluids a release of CO_2 (g) (at the point of CO_2 saturation) will cause a temperature decrease and release of CO_2 and other volatiles to the gas phase. This decrease in the concentration of H_2CO_3 in the fluid will cause it to be undersaturated with respect to calcite. Reed and Spycher (1985) also note that boiling can increase the pH of the solution, which can counteract the effects of cooling and cause calcite precipitation. Platey or bladed calcite is evidence that the system has undergone boiling.

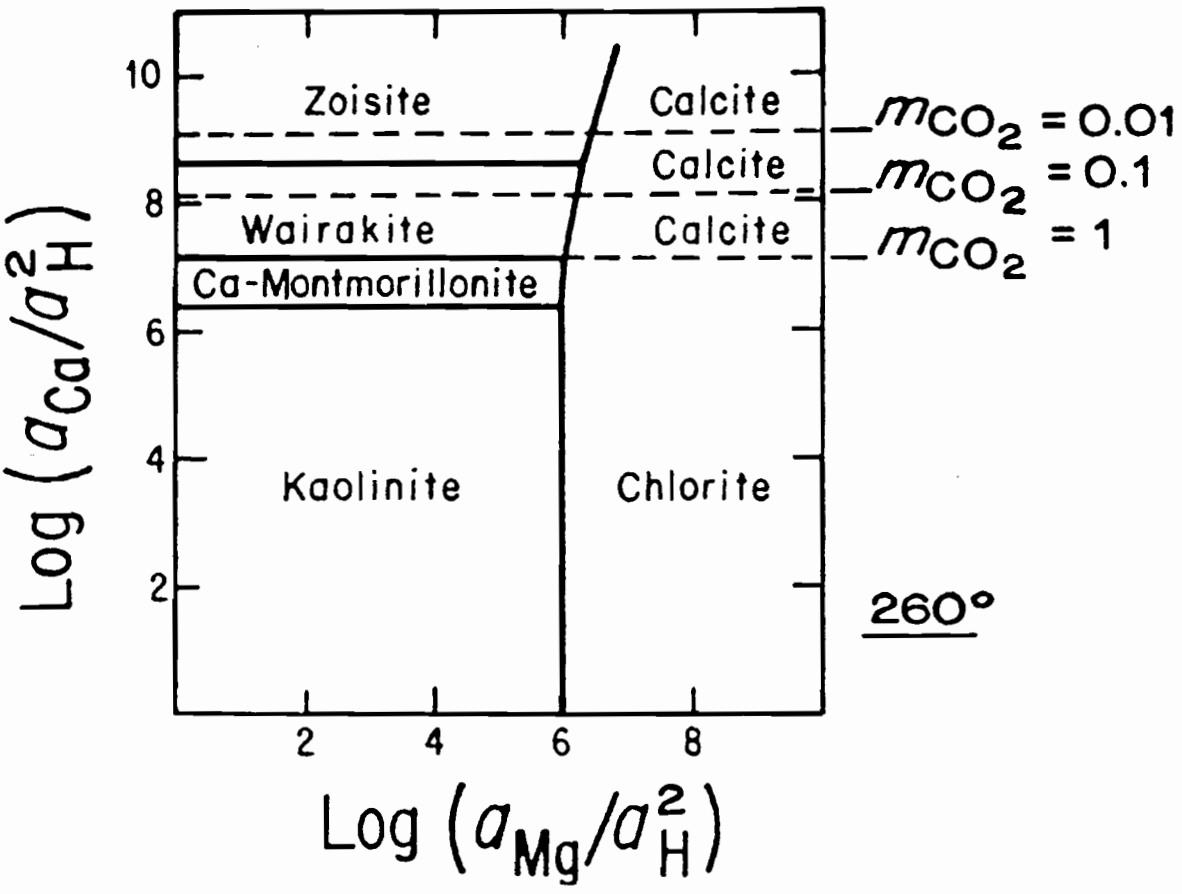

Figure 7.1 Activity diagram for calcium and magnesium minerals at 260°C. At high dissolved CO_2 concentrations, the stability fields for calcium and magnesium minerals are replaced by calcite, or dolomite (after Ellis, 1970)

7.6.3 Dolomite precipitation

Dolomite has a highly ordered structure and consequently grows at a slow rate (Krauskopf and Bird, 1967). According to Holland and Malinin (1979), dolomite precipitates with the same depositional mechanisms as calcite (such as heating, boiling, increasing pH, fluid mixing and water-rock interaction)

Precipitation of calcite or dolomite is dependant on the ratio of the aCa^{2+} to aMg^{2+} (Krauskopf and Bird, 1967). It is most likely that the source of Mg^{2+} is from seawater (Krauskopf and Bird, 1967). Ca^{2+} can be derived from the dissolution of plagioclase, or from seawater (Hill, 1996). Dolomite can also form from the dolomitisation of marine calcite on the seafloor, (Hill, 1996). The dolomites at Hellyer show no evidence of replacement of pre-existing calcite and it is concluded that the dolomites precipitated directly from the hydrothermal fluids.

7.6.4 Discussion

The carbonate alteration assemblages at Hellyer occurs as a patchy and discontinuous zone between the top of the chlorite alteration zone and the ore and within a lower zone 35-45 metres below the ore deposit. The footwall carbonate alteration is more texturally diverse and more prominent in the footwall than the carbonate associated with the ore or the hangingwall basalts.

As discussed in chapter 6, the presence of chlorite in this alteration zone is consistent with the fluids being weakly acidic/alkaline (neutral). The temperatures of formation of the chlorite-carbonate alteration zone (200°-250°C) indicate that the dominant carbon species is H_2CO_3, as at these temperatures H_2CO_3 encroaches into the alkaline field (refer to Fig 6.4.). Under these weakly acidic/alkaline (neutral) conditions, calcite or dolomite may not be stable if CO_2 concentrations are too low, (Fig. 7.1). As discussed earlier, calcite precipitation is favoured by high Ca^{2+} activity and high pH conditions. High CO_2 concentrations in the fluid also favour calcite precipitation as does increasing temperature and boiling. In the syn-mineralisation veins of the Hellyer footwall, there is no textural or fluid inclusion evidence of boiling (Khin Zaw et al., 1996), and a pH increase induced by degassing cannot be applied as a depositional mechanism. Zheng and Hoeffs (1993) argued that there must be a constant replenishment of CO_2 in the hydrothermal fluids to continue the precipitation of calcite. Therefore the confining pressures must be low enough to prevent saturation of CO_2

(boiling) and the fluids must have been constantly replenished by CO_2 (g) to prevent undersaturation.

Dolomites formed in the upper-most part of the Hellyer alteration pipe, where there was probably a sharp temperature gradient due to the influx of seawater. Cooling would favour carbonate dissolution but this could be counteracted by the pH increase caused by mixing with seawater (pH~8, Bischoff and Seigfried, 1978). If the pH induced by mixing counteracts the cooling effects, dolomite would precipitate. Dolomite appears to have formed preferentially in porous rocks which may have been favourable sites for sub-seafloor mixing. The dolomite textures in the footwall could be directly related to the porosity of the host rocks.

There is carbonate alteration in the ore and hangingwall as amydules fill or veinlets (Fulton, 1996), however it is most likely that these carbonates formed where plagioclase crystals altered to calcite upon reaction with CO_2 bearing fluids. The competency of these horizons and lower porosity prevents the abundant carbonate textures as seen in the footwall.

7.7 MODEL FOR THE FORMATION OF THE CHLORITE-CARBONATE ALTERATION ZONE

•Subseafloor volcanics were metasomatised by convecting hydrothermal fluids (evolved seawater) in a topographic low. The volcanics (predominantly andesites and volcaniclastics) were altered to quartz-sericite assemblages. As hydrothermal convection intensified sericite alteration overprinted the quartz-sericite alteration. This was followed by chlorite formation towards the centre of the alteration pipe (Fig. 7.2 a)

• Chlorite and pyrite alteration assemblages were precipitated when 200° to 250°C weakly acidic fluids upwelled through the sub-seafloor volcanic rocks.

Equation (2) shows feldpars in andesites alterating to chlorite

$$CaAl_2Si_2O_8 + 4NaAlSi_3O_8 + 9MgCl_2 + 12H_2O + 4O_2 \longrightarrow$$

Ca-Plagioclase **Na-Plagioclase**

$$3Mg_3Al_2Si_4O_{10}(OH)_8 + CaCl_2 + 4Na^+ + 16Cl^- + 2SiO_2 + 12H^+ \quad (2)$$

Mg-Chlorite

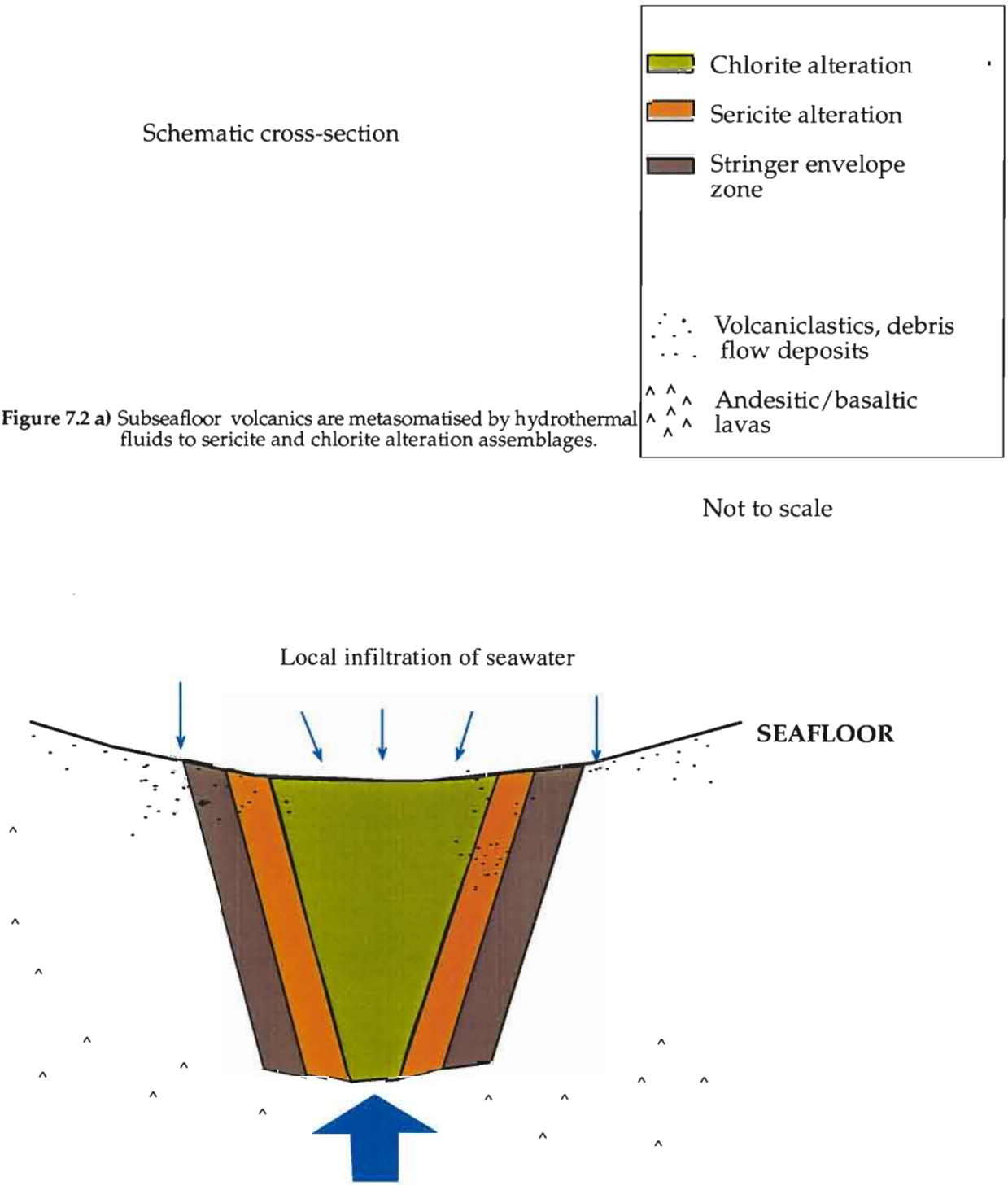

Figure 7.2 a) Subseafloor volcanics are metasomatised by hydrothermal fluids to sericite and chlorite alteration assemblages.

At some point, the fluids became more CO_2-rich, possibly due to magmatic degassing (as H_2CO_3) increased. As the hydrothermal fluids mixed with ambient seawater in porous volcano-sedimentary rocks near the sea-floor a pH increase coupled with increases in Ca^{2+} and Mg^{2+} concentrations caused dolomite to precipitate (equation 3). It nucleated on quartz crystals in the chloritised volcaniclastics just below the seafloor (the contact zone). Carbonate precipitated as the hydrothermal fluids migrated through porous/permeable lithologies. The lower carbonate alteration zone formed as a result of the hydrothermal solutions migrating through and precipitating carbonate in a porous volcaniclastic unit. This unit was close to the main discharge site of hydrothermal fluids which were possibly funnelled to this unit by a structural feature.

$$2H_2CO_3 + CaCl_2 + MgCl_2 \longrightarrow CaMg(CO_3)_2 + 4H^+ + 4Cl^- \quad \textbf{(3)}$$

Dolomite

Based on textural evidence, the carbonate spheroids grew outwards partially replacing the pre-existing chlorite. Pulses of fluid probably passed through the system, each precipitating carbonate of varying compositions. In the northern area, lower in the footwall, fluid discharge was more intense and temperatures were higher based on the evidence obtained by Gemmell and Large (1992). In this region, carbonate textures were controlled by the porosity of the host. In cavities, the fluids could precipitate massive carbonate. In a strongly chloritised zones with only a few nucleation sites, small and large spheroids and rhombs grew. Where there were numerous nucleation sites (such as a volcaniclastic clast), carbonate pods formed. Where there was low primary porosity and no nucleation sites, the carbonate precipitated in fractures (Fig 7.2 b).

• As the hydrothermal activity intensified a quartz alteration assemblage overprinted the chlorite-carbonate alteration (Fig 7.2 c). Metals were leached from the footwall rocks and carried by the syn-mineralisation veins (2B and 2C) to the seafloor.

• During the Devonian, the Jack Fault displaced the ore deposit 30m up and 130m to the north (Fig 7.2 d). The alteration zone on the contact occurs as a halo around the central and northern feeders and the lower alteration zone is closely associated to the Jack Fault on the western side of the east fault block.

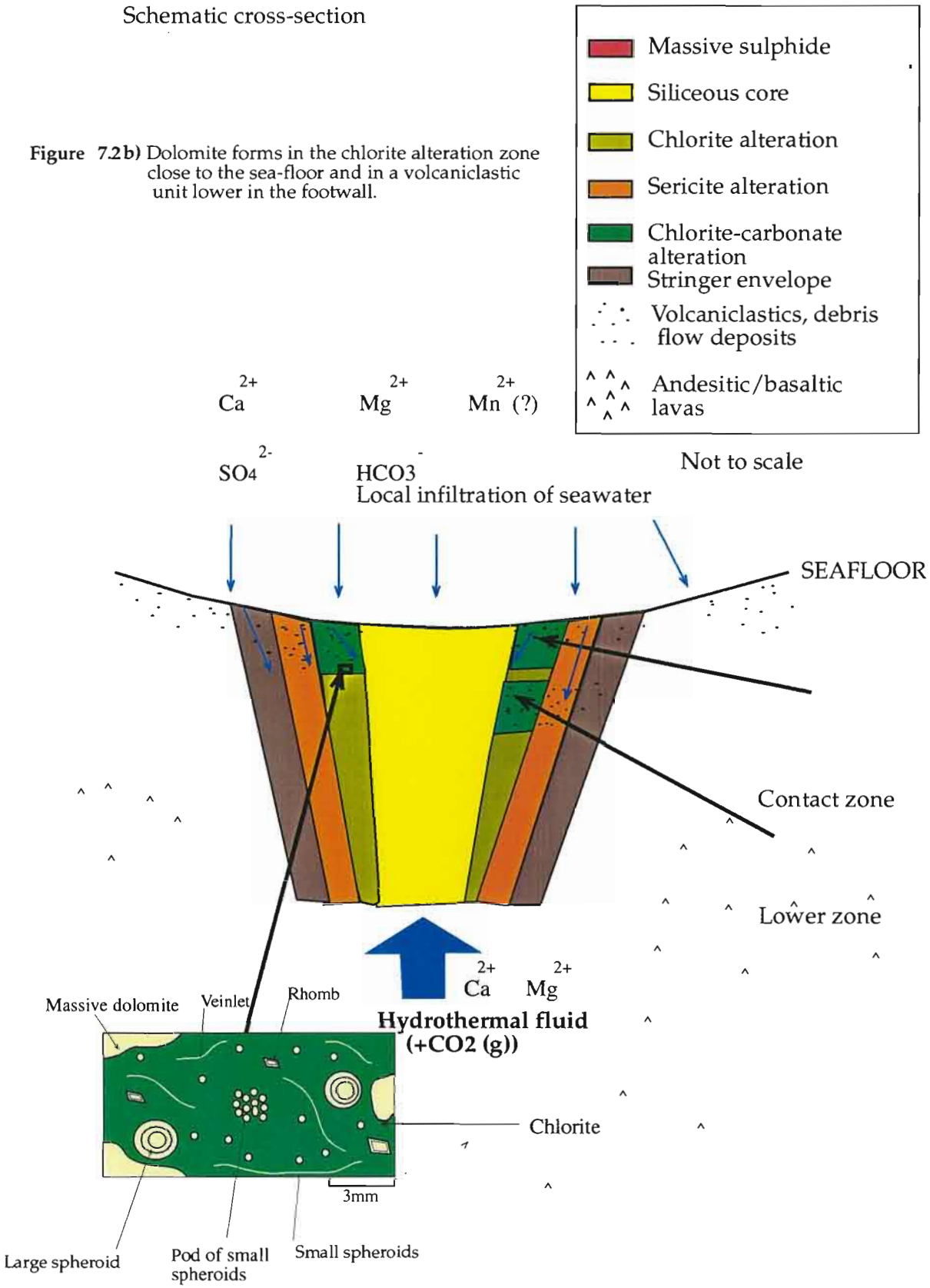

Figure 7.2b) Dolomite forms in the chlorite alteration zone close to the sea-floor and in a volcaniclastic unit lower in the footwall.

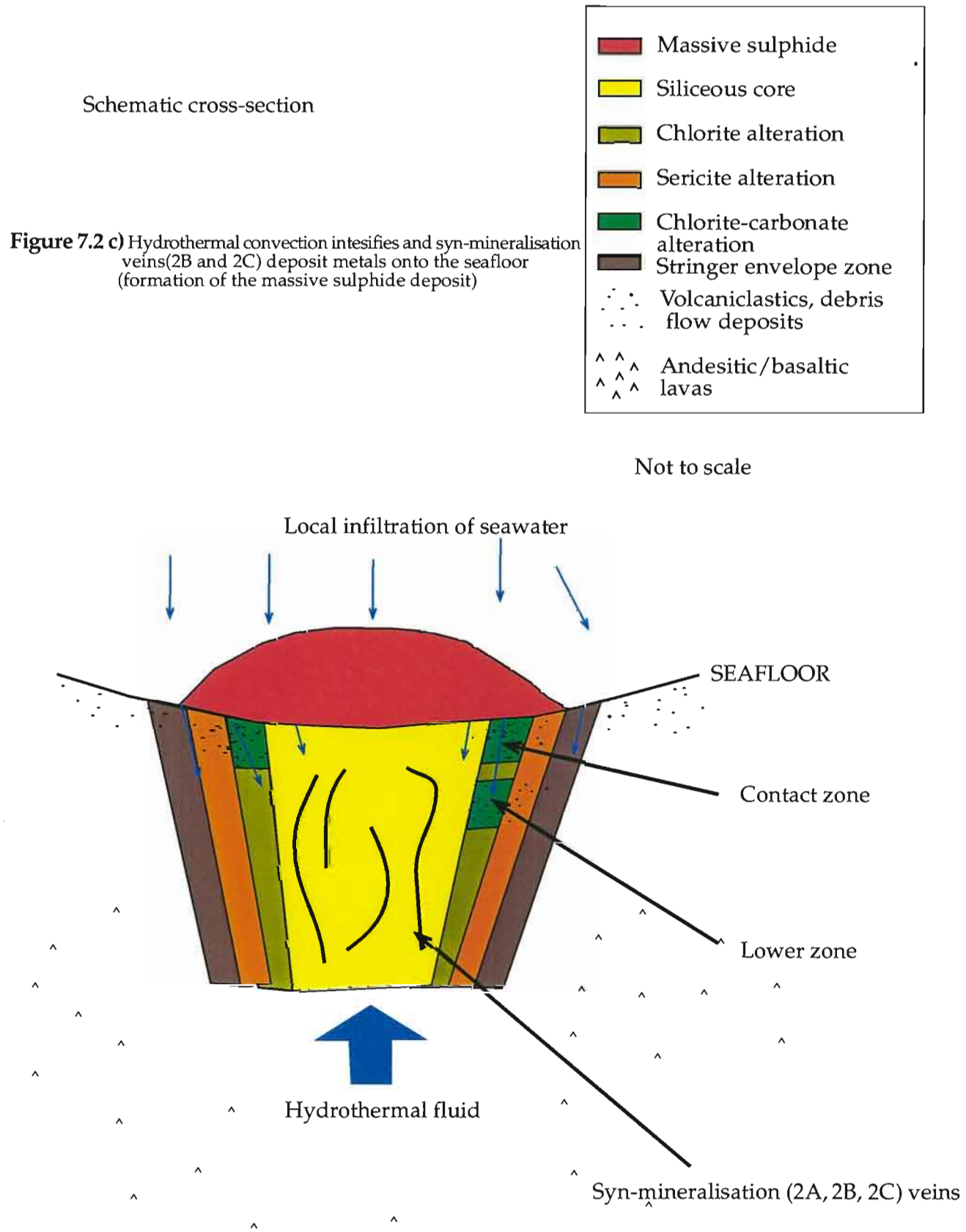

Figure 7.2 c) Hydrothermal convection intesifies and syn-mineralisation veins(2B and 2C) deposit metals onto the seafloor (formation of the massive sulphide deposit)

Schematic cross-section

Figure 7.2 d) During the Devonian, the Jack Fault displaces the ore deposit 30m up and 130m tothe north

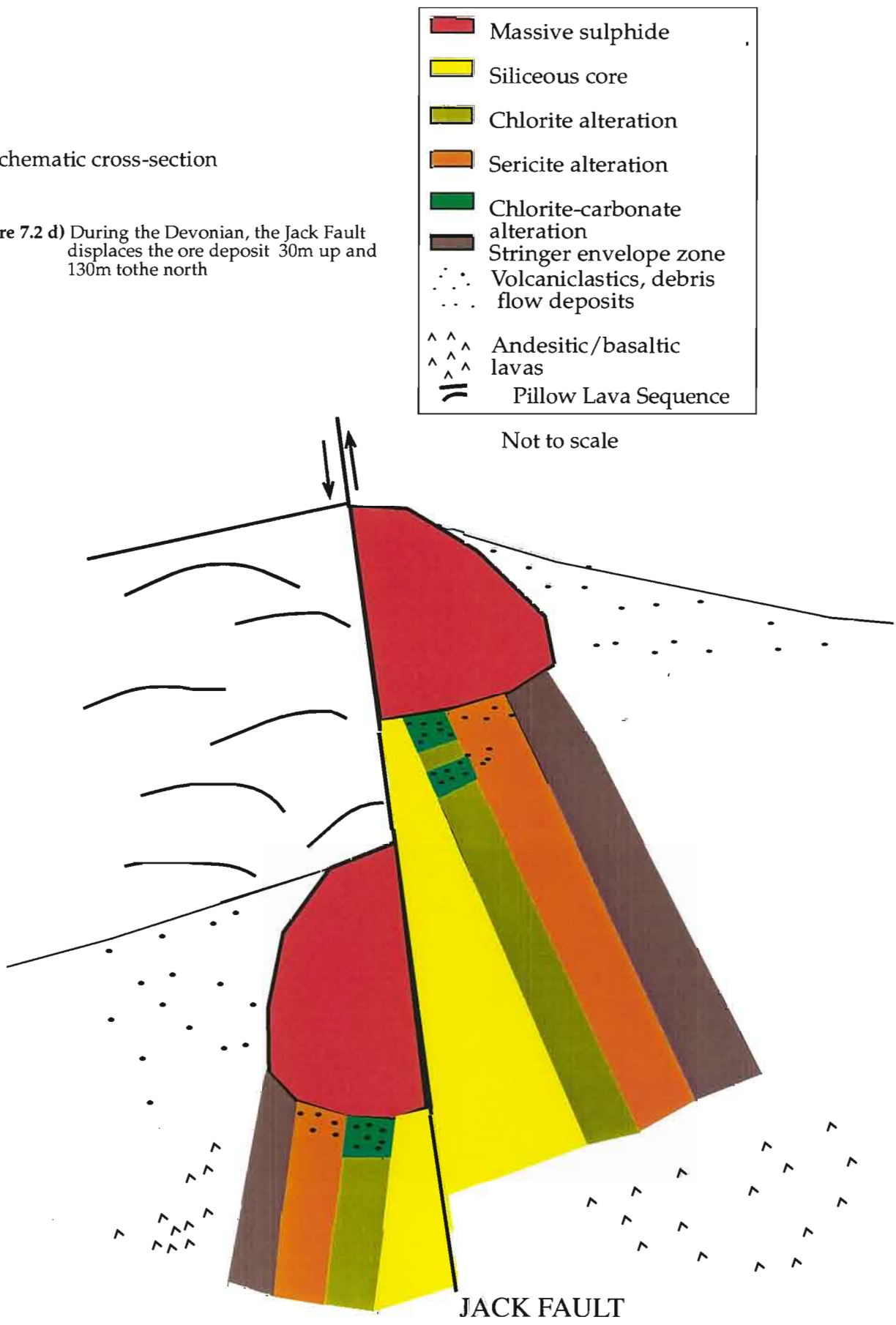

CHAPTER 8

A COMPARATIVE STUDY WITH CARBONATE AND CHLORITE-CARBONATE ALTERATION IN OTHER VHMS DEPOSITS

8.1 Introduction

Studies of VHMS-related alteration have provided insights into the thermal and chemical nature of fluids that precipitated metals onto the sea-floor (Franklin et al., 1981). A number of studies have concentrated on the relationships between each alteration zone surrounding an ore deposit as they impact on exploration.

This study concentrates on chlorite-carbonate alteration assemblages which usually exist in characteristic semi-conformable zones below VHMS ore deposits. At Hellyer, the chlorite-carbonate alteration has distinctive carbonate textures, formed in relatively permeable rocks and is arguably, an alteration assemblage derived from the mixing of seawater and hydrothermal fluids. This type of alteration has been recognised in a number of other deposits in western Tasmania, at Thalanga in northern Queensland; and some Mattabi-type deposits in Canada. This chapter will characterise the similarities between the chlorite-carbonate and carbonate alteration seen at Hellyer and other deposits but will concentrate on comparison with the Que-River deposit.

Chlorite-carbonate alteration is generally not the main focus of publications describing VHMS deposits and carbonate alteration assemblages associated with VHMS deposits are briefly mentioned. For this reason details on texture, distribution and physico-chemical conditions for carbonate deposition are limited.

Table 8.1 characterises the similarities and differences between carbonate and chlorite-carbonate altered VHMS deposits. All of these deposits in western Tasmania, northern Queensland and Canada exhibit carbonate or chlorite-carbonate alteration in close proximity to the ore horizon.

Table 8.1 Summarising the characteristics of chlorite-carbonate and carbonate alteration associated with VHMS deposits

Deposit	Host	Distribution and thickness of the chlorite-carbonate or carbonate alteration zone.	Carbonate composition and textures	Genetic interpretation chlorite-carbonate alteration
Hellyer, western Tasmania, (Gemmell and Large, 1992) Cambrian	Andesites, basalts, volcaniclastics, epiclastic debris flows. Underlain by chlorite, silica and sericite altered rocks	Found in the footwall on the ore contact as a discontinuous horizon, 10-15m thick. Also in a lower, stratabound zone 35-45m below the ore deposit that is more chloritic and continuous.	Mainly Fe-rich dolomite • spheroids • rhombs • massive • pods • veinlets	• At the final stages of alteration, when cooler sea water mixed with warmer hydrothermal fluids. • Direct replacement of Ca-silicates with dolomite •No evidence of dolomitisation on the sea floor.
Que River, western Tasmania (Offler and Whitford, 1992; Whitford and Craven, 1983) Cambrian	Basalts, andesites, dacites, minor rhyolites, tuffs and epiclastics.	Chlorite-carbonate alteration occurs as elongate lenses on the western and eastern sides of the main ore deposits. Also associated with quartz and sericite	In the less altered rocks-ankerites, ferroan-dolomites. In the more altered rocks magnesian-siderite, ferroan-magnesite and calcite Metamorphic and hydrothermal carbonates • coarse-grained carbonate • fine-grained carbonate • irregular veins •rounded aggregates that are suggestive of nodular growth	Chlorite-rich assemblages formed by the mixing of unmodified seawater and hydrothermal fluids
South-Hercules, western Tasmania (Khin Zaw and Large, 1992) Cambrian	Fine-grained, siliceous, tuffaceous sediments. Sericitic feldspar porphyritic volcanics. Underlain by silicified and chloritised rocks.	Chlorite-carbonate blebs are found in the hangingwall epiclastics as a thin lens. Massive carbonate appears as a lateral zone that haloes and interfingers with the sulphide bearing siliceous zone.	Mn-rich kutnohorite and rhodochrosite. • spheroids • botryoidal aggregates • close-packed spheroids • blebby chlorite-carbonate • massive comprising discrete or coalesced spheroids (recrystallised) • cherty carbonate	Cooling and a pH increase. The carbonate formed in the cooler, lateral and stratigraphically higher zones.
Rosebery, western Tasmania (Hill and Orth, 1995; Dixon, 1980; Allen, 1996) Cambrian	sericitic shales, quartz -bearing siltstones, reworked tuffs, carbonate horizons.	Carbonate occurs in lenses immediately along strike from the ore lenses. Massive carbonate is closely associated with the ore which then grades into blebby or poddy carbonate. Associated with quartz, chlorite, and sericite. Overprinted by sulphides	calcite, kutnohorite and rhodochrosite • zoned spheroids • blebby • rhombs • massive • nodules • lozenge • platey • colloform • diagenetic	Carbonates formed early . Carbonates precipitated when seawater mixed with warmer hydrothermal fluids. No evidence of seafloor precipitation. Reaction between hot acidic CO2 bearing fluids and felsic glass replacing pumice with carbonate

Table 8.1 continued

West Thalanga, northern Queensland (Hermann, 1994) Cambrian-Ordovician	Quartz-rich rhyolitic volcaniclastic mass flow sediments and coherent, quartz feldspar porphyry and chlorite-tremolite-carbonate rocks.	Chlorite-carbonate-tremolite rocks exist in a thin (<1m-20m) stratiform lens extending for more than 150m laterally and vertically at the contact between quartz-sericite-pyrite altered rhyolitic volcanic footwall rocks and the ore horizon.	Calcite • massive • veins • sparry patches	Developed in relatively cool parts of the hydrothermal system at the mixing zones of seawater and hydrothermal fluid. Tremolite and chlorite are metamorphic phases. Carbonate is late in the paragenetic sequence. Suggested that these assemblages had precursors of quartz and dolomite that were converted, under metamorphism, to the tremolite-calcite assemblages
Kutcho Creek deposit, North B.C, Canada Permo- Triassic (Barrett et al., 1996)	Rhyolitic pyroclastic and fragmental rocks. The footwall comprises dacites, volcaniclastics, pyroclastics and a felsic lapilli tuff that has been hydrothermally altered	Carbonate, pyrite and sericite alteration are found in the felsic lapilli tuff as a semi-conformable zone. This contains thin beds of mudstone that have been altered by carbonate. The alteration zone extends 200m below the sulphide lenses and 20m above them.	Dolomite, Ankerite • disseminated • veins • clots	Carbonate precipitation is favoured in mafic rather than felsic rocks. Alteration of the volcanics to carbonate preceded the formation of the ore deposit.
Mobrun, north-west Quebec, Canada. (Larocque and Hodgson, 1993) Archean	Lapilli ash tuffs, intermediate flows and tuffs. At the 1100 lens the footwall rocks consists of andesites and the host rocks have been altered to quartz, carbonate, sericite and chlorite.	A broad semi-conformable carbonate alteration occurs close to the ore deposit. Footwall lapilli ash tuff contains lithic pumice fragments which have been altered by chlorite,sericite and carbonate. Carbonate alteration exists in the host sequence and in the hangingwall	Ferroan dolomite • Small amygdales -outer rim of carbonate with an inner core of chlorite carbonate • Large amygdales-consist of coarse grained calcite.Calcite replaced by rhombs and fine grained botryoidal dolomite	Carbonisation was more favoured in mafic rather than felsic rocks. Alteration of the volcanics to carbonate preceded the formation of the ore deposit.
Chisel Lake and North Chisel Lake deposit, Canada (Galley et al.,1993) Early Proterozoic	Felsic volcanics and volcaniclastics.	Footwall alteration consists of chlorite, sericite,carbonate Carbonate is associated with the lower parts of the sericite alteration zone (in the lower semiconformable facies) Dolomite is also associated within parts of the ore.	Dolomite also associated with sericite, quartz and aluminosilicates	Carbonate accumulation occurred during the early formation of the hydrothermal vent. Heated seawater then precipitated calcite on the sea-floor which was dolomitised during hydrothermal alteration (metasomatism). Possible seawater derivation of hydrothermal fluids. Evidence of sub-seafloor boiling.

8.2 Comparison of Hellyer to other VHMS deposits

8.2.1 Carbonate Mineralogy

The composition of the hydrothermal carbonates at Hellyer are Fe-dolomites and dolomites. No detailed investigations into the mineral chemistry could be undertaken*.

From the literature, carbonate compositions associated with VHMS deposits include Fe-rich dolomite, ankerite, kutnohorite, rhodochrosite and calcite and can vary around and within the ore deposit. At the South Hercules deposit the composition of the carbonates varies around the ore horizon, with the most common compositions are Mn-rich kutnohorite and rhodochrosite that contain minor iron and magnesium. Carbonates common to chlorite alteration are Fe-rich dolomite and ankerite. The Fe could have been derived from leaching of the footwall rocks or from the sea-water and the Mn could have also been derived from seawater. Carbonates associated with massive silica, sericite, chlorite are a mixture of Mn-rich kutnohorite and rhodochrosite, and dolomite at south Hercules (Khin Zaw and Large, 1992). At Rosebery, Mn-rich rhodochrosite, kutnnohorite and calcite are common and form a Mn halo around the ore deposit (Khin Zaw, 1991; Lees, 1987). Both the South Hercules and Rosebery deposits display varying carbonate compositions with different textures. Braithwaite (1969) found that the spheroidal carbonate at Rosebery was either rhodochrosite or ferroan-rhodochrosite but massive and veined carbonate were kutnohorite. The carbonates are predominantly calcite or dolomite at Thalanga. Kutnohorite and rhodochrosite are also present at Thalanga, however there is no spatial relationship between Mn and ore (Hill, 1996). The Chisel Lake, Mobrun and Kutcho Creek deposits in Canada only dolomite and ankerite have been identified.

8.2.2 Textures

Studies on various deposits in Tasmania and Canada have characterised a number of different carbonate textures (Hill and Orth, 1995; Khin Zaw and Large, 1992; Offler and Whitford, 1992; Hermann, 1994). These textures include large and small spheroids, botryoidal aggregates, rhombs, spots, nodular pods, massive, amygdale fill, patches, clots, veins and cherty carbonate. Most of these textures are seen at Hellyer, however the more distinct large spheroids are only seen in the chlorite alteration zone in the lower zone at Hellyer.

* The electron microprobe was inaccessible during this year

At the Rosebery deposit (Fig. 8.1) the carbonate alteration is associated with sericite-quartz and chlorite alteration assemblages within a pumiceous mass-flow host. Carbonate textures at Rosebery include small and large spheroids, blebs, pods, rhombs and massive carbonate (Hill and Orth, 1995). In some instances the carbonates nucleate off feldspar crystals and pumice fragments and the spheroids are concentrically zoned. At Hellyer, the chlorite-carbonate assemblages alter predominantly volcaniclastic rocks. The carbonate spheroids nucleate off quartz crystals and envelope pre-existing volcaniclastic clasts. The spheroids at Hellyer are very similar to those at Rosebery.

At the south Hercules deposit (Fig. 8.2) there are also a variety of carbonate textures such as spots, spheroids (with chlorite in the core) and recrystallised massive carbonate comprising coalesced spheroids and a cherty carbonate zone consisting of massive fine-grained carbonate (Khin Zaw, 1991).

The Thalanga deposit in northern Queensland has undergone significant deformation, however there are examples of primary carbonate textures still remaining (Hill, 1996). Carbonate textures consist of zoned rhombs, void fill, zoned spheroids, massive, pods, mesh-veined and banded. As at Hellyer most carbonate spheroids occur in massive to foliated chlorite and are also associated with sericite, quartz and pyrite.

8.2.3 Distribution and occurrence of carbonate and chlorite-carbonate assemblages

In all of the VHMS deposits outlined in Table 8.1 carbonate or chlorite-carbonate alteration is closely associated with the ore. Carbonate textures have only been mapped around a select few ore deposits. At Hellyer, most of the textures show no obvious zonation. One direct correlation between all of the deposits including Hellyer, is the carbonate or chlorite-carbonate alteration assemblages have formed in a porous subseafloor unit. Typical precursors are lapilli tuff breccias, pumice breccias and volcaniclastic units. Morton and Nebel (1984) argue that the distribution of alteration facies at the Helen siderite (Fe-carbonate) deposit in Ontario is partly related to the permeability of the original volcanic rock. In this deposit ankerite alteration is in a narrow zone stratigraphically below and sub-parallel to the siderite deposit.

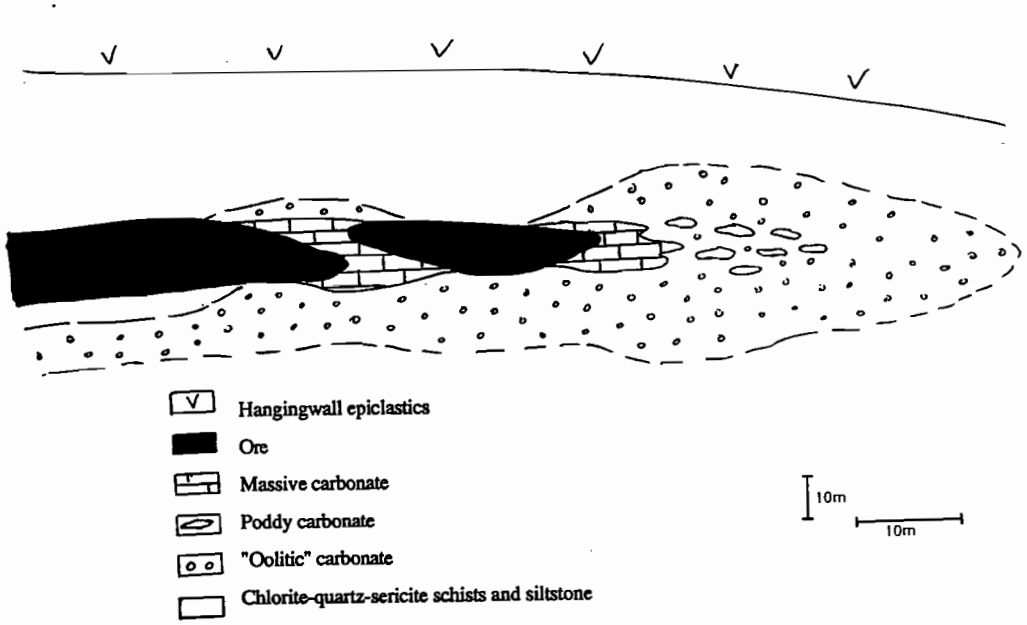

Figure 8.1 Schematic distribution of carbonate textures at the Rosebery Mine, (after Lees, 1987)

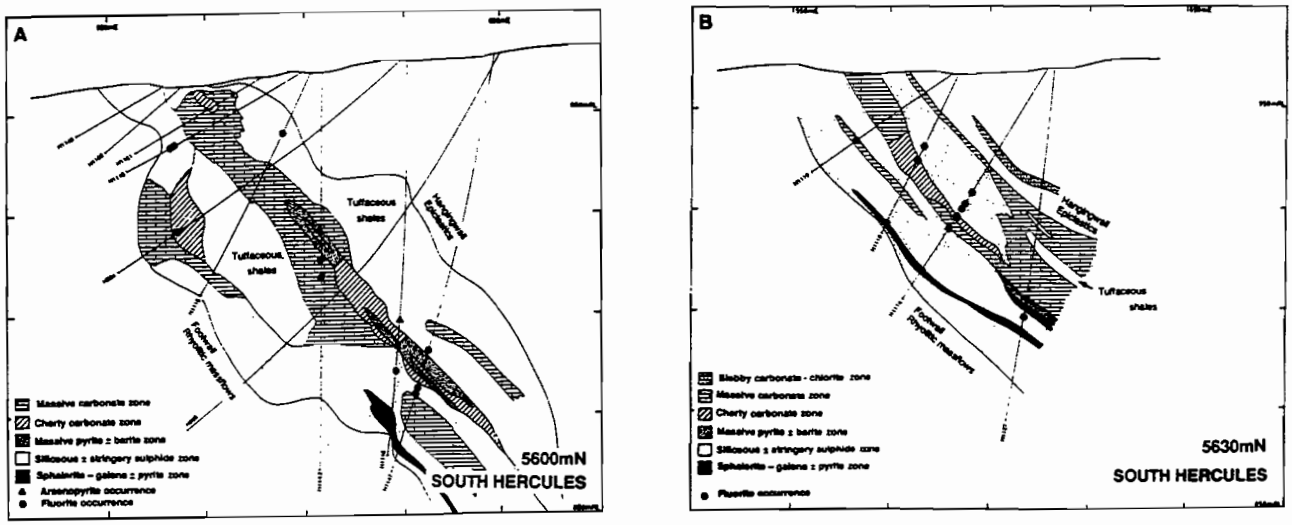

Figure 8.2 Cross-sections at (A) 5600mN and 5630mN (B) through the south Hercules deposit outlining the distribution of carbonate textures (after Khin Zaw and Large, 1992)

At the South Hercules deposit massive recrystallised carbonate alteration envelopes the ore and passes outwards to cherty carbonate (Fig. 8.2). In addition, a blebby chlorite-carbonate zone occurs in the uppermost part of the carbonate facies (Khin Zaw and Large, 1992).

At the west-Thalanga deposit, chlorite-tremolite-carbonate assemblages occur in stratiform lenses up to 6m thick and have been recognised in the host horizons and intercalating with ore lenses (Hill, 1996; Hermann, 1994). Carbonate and chlorite assemblages at the Mobrun deposit in Canada, also alter lithic pumice fragments in a semi-conformable zone proximal to the ore deposit (Larocque and Hodgson, 1993). Both these deposits are comparable to Hellyer where the chlorite-carbonate alteration occurs as thin stratiform lenses on the ore contact. Carbonate alteration at the Rosebery deposit occurs in the footwall of the ore horizon, along strike and rarely in the hangingwall rocks. Massive and blebby carbonate grades into blebby carbonate along strike and pod-like carbonates occur beneath the massive carbonate.

Carbonate alteration associated with VHMS deposits is reinforced by the two-fold Archean volcanic-hosted sulphide deposits in Canada have been divided into categories based on differences in their alteration pipe (Morton and Franklin, 1987). The Noranda-type and Mattabi-type deposits differ with respect to the shape of their alteration pipe, types of host and footwall rocks and styles of alteration. The Mattabi-type deposits have a mineralogically well defined alteration zone and contain mainly fragmental volcanics. Carbonate alteration occurs in these deposits in the alteration pipes and in semi-conformable alteration zones and there is no carbonate alteration associated with Noranda-type deposits (Morton and Franklin, 1987).

8.2.4 Genetic models

Analysis of all the deposits found in Table 8.1 show that carbonate-sericite-quartz alteration and chlorite-carbonate assemblages are an integral part of VHMS alteration. In most of these deposits, carbonate precipitation is associated with chlorite in the most intensely altered parts of the hydrothermal system. Here the salinity, water/rock ratios and temperatures are high and the fluids have high pH (Khin Zaw et al., 1996, Franklin et al., 1981). It is argued that for most deposits carbonate deposition occurs in the cooler parts of the alteration system in the mixing zone between hot hydrothermal solutions and cooler sea water (Khin Zaw and Large, 1992; Hill, 1996; Offler and Whitford, 1992; Hill and Orth, 1995). The Mg^{2+} in the dolomites is sourced from sea-water and the $CO_{2\,(g)}$ is arguably a

volatile incorporated into the circulating hydrothermal solutions, from a distal degassing heat source. These models relate well to Hellyer as the chlorite-carbonate alteration is found only in the hottest part of the system and is in the upper most part of the alteration pipe.

In all of the deposits discussed in Table 8.1, carbonate precipitation is favoured at the point where hydrothermal fluids meet cooler seawater under alkaline conditions. Carbonate can be precipitated directly from seawater (on the seafloor) or from hot, acidic, CO_2 bearing hydrothermal fluids (into a rock unit) when they meet cooler seawater (Offler and Whitford, 1992; Zaw and Large, 1992; Hermann, 1994, Barrett et al., 1996). Hill (1997) argues that the carbonates at the West-Thalanga deposit were formed by precipitation of hot, CO_2 rich fluids because the carbonates show evidence of replacement into a porous substrate, Carbonate at the Chisel Lake deposit in Canada was initially accumulated on the as calcite which was subsequently dolomitised during hydrothermal alteration.
Carbonate alteration, whether associated with chlorite, sericite or quartz alteration appears in the lateral, stratigraphically higher zones of the alteration system where it has more access to sea-water. A porous unit close to the surface would aid the process of carbonate precipitation as it would provide the space for nucleation and growth.

8.3 Comparison of chlorite-carbonate alteration at Que-River with Hellyer.

8.3.1 Carbonate distribution and textures

The Que River deposit is approximately three kilometres to the south-west of the Hellyer deposit and also has chlorite-carbonate alteration assemblages in the footwall. It has been more strongly affected by metamorphism than the Hellyer deposit. The carbonate textures in the footwall at Que-River have been relatively well preserved despite a metamorphic overprint (Offler and Whitford, 1992), however they have not been mapped spatially. The deposit is located in a sequence of tightly folded basalts, andesites, epiclastics, dacites, minor rhyodacites and tuffs (Offler and Whitford, 1992). Mineralisation occurs in five lenses of banded and massive sulphide. Alteration mineralogy consists of quartz, sericite, carbonate, pyrite ± chlorite and occurs in the dacitic, volcaniclastic and andesitic footwall rocks. Chlorite-carbonate alteration forms thin lenses associated with mineralisation. Here, carbonate associated with Mg-rich chlorite is ferroan dolomite and ankerite (Offler and Whitford, 1992). Carbonate (Fe-rich dolomite, ankerite and calcite) and albite alteration are in less altered assemblages below mineralisation. Carbonate in more altered zones is magnesian siderite and

ferroan magnesite and carbonate content decreases with increasing alteration intensity. Quartz and sericite predominate in these zones. In the intensely altered zones volcaniclastic textures are preserved.

In the chlorite-carbonate zone, carbonate occurs as fine and coarse crystalline aggregates (150μm). The fine grained aggregates have a structure indicative of nodular growth. They also form veins that are wispy and contorted, characteristic of growth in a cavity in 'a previously chloritised rock' (Whitford and Craven, 1983). The chlorite-carbonate zone has characteristically low SiO_2 and high MgO. There is also Mn enrichment in the carbonates and chlorites towards the ore deposit. This feature of the carbonate is also present at south-Hercules where the source of the Mn is mainly from seawater. A detailed comparison between the two deposits is given in Table 8.2 and Figure 8.3

8.4 Discussion and recommendations for future work

The main similarity between Hellyer and Que-River, is the close association of carbonate alteration and chlorite-carbonate alteration to the massive sulphide deposit. Chlorite alteration in particular, occurs where hot fluids interact with cooler seawater and in the most pervasively altered part of the system. In both deposits the carbonates are texturally diverse, however no detailed studies on the textural associations and relationships to other alteration types has been conducted at Que-River. Carbonate textures in both deposits are indicative of growth in a relatively porous host, which gives a limitation as to where this type of alteration is found. The chemistry of the carbonates at Que-river differ with different alteration intensity and assemblages and offer a Mn vector to ore. This is an important exploration tool and similar studies should be conducted on the carbonates at Hellyer to find any vertical or lateral changes in chemistry. In both deposits the genetic model proposes that carbonate alteration forms in the mixing zone between seawater and hotter hydrothermal fluids.

Finally, carbonate precipitation is occurring under conditions of high pH (from the interaction with seawater) and at a position where the hydrothermal fluids are the most intense. The rocks that favour this type of alteration are always those that have high porosity and permeability allowing these diverse textures to grow.

Table 8.2 Comparing characteristics of chlorite-carbonate alteration zones at the Hellyer and Que-River deposits

	HELLYER	QUE-RIVER
Footwall Rocks	Massive and fragmented andesitic and basaltic lavas intercalated with polymict mass-flow sediments and volcaniclastics. Chlorite and quartz associated with highly altered zones, sericite on the periphery	Basalt, andesites, volcaniclastics, dacites, closely associated with the ore. Epiclastics and minor rhyodacites. Sericite and quartz in the most highly altered zones, chlorite patchy
Distribution of carbonate and chlorite-carbonate alteration	1-6m discontinuous lenses on the ore -footwall contact. Also as a continuous lens 40m below contact. Carbonate most abundant in chlorite also occurs in sericite and quartz alteration.	Associated with small areas of mineralisation, occurs in intensely altered zones. Occurs in sericite and quartz alteration decreasing towards the ore. Present in separate chlorite zone.
Carbonate textures	Large and small zoned spheroids, rhombs, massive (clots), veinlets. Spheroids and rhombs mainly form in chlorite, veinlets and clots form in sericite, quartz ± chlorite.	Zoned rhombs, irregular and nodular shaped fine and coarse-grained aggregates. No information on where the textural types exist.
Carbonate chemistry and variations around the ore	Dominantly Fe-dolomites, and dolomites, no data on chemistry variation with respect to ore	Highly altered: magnesian siderite, ferroan magnesite, Less altered: Fe-dolomite, ankerite. In chlorite: Fe-dolomites, ankerite. Mn increase towards ore.
Hydrothermal fluid composition	Temperatures variable in footwall based on alteration rank , formed between 200° and 250°C. Ore fluid 8-15 wt. % equiv. salinity	Fluid inclusion data from ankerite and quartz-temperatures at 280°C, assuming 5 wt. % equiv. salinity.
Genetic Model	Carbonate and chlorite assemblages formed near the sea-floor and where there was more access to sea water. Formed in a porous volcaniclastic unit.	Carbonate and (Mg) chlorite assemblages formed under high water/rock ratios where sea-water mixed with hydrothermal fluids.

Figure 8.3 Schematic cross sections comparing occurrences of carbonate alteration at the Hellyer and Que-River deposits

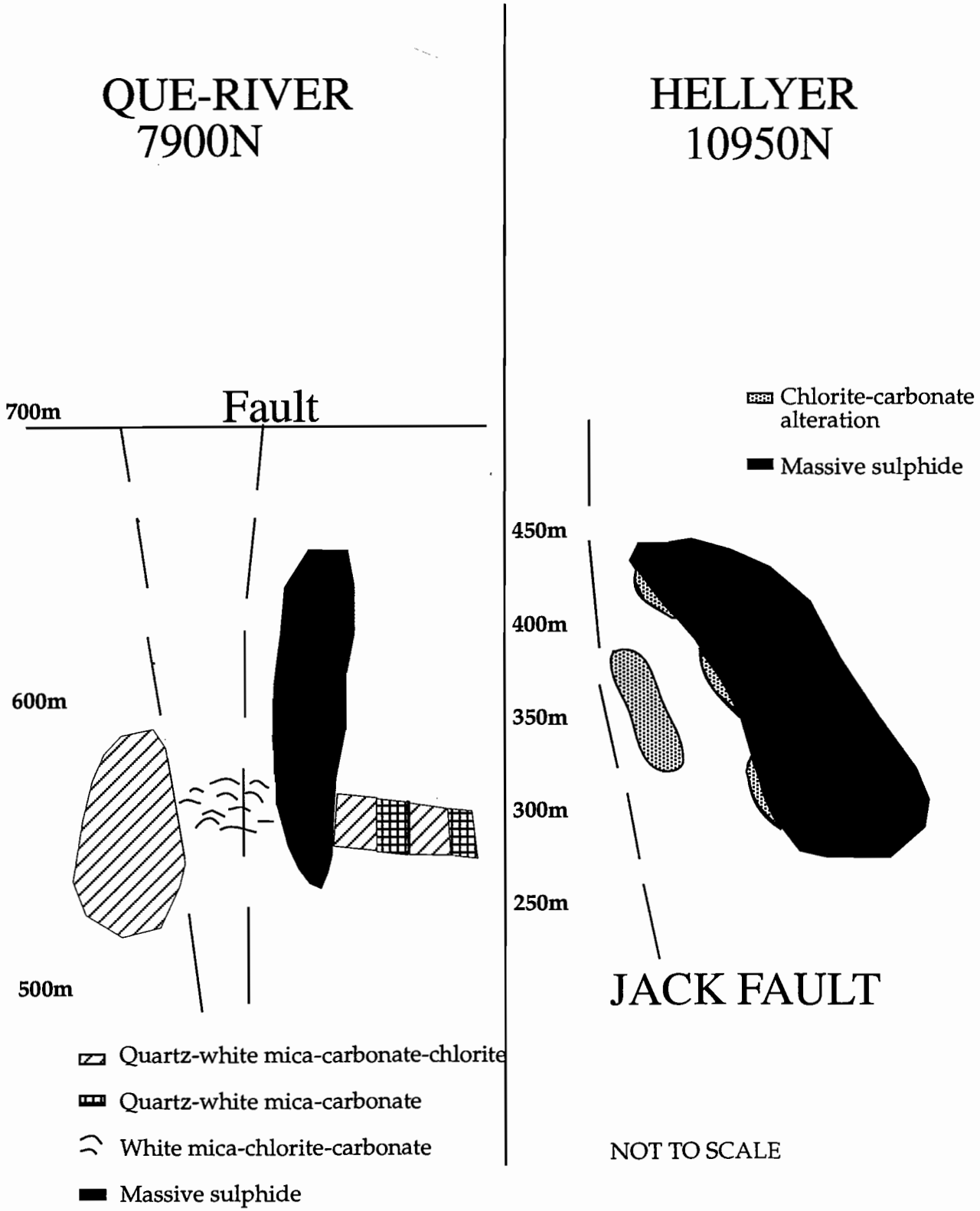

CHAPTER 9

CONCLUSIONS

This study has provided an insight into the distribution, textural characteristics and origin of the chlorite-carbonate alteration in the footwall of the Hellyer massive sulphide deposit. The main conclusions from this study are:

• Chlorite-carbonate alteration at Hellyer is defined as a texturally diverse dolomite in a matrix of fine-grained chlorite. The dolomite may also be associated with sericite and quartz-rich assemblages.

• Chlorite-carbonate alteration zones are concentrated at the top of the chlorite alteration zone around the central and northern hydrothermal discharge sites, as identified by Gemmell and Large (1992). This characteristic alteration assemblage can also be found on the east and west flanks in the northern part of the ore deposit, and as small discontinuous patches in the southern part of the ore deposit

• On the ore contact (the 'contact zone'), the chlorite-carbonate alteration assemblage occurs as thin discontinuous lenses. A lower stratiform chlorite-carbonate alteration zone (the 'lower zone') occurs approximately 40 metres below the contact zone. The lower zone is more laterally continuous than the contact zone and is only occurs on the west side of the east flank of the ore deposit.

• The spatial association of both chlorite-carbonate zones to the ore body implies a close genetic association with mineralisation, as carbonate-chlorite assemblages have not been documented at greater depths within the footwall alteration pipe, or distal to the deposit.

• Carbonate has been identified by staining as predominantly Fe-dolomite and dolomite. The dolomite occurs in five different textural forms; large spheroids, small spheroids, rhombs, veinlets and massive clots. Large and small spheroids have been texturally separated, as the large spheroids have compositional banding whereas the small spheroids do not. The large spheroids have fine-grained cores and the small spheroids, in some instances, nucleate off quartz crystals. Rhombs also have compositional banding. Massive dolomite can surround volcaniclastic clasts and consists of small anhedral grains. The

dolomite textures occur throughout the footwall, however there is no obvious textural zonation. Carbonate textures appear to be associated to the initial permeability of the host rock and it is likely that the dolomite formed in a porous chloritised volcaniclastic unit. The spheroids grew by nucleation on quartz crystals, the rhombs grew in open spaces and the massive carbonate precipitated in voids. The large spheroids preferentially grew in chlorite and it is argued that this could be related to the competency of the chlorite as compared to sericite-quartz alteration. It is also suggested that the Mg in the chlorite could be help activate dolomite precipitation.

- Whole-rock geochemical analysis of the chlorite-carbonate alteration zone has shown that in the alteration process of converting an andesite (assuming that most of the volcaniclastic clasts were andesitic) to chlorite-carbonate involves an elemental mass loss in Na and Si. There is an elemental mass-gain in Mg, Ca, Fe and Mn. The absolute mass gain in this process is approximately 18g/100g.

- Carbon isotopes ($\delta^{13}C$) range between +0.31 and +2.8‰ and oxygen isotopes ($\delta^{18}O$) range between +10.29 to 18.29‰. Isotope studies on the dolomites indicate that they formed either from upwelling hydrothermal fluid (modified seawater with a minor magmatic input) in the lower zone or from the mixing of the hydrothermal fluid with infiltrating seawater in the contact zone. Carbon isotopic values are uncharacteristically high at Hellyer compared with other VHMS deposits and could indicate deep-seated contributions of $\delta^{13}C$.

- Conclusions from a literature review of other VHMS deposits that have carbonate alteration are a) carbonate forms in the mixing zone of hydrothermal fluid and seawater b) it occurs in intensely altered parts of the alteration pipe where water/rock ratios are the highest and c) usually forms in a permeable host such as volcaniclastics, pyroclastics and fragmental rocks. All of these features are similar to the occurrence and characteristics of the footwall carbonate alteration at Hellyer.

- Finally, a model for the formation of the chlorite-carbonate alteration zone has been proposed. Sub-seafloor volcanic rocks were chloritised by convecting hydrothermal fluids. Dolomite only precipitated in chloritised volcaniclastic units near the seafloor or in a shallow sub-seafloor unit. Dolomite precipitation was initiated by CO_2-rich hydrothermal fluids mixing with seawater causing a pH increase. The dolomite preferentially nucleated on quartz grains and clasts in volcaniclastic units. Dolomite only tends to grow in the chlorite as it provided the Mg and was relatively ductile allowing the growth of the dolomites.

References

Allen, R. and Large, R. (1996). Rosebery alteration study. AMIRA Project P439. Studies in VHMS related alteration: geochemical and mineralogical vectors to ore.

Barrett, T.J., and MacLean, W.H. (1993). Lithogeochemical techniques using immobile elements. ***Journal of Geochemical Exploration*, 48 109-133.**

Barrett, T.J. and MacLean, W.H., (1994). Mass Changes in Hydrothermal Alteration Zones associated with VHMS Deposits of the Noranda Area. ***Exploration Mining Geology., Vol 3, No. 2, pp.131-160.***

Barrett, T.J., Thompson, J.F.H. and Sherlock, R.L. (1996). Stratigraphic, lithogeochemical and tectonic setting of the Kutcho Creek massive sulphide deposits, Northern British Columbia. ***Exploration. Mining Geology,*** Vol 5, No 4, pp309-338.

Braithwaite, R.L., (1969). The geology of the Rosebery ore deposit. ***Ph. D Thesis,*** University of Tasmania, Unpub.

Bischoff, J.L., and Seyfried, W.E. (1978). Hydrothermal chemistry of seawater from 25° to 350°C. ***American Journal of Science,*** Vol.278, p838-860.

Browne, P.R.L. (1987). Hydrothermal alteration processes and their recognition *in* ***Proceedings from the Pacific Rim Congress. An international congress on geology, structure, mineralisation and economics of the Pacific Rim***

Calver, C.R (1996). Reconnaissance isotope chemostratigraphy of Neoproterozoic carbonate rocks in western Tasmania. ***Tasmanian Geological Survey,*** **Mineral Resources Tasmania.**

Corbett, K.D. and Komyshan, P., (1989). Geology of the Hellyer-Mt Charter area: Hobart, Tasmania Dept. Mines, Mt. Read Volcanics Proj. Geol. Rept. 1, 48p.

Corbett, K.D., (1992). Statigraphic-Volcanic Setting of Massive Sulphide Deposits in the Cambrian Mount Read Volcanics, Tasmania. ***Economic Geology,*** Vol 87, pp 564-586.

Davidson, G. J. (1993) Carbon/Oxygen Isotopes- their principles and uses in the exploration and understanding of fossil hydrothermal systems. ***Exploration***

Geochemistry and Hydrothermal Geochemistry, **Part 2-** Master of Economic Geology, Course Work Manual 12

Deines, P., Languir, D. and Harmon, R.S (1974) Stable carbon isotope ratios and the existence of a gas phase in the evolution of carbonate ground waters. ***Geochim. Cosmochim.* Acta 38, pp.1147-1164.**

Dixon, G.H. (1980). Geological, geochemical and Stable Isotope studies of the carbonates at Rosebery. ***Honours Thesis,*** University of Tasmania.

Drown, C.G., (1990). The Hellyer Massive Sulphide Deposit. from ***10th Australian Geological Convention, Excursion Guide E1***

Eastoe, C.J., Solomon, M. and Walshe, J.L., (1987). District Scale Alteration with Massive Sulfide deposits in the Mount Read Volcanics, Western Tasmania. ***Economic Geology*** , Vol 87, pp1239-1258.

Ellis, A.J., (1963). The solubility of calcite in sodium chloride solutions at high temperatures. ***Arm Jour. Sci.*** 261 V261: p259-2367.

Evamy, B.D., (1962). The Application of a Chemical Staining technique to a study of dedolomitisation. ***Sedimentology,* 2** pp 164-170.

Franklin, J.M., Lydon, J.W. and Sangster, D.F. (1981). Volcanic-Associated Massive Sulphide Deposits, ***Economic Geology,*** 75th Anniversary Volume, pp 485-627.

Fulton, R. (1996). Hangingwall alteration study, Hellyer Mine, **Amira Project P439.**

Galley, A.G., Bailes, A.H. and Kitzler, G., (1993). Geological setting and hydrothermal evolution of the Chisel lake and North Chizel Zn, Pb, Cu, Ag, Au massive sulphide deposits, Snow Lake, Manitoba. ***Explor. Mining Geol.*** 2: 271-295.

Gemmell, J.B., (1988). Hellyer Stringer Zone Project, Progress Report No.1, ***University of Tasmania.***

Gemmell, J.B., (1989). Hellyer Stringer Zone Project, Progress Report No.2, ***University of Tasmania.***

Gemmell, J.B., (1996). Alteration and stringer zones associated with VHMS deposits. ***CODES Short Coarse Manual 3.***

Gemmell, J.B., and Large, R.R., (1992). Stringer System and Alteration Zones Underlying the Hellyer Volcanic Hosted Massive Sulphide Deposit, Tasmania, Australia. ***Economic Geology,,*** Vol 87, pp 620-649.

Golding, S. D., Huston, D.L., Dean, J.A., Messenger, P.R., Jones, I.. W. O., Taube, A. and White, A.H., (1993), Mount Morgan gold- copper deposit: The 1992 perspective: ***Proceedings of the Australian Institute of Mining and Metallurgy Centenary Conference,*** **Adelaide, April, p.95-112.**

Grant, J.A., 1986, The Isocon Diagram- A simple solution to Gresens' equation for metasomatic alteration **:** ***Economic Geology*** **v. 81, p1976-1982**

Gresens, R.L., (1967). Composition-Volume Relationships of Metasomatism: ***Chem. Geology, V.2, p.47-55.***

Henley, R.W and Ellis, A.J., (1983) Geothermal systems ancient and modern: A geochemical review, ***Earth Science Review., 19: 1-50.***

Hermann, W. (1994) Immobile element geochemistry of altered volcanics and exhalites at the Thalanga deposit, North Queensland, ***Master in Economic geology Thesis,*** University of Tasmania.

Hill, A. and Orth, K. (1995). Textures and origins of carbonate associated with the volcanic-hosted massive sulfide deposit at Rosebery, Tasmania, ***CODES AMIRA Project.*** **P439-Studies of VHMS-related alteration: Geochemical and Mineralogical vectors to ore.**

Hill, A.P. (1996). Structure, volcanic setting, hydrothermal alteration and genesis of the Thalanga massive ulphide deposit. ***PhD Thesis,*** University of Tasmania, Unpub.

Holland, H.D. and Malinin, S.D. (1979) The solubility and occurence of non-ore minerals *in* ***Geochemistry of hydrothermal ore deposits*** (2nd Ed.) Edited by H.L Barnes, John-Wiley and Sons

Huston, D.L., (1997). Stable isotopes and thier significance for understanding the genesis of volcanic-hosted massive sulphide deposits : A Review. *in* ***Volcanic-Associated Massive Sulfide Deposits: Processes and Examples in Modern and Ancient Settings.*** (A volume to accompany a GAC-MDD-SEG co-sponsored short course).

Ishikawa, Y., Sawaguchi, T., Iwaya, S., and Horiuchi M., (1976). Delineation of prospecting targets for Kuroko deposits based on modes of volcanism of underlying dacite and alteration halos: ***Mining Geology,* v.26, p. 105-117 (in Japanese with English Abstracts.)**

Jack, D.J., (1989). Hellyer Host Rock Alteration. ***MSc Thesis,*** University of Tasmania

Khin Zaw (1991). The Effect of Devonian Metamorphism and Metasomatism on the Mineralogy and Geochemistry of the Cambrian VMS Deposits in the Rosebery-Hercules District, Western Tasmania. ***PhD Thesis*** .

Khin Zaw and Large, R.R. (1992). The Precious Metal-Rich South Hercules mineralization, Western Tasmania: A Possible Subsea-Floor Replacement Volcanic-Hosted Massive Sulphide Deposit. ***Economic Geology,* V.87, pp931-952**

Khin Zaw, Gemmell, J.B., Large, R.R., Mernagh, T.P and Ryan, C.G. (1996). Evolution and source of ore fluids in the stringer system, Hellyer VHMS deposit, Tasmania, Australia: evidence from fluid inclusion microthermometry and geochemistry. ***Ore Geology Reviews* 10, 251-278.**

Krauskopf, K.B. and Bird, D.K (1995). Introduction to Geochemistry (3rd Ed.) Mc Graw-Hill, Inc.

Large, R.R, Stoltz, J. and Duhig, N. (1996) Preliminary assessment of MRV geochemical database in terms of possible vectors to ore. ***CODES AMIRA Project P439-*** Studies of VHMS-related alteration: geochemical and mineralogical vectors to ore

Larocque, A.C.L and Hodgson C.J. (1993). Carbonate -rich footwall alteration at the Mobrun Mine, a possible Mattabi-type VMS deposit in the Noranda Camp. ***Exploration Mining Geology,*** Vol. 2, No. 2, pp165-169.

Lees, T.C. (1987). Geology and Mineralisation of the Rosebery-Hercules Area, Tasmania, ***Masters Thesis,* University of Tasmania.**

McArthur, G. J., (1989). Cambrian Mt Read Volcanics and associated mineral deposits-Hellyer. **Geology and mineral resources of Tasmania. Editors Burrett, C.F and Martin, E.L Special Publication 15. Geological society of Australia Inc.**

McArthur, G. J., (1996) ***Main PhD Thesis,*** University of Tasmania, Unpub.

McArthur, G.J., and Dronseika, E.V., (1990). Que River and Hellyer Zinc-lead-Silver Deposits. in ***Geology of the mineral deposits of Australia and Papua New Guinea*** (Ed. F.E Hughes) pp. 1229-1239 (The Australasian Institute of Mining and Metallurgy, Melbourne.

Macrea, J.M, (1950). The Isotope Chemistry of Carbonates and a Palaeotemperature Scale. ***Jour. Chem. Physics,*** v18 p. 849-857.

Matthews, A. and Katz, A. (1977). Oxygen isotope fractionation during dolomitization of calcium carbonate. ***Geochim. Cosmochim*** , Acta 41, pp 1431-1438.

Morton, R.L and Nebel, M.L. (1984). Hydrothermal alteration of felsic volcanic rocks at the Helen siderite deposit, Wawa, Ontario. ***Economic Geology,*** vol. 79, pp1319-1333.

Morton, R.L and Franklin, J.M. (1987). Two-fold classification of Archean volcanic-associated massive sulfide deposits. ***Economic Geology,*** vol. 82 pp 1057-1063

Offler, R. and Whitford, D.J., (1992). Wall-rock alteration and metamorphism of a volcanic-hosted massive sulfide deposit at Que-River, Tasmania: Petrology and mineralogy. ***Economic Geology,*** V.87, p686-705.

Ohmoto, H. and Rye, R. O. (1979). Isotopes of Sulphur and Carbon. In Barnes, H.L. (Ed.) ***Geochemistry of hydrothermal ore deposits,*** 2nd. ed. Wiley, New York:781p.

Reed, M.H and Spycher, N.F. (1985). Boiling, cooling and oxidation in epithermal systems. A numerical modelling approach. ***Geology and Geochemistry of Epithermal Systems.*.** **Reviews in Economic Geology, Vol. 2 Society of Economic Geologists.**

Rollinson, H., (1993). Using Geochemical Data: Evaluation, Presentation, Interpretation. Wiley and Sons Inc., New York.

Simmons, S.F. and Christenson, B.W., (1994). Origons of calcite in a boiling geothermal system. ***American Journal of Science*** v294, p364-400.

Smith, S. Hill, A., Cooke, D and Orth, K., (1994) Application of cathodiluminescence studies to ore deposit research: Examples from carbonated-hosted Zn-Pb, VHMS and epithermal deposits. ***Australian Mineral Foundation Proceeding.***

Taylor, B. (1987). Stable isotope geochemistry of ore forming fluids *in* ***Mineralogical association of Canada,*** Short Course in Stable isotope geochemistry of low temperature fluids, Mineralogical Association Of Canada (Ed. T.K. Kyser)

Urabe, T., Scott S.D and Hattori, K., (1983) A comparison of footwall-rock interaction and geothermal systems beneath some Japanese and Canadian volcanogenic massive sulphide deposits: ***ECON. GEOL. MON 5*** **, p345-364**

Waters, J.C., and Wallace, D. B., (1992). Volcanology and Sedimentology of the Host Succession to the Hellyer and Que-River Volcanic-Hosted Massive Sulphide Deposits, Northwestern Tasmania. ***Economic Geology,*** Vol 87, pp650-666.

Whitford, D.J and Craven, S.J (1983). Petrological and geochemical studies at Que River. ***CSIRO,*** Instituite of Energy and Earth Resources-Division of Mineralogy.

Whitford, D.J, McPherson, W.P.A and Wallace, D.B. (1989). Geochemistry of the host rocks of the volcanigenic massive sulfide deposit at Que River, Tasmania. ***Economic Geology,*** **vol. 84 p1-20.**

Zheng, Y.F. and Hoeffs, J. (1993). Carbon and oxygen isotopic variations in hydrothermal calcites. Theoretical modelling on mixing processes and application to Pb-Zn deposits in the Harz Mountains, Germany. ***Mineral Deposita*** **28, p79-89.**

Appendix 1

HOLE N2
RL 836
110475N

DEPTH (m)	LITHOLOGY	ALTERATION: MINERALOGY %	ALTERATION: TEXTURES	ALTERATION: INTENSITY 1-5	ALTERATION: CHLORITE COLOUR/TEXTURE	ALTERATION: CARBONATE MINERALOGY	ALTERATION: CARBONATE TEXTURE	ALTERATION: CONTACTS	SULPHIDES: MINERALOGY	SULPHIDES: TEXTURES	STRUCTURE	COMMENTS
1–8	STZ	Cl cb PY 65 20 15	• Massive cl • isolated clots of cb • disseminated PY • small cb spheroids • Large Dev veins • 1-2mm veinlets	5	Black, v. fine grained. Massive	Mixture of calcite and dolomite	• 1-2mm small spheroids • 1-2mm veinlets • 10-20cm cross-cutting veins @2-3m @6-10m 1-2mm small spheroids	sharp	PY	• diseam • veined	@6-2m	• between 2 and 5.5m there is a distinct zone where carbonate increases Slight PY increase
9–10	STZ	Si Se cl cb PY 60 15 15 10	• Cl pseudo-brecciated by Si • veinlets of cb	5	Black, patchy	calcite/dolomite	• veinlets of cb • pods	gradational	PY	dissem		decrease in cl
11–20	STZ	Se Si cb py cl 65 15 5 5	• Massive Se/Si • Cb in pods/patches • disseminated PY	5	Black, patchy	calcite/dolomite	@5-10.3m @15-8m	gradational	PY	dissem		increase in sericite
20–24 EOH	HA/BMS	Sericite altered (Massive)		3					PY ga Sph	diseam "		

Cl = chlorite
cb = carbonate
PY = pyrite

Si = silica
Se = sericite
sph = sphalerite

ga = galena
EOH = end of hole

Appendix 1.1: Example of a logging sheet

Drill Hole No.	Northing	Interval logged(m)
HL 799	10340N	166-181
HL 794	10430N	20-29
HL 791	10430N	29-44.5
HL 588	10510N	80-90
HL 727	10520N	89-97
HL 609	10520N	92-105
HL 024	10910N	300-384.4
HL 35A	10910N	396-439.5
HL 199	10910N	93-109
HL 197	10910N	83-102
HL 195	10910N	105-125
HL 416	10910N	10-295
HL 242	10910N	26-112
HL 243	10910N	21-41
HL 241	10910N	7-31
HL 206	10910N	0-20
HL 744	10950N	81-89.
HL 732	10950N	0-12
HL 551	10950N	104-117
HL 174	10950N	115-123.5
HL 173	10950N	113-122
HL 172	10950N	118-129,149-170
HL 056	10950N	341-345
HL 171	10950N	128-144
HL 746	10950N	60-72
HL 253	10950N	18-65
HL 714	10950N	0-88
HL 252	10950N	16-52
HL 202	11010N	145.6-179
HL 109	11010N	121-143
HL 756	11010N	0-26
HL 754	11010N	0-26
HL 807	11010N	10-35
HL 392	11010N	147-162.80
HL 383	11010N	121.5-139.3
HL 534	11010N	205-352
HL 375	11010N	131-163.5
HL 255	11010N	0-25
HL 110	11010N	155-162.7
HL 837	11047.5N	0-17.20
HL834	11047.5N	0-15
HL838	11047.5N	0-16
HL 839	11047.5N	7-28
HL 833	11047.5N	0-16.4
HL 836	11047.5N	0-16
HL 757	11047.5N	11-15
HL 806	11047.5N	1-38.5
HL 129	11047.5N	121-188
HL 758	11047.5N	4-44
HL 141	11047.5N	150-163
HL 127	11047.5N	126-139
HL 470	11047.5N	142-156
HL 137	11047.5N	130-142
HL 284	11047.5N	125-141
HL 128	11047.5N	121-140
HL 542	11090N	152.5-180
HL 830	11090N	0-17
HL 831	11090N	0-17.3
HL 828	11090N	0-15.2

Appendix 1.2: Drill holes logged and intervals

Appendix 2

Thin section samples

Hole No.	Sample No.	Northing	Depth (m)	Zone	Carbonate Texture
HL 755	5	11010N	15.5	Lower	Isltd spheroids (>1/2cm)
HL 807	3	11010N	16.3	Lower	Veins (>1/2cm)
HL 202	8B	11010N	162.5	Lower	Isltd spheroids (<1/2cm)
HL 202	7	11010N	162.2	Lower	Isltd sphds (>1/2cm)+Prvsve
HL 202	8C	11010N	162.7	Lower	Pervasive CO alt.
HL 807	6	11010N	28.8	Lower	"
HL 202	5	11010N	152.8	Lower	Co alt. stops abrubtly
HL 383	1	11010N	125.8	Nr. contact	Pod of sphds (<1/2cm)
HL 392	1	11010N	153.1	Nr. edge	Isltd spheroids (>1/2cm)
HL 807	1	11010N	9.4	Lower	Small spheroids
HL 199	1	10910N	104.3	edge,nr. contact	Isltd spheroids (>1/2cm)
HL 024	2	10910N	345.5	Btwn lower+cntct	Veins (>1/2cm)
HL 35A	1	10910N	408.2	Btwn lower+cntct	Pods of CO
HL 241	1	10910N	20.5	Nr. Jack Fault	Pods+Isltd sphd (>1/2cm)
HL 243	3	10910N	40.3	Contact	Devonian vein
HL 757	3	11047.5N	24.2	Lower	Devonian veins, sml sphds
HL 470	2	11047.5N	152	Nr. contact	Veins (>1/2cm)
HL 141	3	11047.5N	162.5	Nr. edge	Veinlets (<1/2cm)
HL 129	2	11047.5N	139	Lower	Isltd sphds (<1/2cm)+rhombs
HL 757	5	11047.5N	41.9	Nr. contact	Islt/colscd CO in pods/zones
HL 833	2	11047.5N	4.8	Nr. contact	Pods of veinlets (<1/2cm)
HL 252	1	10950N	26.5	Nr. contact	Veinlets (<1/2cm)
HL 172	2	10950N	150.8	Lower	Isltd/coalscd CO in pods/zns
HL 732	1	10950N	0.2	Lower	Pods
HL 714	1	10950N	14.8	Lower	Vns/vnlts,Isltd pods,(<1/2cm)
HL 172	4	10950N	165.7	contact	Pervasive
HL 542	3	11090N	166.7	Nr. contact	Veinlets (<1/2cm)
HL 602	2	11090N	102.6	Nr. edge	Veinlets(<1/2cm)
HL 609	1	10520N	98	Nr. edge	Pods
HL 799	1	10340N	172.5	Nr. contact	Isltd spheroids (<1/2cm)

Isltd sphds- isolated spheroids
Coalsd- coalesced
Vnlts- veinlets
Vns- veins

Appendix 2.1: Thin section sample locations and descriptions

HELLYER MINE, CHLORITE-CARBONATE ALTERATION STUDY
PETROLOGICAL INTERPRETATION

Date: 16/7/97

Sample No: 5

Hole No: HL 202, 1101oN

Depth: 152.8m

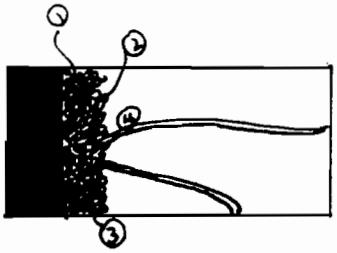

Hand Sample Description: Veinlets of dolomite (< ½cm) that seem to lead to a group of coalesced small dolomite spheroids. There is a sharp contact between chlorite alteration.

Remnant Host Rock textures : none.

Deformational Textures: pressure shadows in the pyrite, coarser sericite on rims of carbonate spheroids.

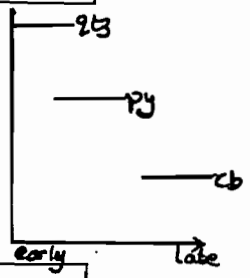

Alteration Mineralogy:

% Calcite	% Dolomite	%Cl	%Qtz	%Other
	Fe^{2+} (stained) 75%	10%	20%	Sericite 5%

Carbonate Textures:

1. Close-packed spheroids < ½ cm in a distinct zone. On the edges some crystals are radiating, towards the centre, they are more closely packed
2. Centre of spheroids is finer grained
3. Quartz seems to be everywhere in matrix (Euhedral)
4. Fine-grained matrix of chlorite/carb quarty

Some relict cb, anhedral clots overprinted by Silse alteration.

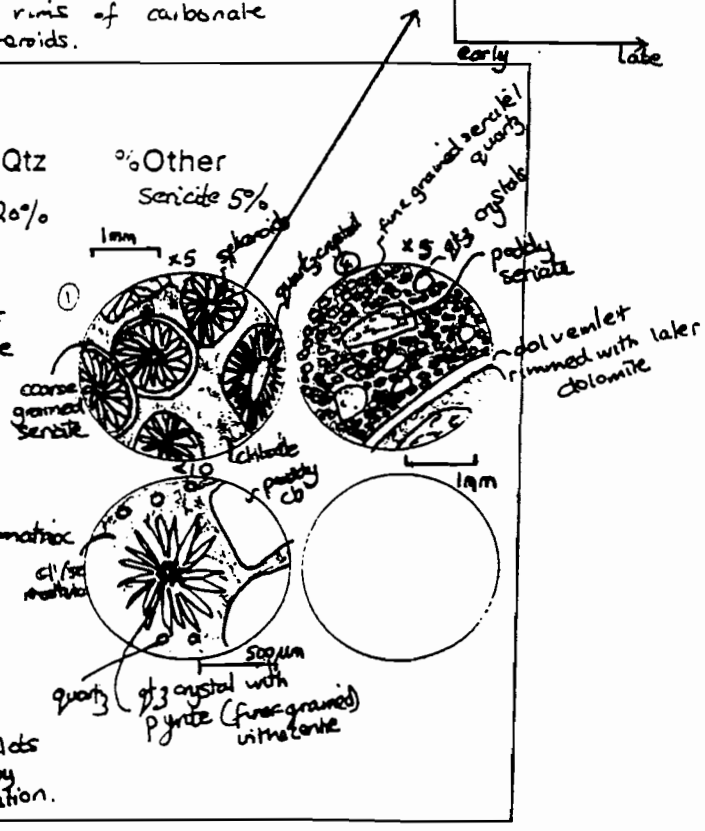

Appendix 2.2: Example of a petrological interpretation sheet

Alteration Mineral Paragenisis:

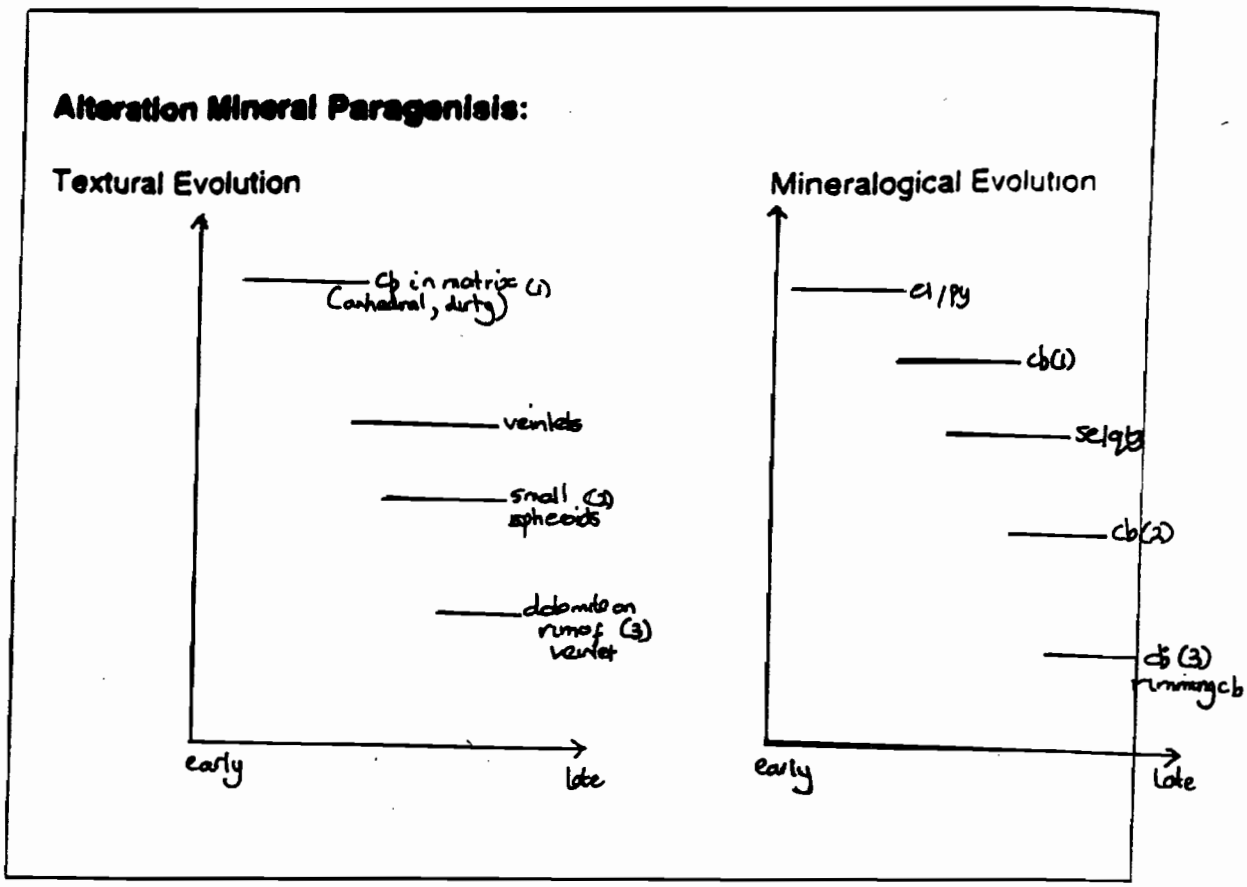

Comments:

- Spheroids appear to be nucleating off quartz crystals.
- pyrites mainly concentrated in the centre of the spheroids
- pervasive se/si alteration over original anhedral dolomites in a sericite matrix
- possibly pervasive alteration front (?)

Appendix 3

	C	O	N	T	A	C	T		L	O	W	E	R		
Sample	1	1	1	3	4	1	**MEAN**		2	2	4B	1	1	**MEAN**	**MEAN ALL**
Hole	HL 128	HL 199	HL 241	HL 551	HL 109	HL 833			HL 252	HL 35A	HL 202	HL 732	HL 757		
Northing	11047.5N	10910N	10910N	10950N	11010N	11047.5N			10950N	10910N	11010N	10950N	11047.5N		
Depth (m)	123.9	104.5	20.5	119.9	128	0.5			32.9	409.2	152.3	0.2	16.1		
Lithology	STZ	STZ	STZ	STZ	STZ	STZ			STZ	STZ	STZ	STZ	STZ		
Alteration	ClCbSePy	ClCbSi	ClCbPy	ClCbPy	ClCbPy	ClCbPy			CbClPy	ClCbPy	ClCbPy	ClCb	ClCbPy		
Zone	Contact	Contact	Contact	Contact	Contact	Contact			Lower	Lower	Lower	Lower	Lower		
Textures	Vlts	Vnlts, Ss	Vlts, Pods	Vlts, Pods	Vlts, Diss	Vlts, Pods			Patchy	Ls	Ss	Ss/Pods	Pods		
SiO2	57.0	18.4	28.4	20.2	32.2	27.6	25.4		31.6	21.7	23.1	23.2	13.2	22.6	27
TiO2	0.3	0.4	0.4	0.5	0.6	0.5	0.4		0.1	0.6	0.6	0.5	0.4	0.44	0.43
Al2O3	9.0	11.3	8.5	10.7	18.0	10.9	11.4		3.4	14.6	15.1	8.5	16.4	11.6	11.8
Fe2O3	4.1	14.9	6.5	19.3	9.1	8.4	10.4		4.8	13	8.2	14.8	3.2	8.8	9.6
MnO	0.5	1.0	0.6	0.8	1.1	0.6	0.7		0.6	0.9	0.5	0.6	0.8	0.68	0.71
MgO	5.0	16.0	15.2	13.0	12.4	17.7	13.2		11.2	19.9	17.2	21.1	22.9	18.5	14.1
CaO	8.1	11.7	16.9	7.0	6.6	9.0	9.9		17.8	9	11.5	6.1	9.8	10.8	10.9
Na2O	0.02	0.03	0.03	0.03	0.016	0.03	0.025		0.03	0.0025	0.0025	0.03	0.025	0.024	0.067
K2O	2.49	0.59	0.01	0.48	3.3	0.69	1.26		0.2	0.7	2	0.03	0.0025	0.58	0.095
P2O5	0.07	0.12	0.08	0.14	0.14	0.05	0.1		0.08	0.14	0.13	0.11	0.05	0.102	0.01
LOI	12.7	20.4	21.7	17.1	14.9	19.7	17.73		22	19.7	21.7	16.6	29.9	21.9	19.7
TOTAL	99.2	94.8	98.3	89.2	98.4	95.2	90.5		91.8	100.24	100.03	91.57	96.68	96.07	95.4
S	2.0	5.4	3.6	12.5	3.9	3.4	5.1		3.4	2.7	1.1	1.6	0.2	1.8	3.61
Zr	80.0	88.0	93.0	80.0	133.0	118.0	98.6		44.0	139.0	126.0	109.0	115.0	106.6	102.2
Nb	6.0	5.0	6.0	5.0	9.0	8.0	6.5		2.0	8.0	8.0	6.0	8.0	6.4	6.5
Y	21.0		16.0	25.0	30.0		23.0			31.0		19.0	33.0	27.6	27.7
Sr	84.0	102.0	132.0	43.0	65.0	111.0	89.5		175.0	160.0	135.0	69.0	195.0	146.8	115.5
Rb	84.0	20.0	0.3	16.0	111.0	24.0	42.5		7.0	23.0	56.0	1.0	0.3	17.5	31.3
Ba	745.0	447.0	42.0	166.0	948.0	412.0	460.0		197.0	878.0	1028.0	70.0	43.0	443.2	452.4
Cu	6.0	156.0	22.0	1409.0	23.0	60.0	279.3		50.0	14.0	5.0	11.0	0.5	13.4	159.6
Pb	9.0	6500.0	1043.0	2600.0	83.0	3600.0	2305.8		15800.0	121.0	29.0	175.0	1444.0	3513.8	2854.9
Zn	21.0	13200.0	873.0	54300.0	247.0	3750.0	12065.0		21636.0	314.0	148.0	1194.0	1866.0	5631.6	8868.1
Cu Ratio	22.2	1.2	2.5	2.5	8.5	1.6	6.4		0.2	4.3	3.3	0.9	0.0	1.7	4.3
Zn Ratio	70.0	67.1	45.6	95.4	74.8	51.0	67.3		57.8	72.2	83.6	87.2	56.4	71.4	69.1
Ti/Zr	24.0	28.0	22.6	34.5	26.1	24.3	26.6		17.7	24.1	27.1	28.5	20.3	23.2	25.2
Alt. Index	48.4	58.5	47.1	65.6	70.3	65.2	59.2		38.9	69.5	62.5	77.5	57.9	61.3	60.1
Cl/Cb/Pyldx	78.6	98.0	99.8	98.5	86.7	97.3	93.1		98.8	97.9	92.6	99.8	99.9	97.8	95.3
Mn Carb Idx	84.0	97.2	99.9	96.7	83.9	95.3	92.7		99.2	96.3	88.4	99.5	88.9	96.7	94.5

Ss- Small spheroids	Se-Sericite alteration
Ls- Large spheroids	Cl- Chlorite alteration
Vlts- Veinlets	Si-Quartz alteration
STZ-Stringer Zone	Cb- Carbonate alteration
	Py -Pyrite alteration

Appendix 3.1: Whole-Rock XRF results

UNALTERED PRECURSOR XRF DATA

Hole	841B	HL 841B	HL 844	HL 841B	MEAN
Depth (m)	830.9	947.7	373.1	1029.7	
Lithology	Andesite	Andesite	Andesite	Andesite	
SiO2	53.8	53	57.3	56.6	55.18
TiO2	0.6	0.65	0.58	0.63	0.615
Al2O3	15.2	15.8	14.6	16	15.4
Fe2O3	7.6	8.82	6.54	7.47	7.61
MnO	0.13	0.13	0.17	0.14	0.142
MgO	4.1	4.25	2.55	5	3.98
CaO	4.4	3.25	6.82	2.84	4.33
Na2O	5.2	5.09	3.94	5.3	4.88
K2O	0.21	0.64	1.26	0.35	0.62
P2O5	0.12	0.15	0.15	0.14	0.14
S	0.5	0.5	0.3	0.05	0.34
Zr	141	151	135	145	143
Ti/Zr	25.5	25.8	25.8	26	25.78
Alt. Index	31	37	26	40	33.5

Appendix 3.2: Unaltered andesite XRF analyses (Courtesy Aberfoyle Resources Ltd.)

	FPS MEAN N=6	FPS STD. DEV.	SEZ MEAN N=33	SEZ STD. DEV.	Se/Cl MEAN N=12	Se/Cl STD. DEV.	Cl/CO MEAN N=5	Cl/CO STD. DEV.	Cl MEAN N=7	Cl STD. DEV.	SiSe MEAN N=9	SiSe STD. DEV.
SiO2	56.94	1.64	62.29	5.24	59.31	10.54	41.23	17.76	42.97	19.73	73.08	6.81
TiO2	0.67	0.04	0.63	0.13	0.57	0.15	0.71	0.13	0.67	0.20	0.33	0.16
Al2O3	18.66	1.08	16.64	3.23	15.79	2.60	18.47	4.29	18.33	4.99	8.81	4.34
Fe2O3	7.97	0.91	8.42	2.75	11.90	9.39	15.24	8.61	21.50	15.68	13.37	9.81
MnO	0.09	0.03	0.11	0.07	0.23	0.13	0.94	0.53	0.47	0.27	0.08	0.09
MgO	3.95	1.16	3.81	3.74	5.62	3.60	15.45	7.18	12.97	10.11	1.54	1.46
CaO	3.27	1.16	2.94	2.84	1.60	1.49	5.75	5.25	0.73	0.57	0.35	0.26
Na2O	6.72	1.27	1.40	1.36	0.98	1.58	0.01	0.00	0.14	0.33	0.03	0.02
K2O	1.61	1.50	3.63	1.74	3.90	1.46	2.04	1.97	2.07	1.39	2.35	1.30
P2O5	0.12	0.03	0.14	0.05	0.11	0.05	0.15	0.04	0.14	0.04	0.05	0.05
TOTAL	100		100		100		100		100		100	
LOI	3.96	0.68	7.89	2.55	8.11	4.19	15.40	5.73	12.29	5.70	7.74	3.75
S	1.92	1.21	4.15	2.95	6.02	6.75	4.13	2.83	8.65	10.38	8.87	7.09
Ni	368	626	39	34	35	27	34	19	34	16	16	13
Cr	115	34	144	230	93	86	90	17	89	34	74	83
V	256	38	188	60	219	121	205	67	250	82	101	69
Zr	125	15	123	52	94	41	124	24	140	58	74	23
Nb	7	1	7	4	6	3	9	2	8	2	4	2
Y	19	3	26	8	18	9	28	5	25	6	28	15
Sc	8	16	11	13	21	16	30	7	34	8	5	6
La	31	25	46	26	26	15	32	8	17	11	27	21
Sr	299	47	97	70	121	190	58	37	39	41	15	10
Rb	68	62	127	63	117	42	66	62	79	56	79	36
Ba	744	386	1587	1351	1986	979	1074	1000	2235	1829	2429	2020
Cu	1700	2865	312	742	119	136	67	108	1116	1786	308	547
Pb	62	34	4523	20027	392	785	257	229	113139	280295	3892	8039
Zn	1433	1997	11697	57713	500	998	526	307	39	41	42948	113246
Ag	2	1	4	7	2	2	2	2	16	24	7	9
As	47	10	114	106	170	159	130	110	281	345	354	297
Zn RATIO*	96	11	72	19	56	21	67	14	0	38	92	28
Cu RATIO*	54	17	3	21	19	15	11	8	97	35	1	19
Ti/Zr	32	3	31	12	36	14	34	3	29	9	27	11
Zr/Y	7	1	5	2	5	3	4	1	6	2	3	2
Zr/Nb	18	4	18	25	16	12	14	1	17	6	17	15
ALT INDEX**	36	7	64	19	79	22	75	11	95	4	91	6

* Alteration: Si- silica, Se-sericite, Cl-chlorite, CO-carbonate, Py-pyrite, SEZ - stringer envelope zone, FPS - feldspar phyric sequence (footwall andesite)
* Zn RATIO=100*Zn/Zn+Pb, Cu RATIO=100*Cu/Cu+Zn
** ALTERATION INDEX= K20+MgO/K2O+Na2O+CaO+MgO*100 (Ishikawa et al. (1976)

Appendix 3.3: Chlorite-carbonate XRF analyses (Gemmell, 1989)

Unit	Drill Hole No.	Depth (m)	TiO_2	Zr
Mixed dacitic sequence	MAC 35	1100	0.4	186
"	QR 1001	267	0.33	170
"	MAC 21	160	0.22	200
"	MAC 17	136.7	0.34	188
"	HAT 9	123	0.21	220
Hellyer Basalt	HL 55	154.2	0.47	54
"	HL 55	167.1	0.4	53
"	HL 55	198.4	0.7	86

Appendix 3.4: Location, TiO_2 and Zr data for the mixed dacitic sequence and Hellyer basalt (Courtesy Aberfoyle Resources Ltd.)

Appendix 4

SAMPLE	VEIN STAGE	DEPTH BELOW OREBODY	FEEDER	ALTERATION ZONE	MINERAL	δ13C (PDB) (per mil)	δ18O (SMOW) (per mil)
HL 058-4	2A	10 m	N	Chlorite/Carb	Cal/Dolm	0.87	13.72
HL 093-10	2A	25 m	C	Silica	Dolomite	0.42	11.42
A/HL-27	2A	50 m	C	Silica	Dolm/Cal	-0.15	9.90
HL 093-61	2A	95 m	C	Silica	Dolomite	1.07	10.43
HL 306-100	2A	190 m	C	Silica	Dolomite	1.48	10.24
HL 306-114	2A	240 m	C	Silica	Dolomite	1.26	10.21
HL 306-126	2A	293 m	C	Silica	Dolm/Cal	1.30	9.58
HL 306-148	2A	350 m	C	Silica	Dolomite	1.22	10.61
HL 306-171	2A	426 m	C	Chlorite	Dolomite	1.65	10.80
HL 306-186	2A	480 m	C	Chlorite	Dolomite	1.06	10.70
HL 306-195	2A	550 m	C	Chlorite	Dolomite	0.19	11.69
HL 093-10	2B	25 m	C	Silica	Dolomite	0.56	11.70
A/HL-26	2B	50 m	C	Silica	Dolomite	1.33	10.55
HL 306-130	2B	296 m	C	Silica	Dolm/Cal	1.61	9.94
HL 306-139	2B	328 m	C	Silica	Dolomite	1.55	10.08
HL 306-141	2B	332 m	C	Silica	Dolomite	-1.81	13.37
HL 022-3	2C	45 m	N	Chlorite	Dolm/Cal	-0.33	12.10
A/HL-23	2C	50m	C	Silica	Dolm/Cal	0.98	10.43
HL 306-49	2C	55 m	C	Silica	Dolomite	0.81	9.34
HL 177-2	4	5 m	N	Chlorite/Carb	Cal/Dolm	0.56	9.90
HL 022-4	4	50 m	N	Sericite	Dolomite	0.68	9.24
HL 306-56	4	74 m	C	Silica	Dolomite	-0.80	12.45
HL 306-74	4	121 m	C	Silica	Dolomite	0.29	9.12
HL 306-117	4	245 m	C	Silica	Cal/Dolm	0.65	8.64
HL 306-142	4	334 m	C	Silica	Dolomite	0.15	11.27
HL 306-188	4	480 m	C	Chlorite	Dolomite	0.71	9.15
HL 306-78	5	138 m	C	Silica	Cal/Dolm	-0.51	11.66
HL 306-121	5	259 m	C	Silica	Cal/Dolm	0.75	11.34
HL 306-138	5	326 m	C	Silica	Dolomite	0.18	11.25
HL 006-10	6	40 m	S	Silica	Cal/Dolm	-1.78	12.56
HL 306-72	6	117 m	C	Silica	Cal/Dolm	-0.33	12.04
HL 177-4	Alt.	5 m	N	Chlorite-Carb	Cal/Dolm	0.60	11.13
HL 58-7	Alt.	5 m	N	Chlorite-Carb	Dolomite	0.43	11.62
HL 256-6	Alt.	15 m	N	Chlorite-Carb	Calcite	-0.21	10.43
HL 006	Alt.	40 m	S	Chlorite-Carb	Dolomite	-1.51	8.20

Appendix 4.1: $\delta^{13}C$ and $\delta^{18}O$ stable isotope locations for the stage 2A, 2B and 2C syn-mineralisation veins and the stage 4, 5 and 6 post-mineralisation veins (Gemmell, 1988)

CARBON AND OXYGEN ISOTOPE DATA

Sample No.	Hole No.	Description	Depth(m)	Northing	Easting	$^{13}C_{PDB}$(‰)	$^{18}O_{SMOW}$(‰)	Altn. zone
2	HL 024	Calcite veins	345.5	10910N	5798E	-0.178	10.631	
5	HL 024	clts/lge sphds	378	10910N	5810E	0.969	12.55	Lower
1	HL 35A	clots	408.2	10910N	5817E	0.309	12.882	Contact
2	HL 195	vnlts/sml sphds	121.8	10910N	5792E	1.247	14.541	Contact
1	HL 199	lge sphds	104.3	10910N	5836E	2.154	17.467	Contact
1	HL 241	clots/lge sphds	20.5	10910N	5757E	2.013	12.979	Lower
1	HL 172	veinlets	122.6	10950N	5818E	0.837	13.022	Contact
2	HL 172	sml sphds in pod	150.8	10950N	5790E	1.797	15.247	Lower
1	HL 252	veinlets	26.5	10950N	5779E	1.622	14.003	Contact
2	HL 252	calcite vein	32.9	10950N	5775E	0.96	13.295	
1	HL 714	vnlts/sml sphds	14.8	10950N	5786E	1.587	15.775	Lower
1	HL 732	clots	0.2	10950N	5800E	2.319	16.827	Lower
5	HL 253	vscle fill	64.2	10950N	5761E	-0.964	12.554	
7	HL 732	lge sphds	7.5	10950N	5793E	1.85	18.285	Lower
5	HL 202	sml sphds	152.8	11010N	5797E	1.221	15.045	Lower
7	HL 202	lge sphds	162.2	11010N	5789E	2.226	17.547	Lower
8C	HL 202	sml sphds/vnlts	162.7	11010N	5779E	1.594	15.194	Lower
1	HL 383	sml sphds in pod	125.8	11010N	5844E	0.647	12.995	Contact
1	HL 392	lge sphds	153.1	11010N	5855E	-0.74	12.74	Lower
8B	HL 202	sml sphds	162.5	11010N	5782E	1.949	17.631	Lower
2	HL 754	massive/clt vein	9.5	11010N	5790E	1.357	16.395	Lower
5	HL 755	lge sphds	15.5	11010N	5781E	1.464	17.429	Lower
3	HL 807	clct veins	16.3	11010N	5803E	1.082	16.541	Lower
4	HL 807	veinlets	18.9	11010N	580OE	1.675	16.562	Lower
6	HL 807	sml sphds/vnlts	28.8	11010N	5795E	0.813	10.758	Lower
2	HL 129	sml sphds	139	11047.5N	5818E	1.822	16.781	Lower
2	HL470	calct vein	152	11047.5N	5860E	6.007	23.814	
3	HL 141	veinlets	162.5	11047.5N	5777E	2.755	16.172	Lower
5	HL 757	sml sphds in pod	41.9	11047.5N	5786E	2.32	17.615	Lower
2	HL 833	Vnlts in pods	4.8	11047.5N	5860E	1.453	15.069	Contact
2	HL 836	clots	6.2	11047.5N	5860E	1.484	15.627	Contact
4	HL 758	clot	30.3	11047.5N	5785E	1.834	16.787	Lower
4A	HL 806	calcite vein	15.4	11047.5N	5810E	1.957	15.964	
1A	HL 141	lge sphds/vnlts	155.7	11047.5N	5777E	1.51	17.574	Lower
3	HL 542	veinlets	166.7	11090N	5868E	0.729	10.293	Contact
2	HL 831	sml sphds in pod	7	11090N	5863E	1.304	14.22	Contact

Sml sphds- small spheroids
Lge sphds- large spheroids
Calct- calcite
Lge sphds- large spheroids
Vscle- vesicle
Clts- clots
Vnlts- veinlets

Appendix 4.2: $\delta^{13}C$ and $\delta^{18}O$ stable isotope sample locations and descriptions

Appendix 5

Rock Catalogue

Catalog #	Field #	Textures	Mine - N	Mine - E	DDH	Depth	Locality	Preparations
135740	S1	chl/carb overprinted by se/qz	11010	5807	HL 807	9.4	footwall	R
135741	S2	Large spheroids joined to form a vein	11090	5854	HL 828	8.8	footwall	R
135742	S2	massive dolomite and veinlets	11047.5	5779	HL141	161.1	footwall	R
135743	S2	massive dolomite pod in a chlorite matrix	11010	5802	HL202	149.3	footwall	R
135744	S2	small spheroids in chlorite matrix	11047.5		HL137	132.8	footwall	R
135745	S5	calcite vein cross-cutting chlorite/quartz alteration	11047.5	5785	HL758	35.2	footwall	R
135746	S1	isolated large spheroids	10910	5836	HL199	104.3	footwall	PS/CH/SOdol/Cldol
135747	S2	veins	10910	5798	HL 024	345.5	footwall	PS/CH/SOdol/Cldol
135748	S1	isolated small spheroids	10910	5817	HL 35A	408.2	footwall	PS/CH/SOdol/Cldol
135749	S1	isolated large spheroids	10910	5757	HL 241	20.5	footwall	PS/CH/SOdol/Cldol
135750	S3	veins	10910	5740	HL 243	40.3	footwall	PS
135751	S1	veins	10947.5	5779	HL 252	26.5	footwall	PS/CH/SOdol/Cldol
135752	S2	isolated pods of dolomite	10947.5	5818	HL 172	150.8	footwall	PS/CH/SOdol/Cldol
135753	S1	pods	10947.5	5800	HL732	0.2	footwall	PS/CH/SOdol/Cldol
135754	S1	veinlets / isolated pods	10947.5	5786	HL714	14.8	footwall	PS/SOdol/Cldol
135755	S4	massive	10947.5	5790	HL172	165.7	footwall	PS
135756	S5	isolated large spheroids	11010	5781	HL 755	15.5	footwall	PS/CH/SOdol/Cldol
135757	S3	veins	11010	5803	HL 807	16.3	footwall	PS/SOdol/Cldol
135758	S8B	isolated small spheroids	11010	5782	HL 202	162.5	footwall	PS/CH/SOdol/Cldol
135759	S7	isolated large spheroids	11010	5789	HL 202	162.2	footwall	PS/CH/SOdol/Cldol
135760	S8C	massive	11010	5795	HL 807	28.8	footwall	PS/CH/SOdol/Cldol
135761	S5	massive	11010	5797	HL 202	152.8	footwall	PS/CH/SOdol/Cldol
135762	S1	small spheroids	11010	5844	HL 383	125.8	footwall	PS/CH/SOdol/Cldol
135763	S1	pod of small spheroids	11010	5855	HL 392	153.1	footwall	PS/CH/SOdol/Cldol
135764	S6	isolated large spheroids	11010	5807	HL 807	9.4	footwall	PS/SOdol/Cldol
135765	S1	mssve qz/ser overprint	11010	5807	HL 807	28.8	footwall	PS

Cambrian
Que-Hellyer Volcanics

All lower greenschist facies
AMG ~ 55GCQ 875340

135740-135798

Catalog #	Field #	Textures	Mine - N	Mine - E	DDH	Depth	Locality	Preparations
135766	S2	veins	11047.5	5860	HL 470	152	footwall	PS/CH/SOdol/CIdol
135767	S3	veinlets	11047.5	5777	HL 141	162.5	footwall	PS/CH/SOdol/CIdol
135768	S2	isolated small spheroids	11047.5	5818	HL 129	139	footwall	PS/CH/SOdol/CIdol
135769	S5	pods	11047.5	5786	HL 757	41.9	footwall	PS/CH/SOdol/CIdol
135770	S2	veins	11047.5	5860	HL 833	4.8	footwall	PS/CH/SOdol/CIdol
135771	S3	veinlets	11090	5868	HL 542	166.7	footwall	CH/SOdol/CIdol
135772	S2	veinlets	10520	5614	HL 602	102.6	footwall	PS/CH/SOdol/CIdol
135773	S1	pods	10520	5653	HL 609	98	footwall	PS/CH/SOdol/CIdol
135774	S1	isolated small spheroids	10340	5652	HL 799	172.5	footwall	PS/CH/SOdol/CIdol
135775	S2	veinlets/small spheroids	10910	5792	HL 195	121.8	footwall	SOdol/CIdol
135776	S5	large spheroids	10910	5810	HL 024	378	footwall	SOdol/CIdol
135777	S1	veinlets	10947.5	5818	HL 172	122.6	footwall	SOdol/CIdol
135778	S7	isolated large spheroids	10947.5	5793	HL 732	17.5	footwall	SOdol/CIdol
135779	S2	veins	10947.5	5775	HL 252	39.2	footwall	SOdol/CIdol
135780	S5	carb in vesicle	10947.5	5761	HL 253	64.2	hangingwall	SOdol/CIdol
135781	S2	massive	11010	5790	HL 754	9.5	footwall	SOdol/CIdol
135782	S4	veinlets	11010	5800	HL 807	18.9	footwall	SOdol/CIdol
135783	S2	pods	11047.5	5860	HL 836	6.2	footwall	SOdol/CIdol
135784	S4	pods	11047.5	5785	HL 758	30.3	footwall	SOdol/CIdol
135785	S4A	veins	11047.5	5810	HL 806	15.4	footwall	SOdol/CIdol
135786	S1A	veinlets/large spheroids	11047.5	5777	HL 141	155.7	footwall	SOdol/CIdol
135787	S2	pods of small spheroids	11090	5863	HL 831	7	footwall	SOdol/CIdol
135788	S1	veinlets	11047.5	5815	HL 128	123.9	footwall	PD
135789	S1	small sphedoids/veinlets	10910	5804	HL 199	104.5	footwall	PD
135790	S1	veinlets/pods	10910	5755	HL 241	20.5	footwall	PD
135791	S3	veinlets/pods	10950	5871	HL 551	119.9	footwall	PD
135792	S4	dissem carb/veinlets	11010	5835	HL 109	128	footwall	PD
135793	S1	veinlets/pods	11047.5	5860	HL 833	5	footwall	PD

Cambrian
Que-Hellyer Volcanics

All lower greenschist facies
AMG ~ 55GCQ 875340

135740-135798

Catalog #	Field #	Textures	Mine - N	Mine - E	DDH	Depth	Locality	Preparations
135794	S2	patchy	10947.5	5770	HL 252	32.9	footwall	PD
135795	S2	large spheroids	10910	5821	HL 35A	409.2	footwall	PD
135796	S4B	small spheroids	11010	5775	HL 202	152.3	footwall	PD
135797	S1	small spheroids/pods	10947.5	5800	HL 732	2	footwall	PD
135798	S1	pods	11047.5	5800	HL 757	16.1	footwall	PD

Cambrian
Que-Hellyer Volcanics

All lower greenschist facies
AMG ~ 55GCQ 875340

135740-135798